

**SECRET**



3 4456 0050899 3

ORNL 159  
PROGRESS REPORT

**CENTRAL RESEARCH LIBRARY  
DOCUMENT COLLECTION**

**LABORATORY SECURITY**

PHYSICS DIVISION

PROGRESS REPORT FOR THE QUARTER JUNE, JULY, AUGUST 1948

A.M. WEINBERG, DIRECTOR

**CENTRAL RESEARCH LIBRARY  
DOCUMENT COLLECTION  
LIBRARY LOAN COPY  
DO NOT TRANSFER TO ANOTHER PERSON  
If you wish someone else to see this  
document, send in name with document  
and the library will arrange a loan.**

# OAK RIDGE NATIONAL LABORATORY

OPERATED BY  
CARBIDE AND CARBON CHEMICALS CORPORATION  
FOR THE  
ATOMIC ENERGY COMMISSION  
POST OFFICE BOX P  
OAK RIDGE, TENNESSEE

**SECRET**

~~SECRET~~

ORNL-159

This document consists of  
125 pages

Copy 7 of 89 .Series A

ISSUED: *Training School  
Library*

**DECLASSIFIED**

CLASSIFICATION CHANGED TO:

BY AUTHORITY OF: T10-11.49  
By: *D. Morrison* 2/8/52

Contract No. W-7405, eng. 26

PHYSICS DIVISION

PROGRESS REPORT

FOR THE QUARTER

JUNE, JULY, AUGUST

1948

A. M. Weinberg, Director

OCT 14 1948

OAK RIDGE NATIONAL LABORATORY  
OPERATED BY  
Carbide and Carbon Chemicals Corporation  
For the  
Atomic Energy Commission  
Post Office Box P  
Oak Ridge, Tennessee

MARTIN MARIETTA ENERGY SYSTEMS LIBRARIES



3 4456 0050899 3

~~SECRET~~

[REDACTED]

INDEX

|   | Page No. |
|---|----------|
| SUMMARY, A. M. Weinberg                       | 4        |
| NEUTRON PHYSICS, A. H. Snell                  | 8        |
| NEUTRON AND NUCLEAR PHYSICS, E. O. Wollan     | 14       |
| PHYSICAL ELECTRONICS, W. H. Jordan            | 28       |
| NUCLEAR STATES AND RADIATIONS, S. DeBenedetti | 49       |
| CRITICAL EXPERIMENTS, M. M. Mann              | 61       |
| PHYSICS OF SOLIDS, S. Siegel                  | 82       |
| MATHEMATICS AND COMPUTING, A. S. Householder  | 91       |
| SHIELDING, E. P. Blizard                      | 104      |
| THEORETICAL PHYSICS, M. E. Rose               | 124      |

SUMMARY

QUARTERLY REPORT

PHYSICS DIVISION

A. . Weinberg, Director

Personnel Changes

The following people have left the Division during the last quarter:

|                  |   |
|------------------|---|
| H. L. Garabedian | E.E. Conrad (U. S. Navy loan)                   |
| G. H. Goertzel   | A. V. H. Masket (NRL loan)                      |
| E. Greuling      | R. C. L. Mooney (Sarah Newcomb College<br>Loan) |
| G. J. Haines     |   |
| L. D. Norris     | R. E. Rundle (Iowa State College loan)          |
| R. D. Present    | W. Yatchmenoff (U. S. Navy loan)                |
| M. J. Valentine  |   |
| D. K. White      |   |

The following have joined the Division:

L. Gordon  
K. G. Libbey  
F. T. Rogers  
F. A. Sherrill  
L. C. Templeton

The following are on loan to the Division:

J. K. Bair, NEPA  
J. A. Barker, U. S. Navy  
R. W. Coyle, NEPA  
H. M. James, Purdue University  
R. H. Kernohan, NEPA  
E. Rodgers, University of Alabama  
E. B. Roth, U. S. Navy.

[REDACTED]

Low Temperature Conference - A conference on Low Temperatures and Nuclear Physics was held under the sponsorship of the Division on August 7. The conference was attended by about 100 scientists, of whom 35 came from outside the area. The four invited papers which were presented by M. E. Rose, H. B. G. Casimir, E. M. Purcell and F. London will be issued as an ORNL publication.

Hi-Flux Pile - Emphasis in the hi-flux reactor project has shifted from the original 30 megawatt design to consideration of rather more moderate outputs of the order of 3 megawatts. This change has come about as a result of decisions of the Reactor Safeguard Committee to limit output in inhabited areas.

Critical experiments with Be and graphite reflectors continue. The adequacy of the Cd and Th safety rods has been demonstrated, and  $\gamma$  ray heating near the experimental holes has been measured. The flux of very fast neutrons ( $> 1$  MeV) has been found to be about 40% of the thermal flux at the center of the assembly.

Shielding Program - Core borings on the present pile shield show little evidence of radiation damage. Arrangements for lid type experiments are being made; and future attenuation tests will all be made in lid geometry. The advantage of lid experiments is that boundary effects are essentially eliminated in them.

Neutron Physics - Coincidences between decay  $\beta$ 's and protons have been observed in the neutron decay experiment. The coincidence rate is lower than would be expected from the single counting rate.

An absorption resonance at 0.5 eV of at least 1700 barns has been found in very pure  $\text{Er}_2\text{O}_3$ . Transmission experiments on  $\text{Ni}^{58}\text{O}$  with neutrons of energy 0.03 to 0.5 eV show marked diffraction maxima; the coherent scattering cross section of  $\text{Ni}^{58}$  has been found to be 26 barns, in agreement with the value obtained from powder diffraction studies.

Neutron diffraction studies have been directed toward

[REDACTED]

establishing the scattering properties of the Ni isotopes, and the determination of the scattering phases of Zr, N, Th, Rb and Sr.

Capture  $\gamma$ -ray work is progressing along three lines -- measurement of capture  $\gamma$ -rays from Cl by production of pairs in a cloud chamber with Pb radiator; study of capture  $\gamma$ -rays with a crystal counter; and photographic plate studies with D<sub>2</sub>O impregnated plates.

Slowing down distributions of neutrons from a fission source in a 1-1 H<sub>2</sub>O-Al mixture have been measured. The mean square slowing range is 473 cm<sup>2</sup> compared to a calculated value of 440 cm<sup>2</sup>.

Theoretical and Mathematical Physics - Coding procedures for computation of internal conversion coefficients have been almost completed. It has been decided to place the problem on the Harvard Mark I Computer.

A long term program of exploration of stochastic methods for solution of differential equations is being set up. This program, which is pointed toward the ultimate exploitation of a high speed computing machine, has promise of yielding extremely powerful methods for solving differential equations in many dimensional spaces.

Theoretical studies of the problem of lining up nuclear spins at low temperatures in high magnetic fields have continued. A talk on this subject was given by M. E. Rose at the Conference on Nuclear Physics and Low Temperatures.

Miscellaneous Nuclear Physics - Study of the  $\beta$  spectrum of W<sup>187</sup> indicates the presence of a hitherto unreported  $\gamma$ -ray line at .767 MeV.

The "Rodgers Effect" (change in scattering of polarized X-rays from a scatterer caused by an AC magnetic field) has been sought with Au<sup>197</sup>  $\gamma$ -rays (.4 MeV). Although the experiments are not entirely consistent, there seems to be some evidence that an AC field does increase the scattering of polarized  $\gamma$ -rays from a scatterer. So far there is no satisfactory explanation of the effect.

~~SECRET~~

Physical Electronics - The effect of temperature on the pulse sizes of anthracene and naphthalene scintillation has been studied. In accordance with theory, it is found that naphthalene shows a greater pulse height increase than anthracene as the temperature is lowered.

Alkali halide and anthracene counters have been compared. The alkali halides give larger pulses than anthracene, but the duration of the light flashes (and therefore the resolving time) is longer.

Extensive studies of the mechanism of Geiger counter discharge indicate that electron collection plays an important role in the discharge when the counter voltage is well above threshold.

Physics of Solids - The release of radioactive gas from irradiated Al-U alloys at temperatures between 200° C and 500°C has been measured. It appears that Kr<sup>85</sup> (half life 9.8 days) is released at a maximum rate at 250°C. This observation is of importance in estimating the inherent safety of a plate type reactor which has lost its water.

A refined calculation of the rate of energy loss from recoil C atoms shows that the amount of energy used up in damaging the lattice depends only weakly on the energy of the C recoil. This means that the number of collisions of fast neutrons per c.c., rather than the energy transfer per c.c. is a more relevant measure of the damage produced in the lattice.

Equipment for making Hall effect measurements on irradiated semi-conductors has been set up.

██████████

SECTION I - NEUTRON PHYSICS

A. H. Snell, Section Chief  
S. Bernstein, Associate Section Chief

Neutron Decay Experiment - (Snell, Bernstein) . Efforts have been continued in looking for coincidences between the expected products of neutron decay, viz; beta particles counted in a thin-window Geiger counter, and protons accelerated and focused upon a secondary electron multiplier. The situation at present may be summarized by saying that we get repeating positive effects, but they are much smaller than would be expected from the individual proton counting rate.

This may be illustrated as follows:

In a typical run, there were 593 cpm of foil-sensitive counts in the multiplier. The efficiency of the counter for registering betas from the position of the decaying neutrons had been separately evaluated as 0.004. Therefore, if all of the 593 foil-sensitive counts in the multiplier really were caused by protons from the decaying neutrons, there should be  $593 \times 0.004 = 2.4$  genuine coincidences observed per minute. Actually, we observe at most about 1/10 of this amount. The problem at the moment is to see whether this discrepancy is instrumental in origin, or whether it means that the neutron half-life is longer than would be expected from the multiplier single counting rates alone.

Photoneutron Yields - (Snell). Some old (1945) experimental data on photoneutron yields have been re-evaluated and corrected for effects such as the absorption of the gamma rays in the D<sub>2</sub>O and Be spheres surrounding the radioactive sources. The results stand as follows:

| Photoneutron Source                 | Standard Yield   |
|-------------------------------------|--|
| Na <sup>24</sup> - Be               | 14.1x10 <sup>4</sup> neutrons per sec<br>per gram of target<br>material at 1 cm. |
| Na <sup>24</sup> - D <sub>2</sub> O | 27.0   |
| Ga <sup>72</sup> - Be               | 4.5  |
| Ga <sup>72</sup> - D <sub>2</sub> O | 5.3  |

The Ga<sup>72</sup> data are not uniquely interpretable in terms of photo-dissociation cross sections because of the complexity of the decay scheme. The Na<sup>24</sup> results are directly interpretable, and lead to the following results for the photo-dissociation cross section for 2.76 Mev gamma rays:

$$\sigma_{\text{Be}} = 7.1 \times 10^{-28} \text{ cm}^2$$

$$\sigma_{\text{D}} = 15.1 \times 10^{-28} \text{ cm}^2$$

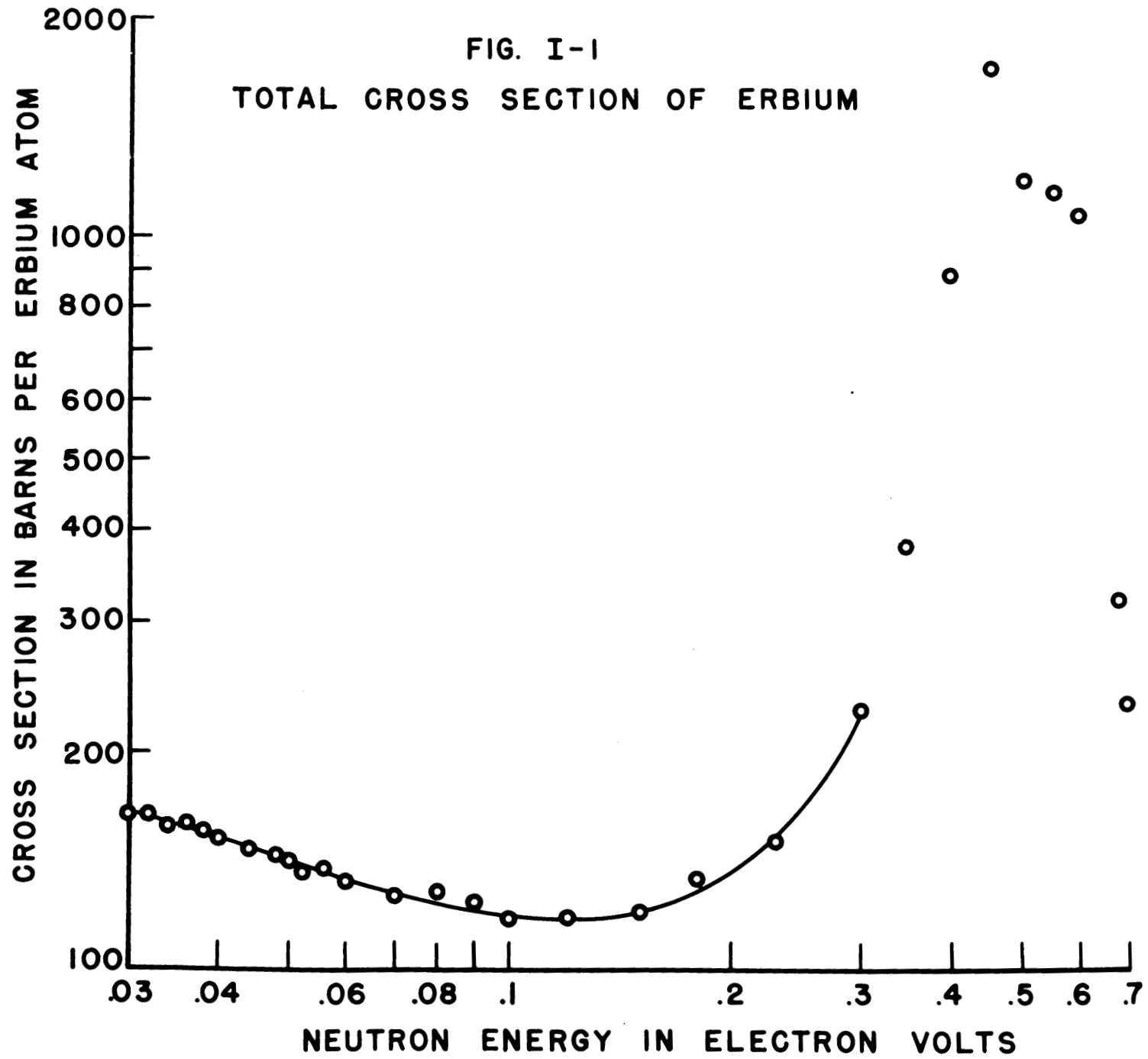
It is thought that in absolute magnitude these are correct within about 12%.

Possible Neutron Absorption Resonance in Erbium - (Stanford, Stephenson). The neutron cross-section of erbium was measured from .03 ev to 0.7 ev with the bent quartz crystal spectrometer. The sample used consisted of very pure Er<sub>2</sub>O<sub>3</sub>. According to reports of members of the Chemistry Division spectroscopic and activation measurements showed that it contained less than 0.01% by weight of other rare earths. It contained also 2.2% by weight of water. Several samples were used, the largest sample consisting of 54 mg of Er<sub>2</sub>O<sub>3</sub> in a capillary tube of 2 mm inside diameter.

The accompanying curve, Figure I-1, shows the total cross-section in barns per erbium atom as a function of neutron energy in ev. A resonance was found in the neighborhood of 0.5 ev having a

Dr 6150

FIG. I-1  
TOTAL CROSS SECTION OF ERBIUM



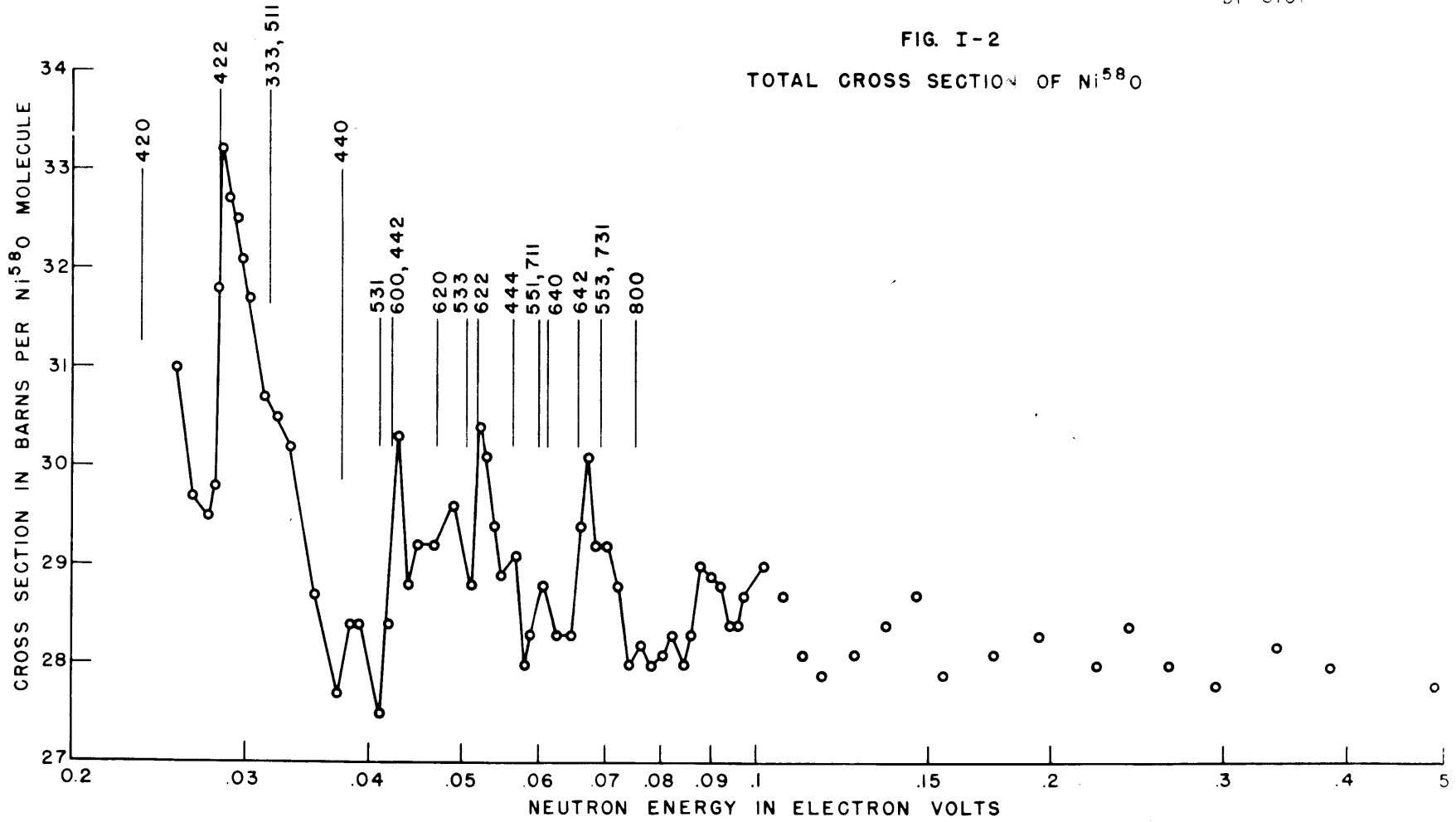
SECRET

maximum value of at least 1700 barns. The exact position of the peak and the maximum value of the cross-section cannot be given with any great accuracy, since the instrument has been set up for special work at lower energies. The shape of the curve seems to suggest also that there is a possibility that the hump in the cross-section at about 0.5 ev may consist of more than one resonance, the resolving power of the instrument being not great enough to prove or disprove this possibility. It should be pointed out that Sturm, et al (Reviews of Modern Physics 19, 288 (1947)) find a resonance in europium at about 0.45 ev with a peak cross-section of about 6000 barns. However, the chemists contend that the presence of a significant amount of Eu in our sample is extremely unlikely. From the curve, it can be seen that the cross-section per erbium atom at .03 ev is 165 barns.

Total Cross-Section of Ni<sup>58</sup>O - (Stanford, Stephenson, Bernstein, Shapiro, Dial). Measurements were taken of the transmission of a sample of Ni<sup>58</sup>O from about 0.03 ev to 0.5 ev. The results are shown in Figure I-2, in which the total cross-section per molecule of Ni<sup>58</sup>O is given as a function of neutron energy. As can be seen from the graph, crystalline diffraction effects are very distinct. The fact that such large crystalline effects persist in this case at such high energy values, or for such small grating-space values, indicates at once that Ni<sup>58</sup> is the nickel isotope which is responsible for the anomalously high scattering cross-section for normal nickel, as has been previously shown by Shull and Wollan. The Miller indices responsible for the various peaks are indicated at the appropriate energy values on the graph. Since the crystal structure of nickel oxide is the same type as NaCl, the fact that the (422) discontinuity is much larger than the (333,511) discontinuity proves that the phase of scattering from Ni<sup>58</sup> is of the same sign as the phase of scattering from oxygen. The value of coherent scattering cross-section of the bound Ni<sup>58</sup> nucleus has been calculated from the height of the 422 discontinuity and found to be 26. barns.

SECRET

FIG. I-2  
TOTAL CROSS SECTION OF Ni<sup>58</sup>O



~~SECRET~~

This value was obtained from the expression

$$\sigma_{hkl} = \frac{\lambda^2 M}{2} [j_{hkl}] [d_{hkl}] [F_{hkl}^2]$$

molecule

in which  $\sigma_{hkl}$  = height of the discontinuity of the cross-section of the bound nucleus due to reflection from the plane hkl.

$\lambda$  = wave length of the neutrons

$M$  = number of molecules per  $\text{cm}^3$

$j_{hkl}$  = multiplicity of the planes hkl

$d_{hkl}$  = grating-space of the planes hkl

$F_{hkl}$  = crystal structure factor per molecule.

In calculating the crystal structure factor the value obtained by Shull, Wollan and Marney of 4.15 barns for the scattering cross-section per bound nucleus of oxygen was used.

The value of 26 barns corresponds to a scattering cross-section for the free nucleus of about 25 barns. This value of 25 barns agrees quite well with the value 24.3 barns obtained by using the average value of 28 barns given by the data in the region from about 0.2 ev to 0.5 ev, where crystalline and molecular binding effects should be small, and subtracting from it the value 3.68 b obtained by Shull, Wollan and Marney for the free nuclear scattering cross-section of oxygen. The value 26 barns for the coherent scattering cross-section of  $\text{Ni}^{58}$  agrees also with the value of 27 barns obtained by Shull, Wollan and Marney from their powder diffraction studies, recorded elsewhere in this report. The general features of the curve, in addition to the 422, and 333 reflections, agree also with preliminary calculations of the energies at which the discontinuities should appear and of the magnitude of these discontinuities.

██████████

SECTION III - NEUTRON AND NUCLEAR PHYSICS

E. O. Wollan, Section Chief  
C. G. Shull, Associate Section Chief

Neutron Diffraction Studies - (C. G. Shull, E. O. Wollan, M. C. Marney).

Scattering Cross Section and Phase Scattering for Ni<sup>58</sup> and Ni<sup>60</sup>.

Various scattering cross section determinations for Ni have indicated a much larger scattering than suggested by simple potential scattering. Normal nickel contains two major isotopes, Ni<sup>58</sup> (68.0%) and Ni<sup>60</sup> (27.2%), along with the minor isotopes Ni<sup>61</sup>, Ni<sup>62</sup> and Ni<sup>64</sup>. In attempting to assign the anomalous scattering cross section to a particular isotope, samples of Ni<sup>58</sup>O and Ni<sup>60</sup>O were obtained from the Isotopes Production Division at Y-12 and were examined in the neutron diffraction spectrometer.

Figure III-1 shows the diffraction patterns obtained for the three nickel oxide preparations consisting of Ni<sup>58</sup>, Ni<sup>60</sup> and normal Ni. The experimental data for the three samples have been corrected for specimen weight, absorption, etc. so that the patterns are directly comparable. Since nickel oxide crystallizes in the NaCl-type face centered cubic structure, a comparison of the (111) and (200) intensities permits a direct determination of the phase of scattering of the nickel isotopes. It is seen in Figure III-1 that the (200) reflection is stronger than the (111) reflection for all three specimen and hence it follows that Ni<sup>58</sup> and Ni<sup>60</sup> and elemental Ni scatter neutrons with positive phase, the same as does oxygen. It is also seen that the patterns differ markedly in intensity, signifying that the scattering cross sections are widely different. From the measured intensities of the diffraction peaks, the coherent scattering cross sections for Ni<sup>58</sup>, Ni<sup>60</sup> and elemental Ni have been determined as 27, 2 and 14 barns respectively. Since potential scattering ( $4\pi R^2$ ) according to the physical size of these nuclei should contribute a scattering cross section of only about 5.7 barns, it is seen that the anomalously high scattering for

██████████

Dr. No. 5889

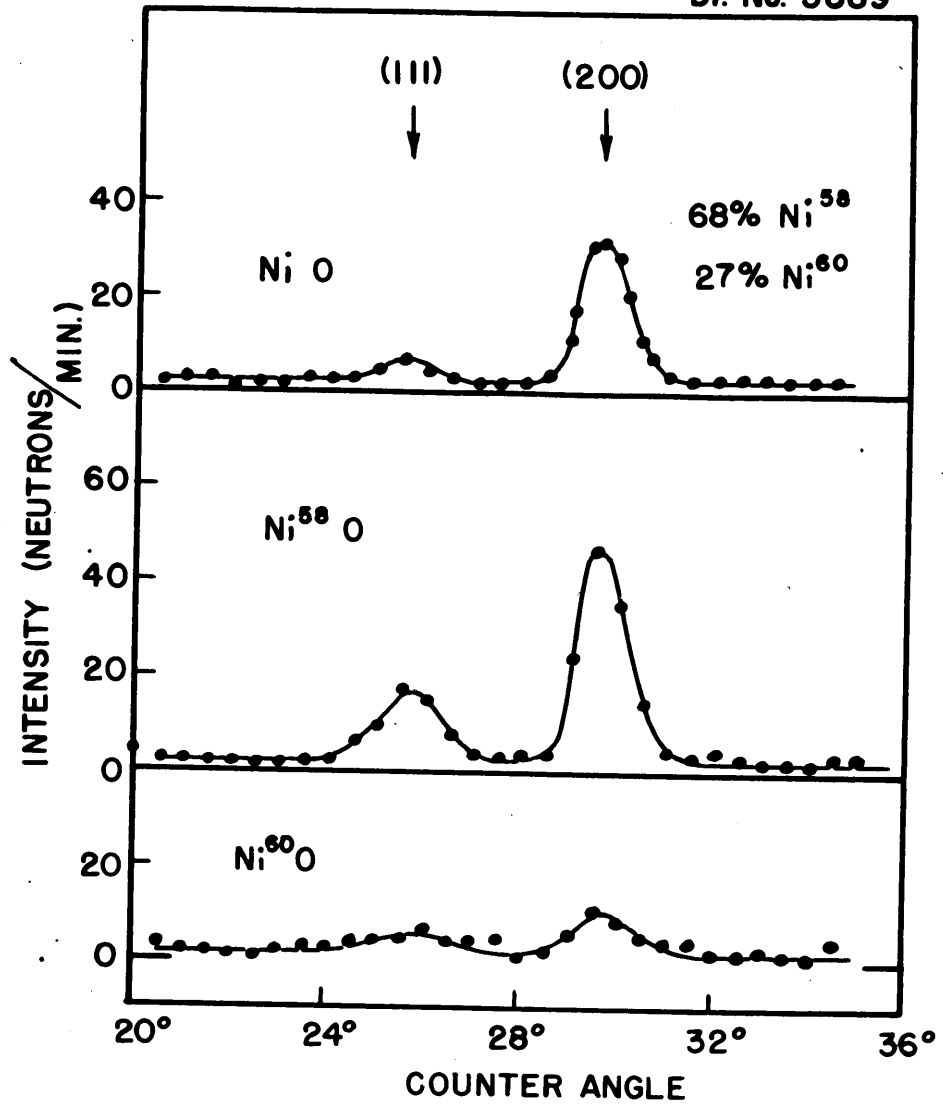


FIG. III-1

SECRET

nickel is caused by the  $\text{Ni}^{58}$  isotope in spite of the fact that the scattering by  $\text{Ni}^{60}$  is lower than the expected potential scattering.

Both  $\text{Ni}^{58}$  and  $\text{Ni}^{60}$  are even-even nuclei with presumably zero spin and hence their coherent scattering cross sections should be the same as their total scattering cross sections. From transmission measurements on the nickel oxide samples, the total scattering cross sections for  $\text{Ni}^{58}$ ,  $\text{Ni}^{60}$  and elemental Ni were determined as 25, 3 and 17 barns respectively, as shown in Table 1.

Table 1 - Scattering Cross Sections for Isotopic and Elemental Nickel Samples

|                  | Coherent Scattering<br>Cross Section | Total Scattering<br>Cross Section |
|------------------|--------------------------------------|-----------------------------------|
| $\text{Ni}^{58}$ | 27 barns                             | 25 barns                          |
| $\text{Ni}^{60}$ | 2                                    | 3*                                |
| Ni element       | 14                                   | 17                                |

\* Not corrected for residual water content in sample

The agreement between the two cross section values of  $\text{Ni}^{58}$  is satisfactorily within experimental error while the presence of uncorrected residual water in the  $\text{Ni}^{60}$  sample makes the total scattering larger than the coherent scattering. It would not be expected that the total and coherent scattering for elemental Ni should be the same because of isotopic incoherence. A calculation of the incoherent scattering to be expected for Ni using the above coherent scattering cross sections for the isotopes leads to a value of 2.7 barns and this added to the coherent scattering agrees satisfactorily with the total scattering cross section for elemental Ni.

The large value for the scattering cross section of  $\text{Ni}^{58}$  coupled with the fact that this nucleus scatters with positive phase suggests on the Feshbach-Peaslee-Weisskopf picture the presence of a scattering resonance at a nearby virtual energy. On the other

hand, the smaller-than-expected scattering cross section for Ni<sup>60</sup> along with its positive phase of scattering suggests the presence of a nearby resonance at a higher-than-thermal energy. Havens, et al have reported evidence for a resonance at several hundred volts energy and this presumably is to be associated with the Ni<sup>60</sup> nucleus.

Scattering Data for Miscellaneous Elements. A number of elements and compounds were examined in the past period with the neutron diffraction spectrometer in continuation of the survey of the scattering properties of various elements and isotopes. The materials studied included ZrC, ZrN, Th, ThO<sub>2</sub>, RbCl and SrO. From the pattern intensities, the coherent scattering cross sections and phases of scattering have been determined and these are listed in Table 2.

Table 2 - Scattering Data for Miscellaneous Elements

| Element | Material Studied     | Phase of Scattering Amplitude | Scattering Cross Sections |       |
|---------|----------------------|-------------------------------|---------------------------|-------|
|         |                      |                               | Coherent                  | Total |
| Zr      | ZrC, ZrN             | Positive                      | 4.9 barns                 | 8*    |
| N       | ZrN                  | "                             | 4.6                       | ~ 6*  |
| Th      | Th, ThO <sub>2</sub> | "                             | 11                        | 12*   |
| Rb      | RbCl                 | "                             | 5.3                       | 12**  |
| Sr      | SrO                  | "                             | --                        | 9.5** |

\*From transmission measurements at 0.07 e.v.

\*\*Thermal scattering cross sections

All of these elements are seen to scatter with positive phase. The coherent scattering for Zr and Rb appears to be considerably smaller than the total scattering and this indicates the presence of a considerable isotopic incoherence in the overall scattering. On the other hand, Th (being monoisotopic with a zero spin)

██████████

shows no significant difference in the two cross sections as is to be expected for nuclei with these properties. The data for N are somewhat uncertain but taken as such, they indicate the presence of spin dependent scattering for nitrogen because of the lower value for coherent scattering than for total scattering. Since nitrogen is practically monoisotopic, such a comparison is indicative of spin incoherence. The diffraction pattern for SrO has not been analyzed quantitatively as yet because of the presence of unidentified impurity.

Stopping of Fission Fragments in Gases - (E. C. Campbell, W. M. Good, W. A. Strauser). Results on the ranges of the fission fragments emitting delayed neutrons have already been reported for air, helium and argon in ORNL-51, p. 79. The study has been extended to hydrogen and deuterium. Experimental curves of the measured delayed neutron activity as a function of gas pressure in the rabbit are shown in Figures III-2 and III-3. Table 3 summarizes the data so far obtained for U<sup>235</sup> fragments in all gases. Here R<sub>0</sub> is the gas pressure in cm. Hg corresponding to a mean range equal to the length of the rabbit (5.06 cm.) and 2s is the width of the stepwise fall-off of the experimental curves. The relative straggling is then S/R<sub>0</sub>. A correction has been applied to both to compensate for the effect of the thickness of the U<sup>235</sup> source (0.3 mg/cm<sup>2</sup>)

TABLE 3

|           | <u>22 second activity</u> |     |                  | <u>55 second activity</u> |     |                  |
|-----------|---------------------------|-----|------------------|---------------------------|-----|------------------|
|           | R <sub>0</sub>            | S   | S/R <sub>0</sub> | R <sub>0</sub>            | S   | S/R <sub>0</sub> |
| Hydrogen  | 113.3                     | 2.5 | .022             | 139.5                     | 3.6 | .025             |
| Deuterium | 119.3                     | 4.3 | .03              | 144.3                     | 5.2 | .035             |
| Helium    | 174                       | 5.9 | .03              | 221                       | 7.5 | .03              |
| Air       | 27.8                      | 2.2 | .08              | 38.0                      | 2.1 | .05              |
| Argon     | 28.2                      | 2.6 | .09              | 40.3                      | 2.8 | .07              |

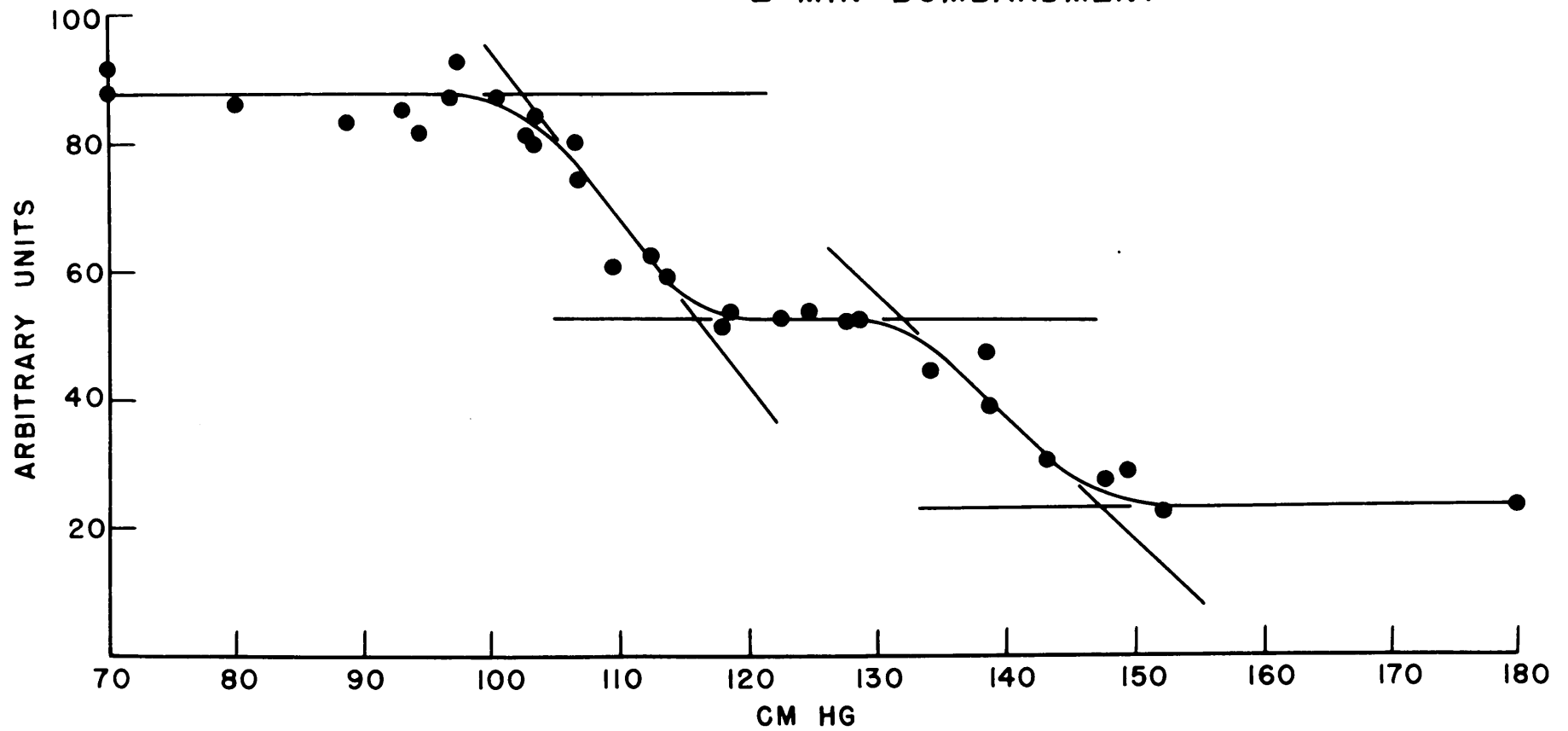
No correction has been made for the "instrument straggling" due to the finite size of source and detector discs. This effect could give a value of S/R<sub>0</sub> not greater than .025 and is the same for all runs. The fact that the observed value of S/R<sub>0</sub> increases with mass

Dr 6164

FIG. III-2

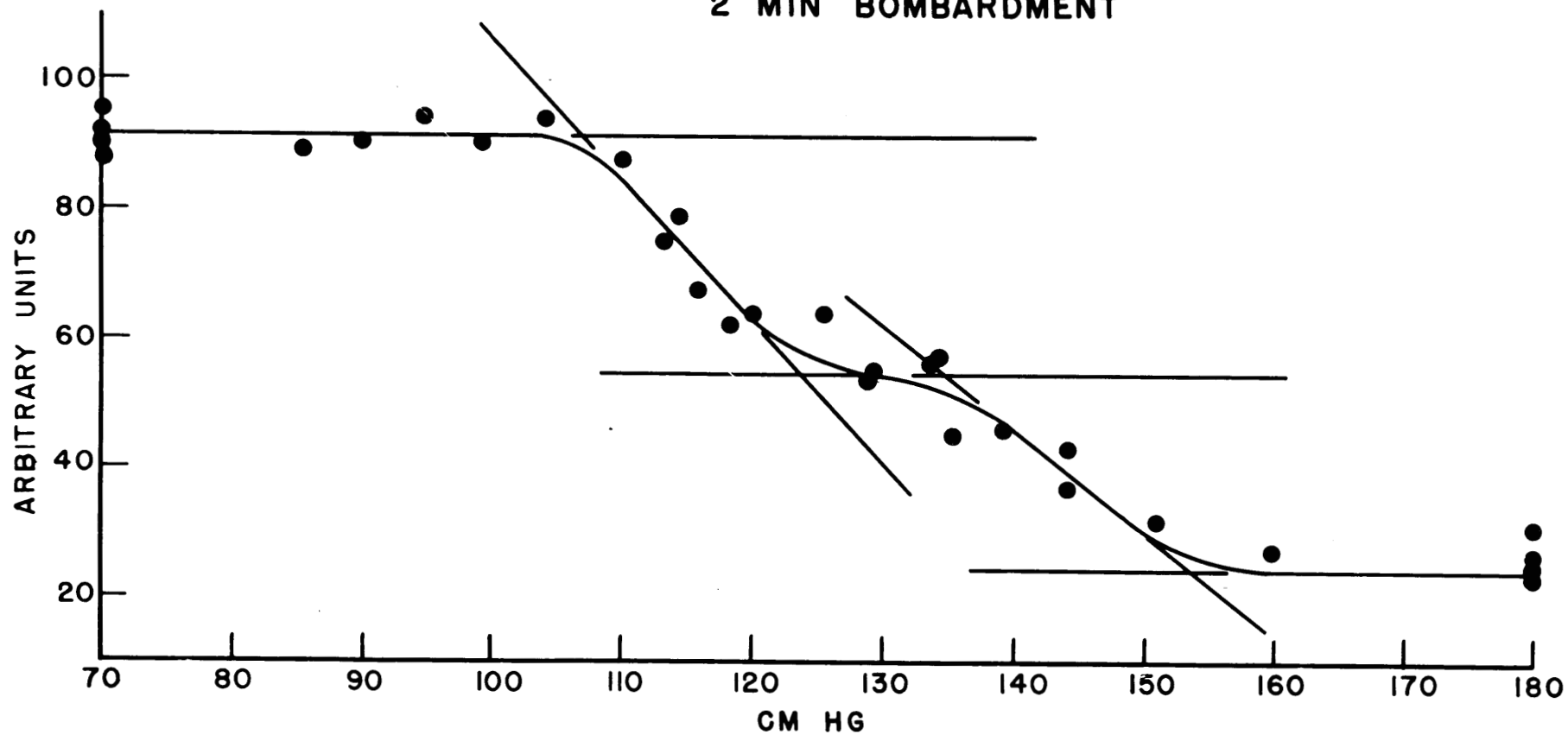
U<sup>235</sup> IN HYDROGEN  
2 MIN BOMBARDMENT

NOT CLASSIFIED



NOT CLASSIFIED

FIG. III-3  
U<sup>235</sup> IN DEUTERIUM  
2 MIN BOMBARDMENT



██████████

number of the stopping gas is a new experimental result, in agreement with the prediction of Bohn, which shows up clearly the importance of nuclear stopping. The importance of nuclear stopping is further shown in the relatively shorter range of fission fragments in hydrogen as compared with the range in deuterium, although the electronic stopping of these gases is the same. The difference is due entirely to the influence of the nuclear collisions; in a collision with a hydrogen nucleus twice as much energy is lost by the fission fragment as in a similar collision with a deuterium nucleus.

Capture Gamma Rays from Chlorine - (C. D. Moak and J. W. T. Dabbs). A number of improvements have been made in the cloud chamber equipment. These include a more intense beam (factor of about 5, obtained by enlarging the hole in the stringer), better shielding, a target changer, and a data board which is photographed with the chamber. The ratio of Cl pairs to background pairs has not been determined, but is estimated to be greater than 10, by counting all tracks from the Pb foil in the chamber, and by counter measurements in the chamber position. The target changer allows the taking of a cyclic series of three pictures, two of which are backgrounds, and keeps the targets in the beam about one second, thus preventing the build-up of residual activity in the aluminum cells which contain  $\text{CCl}_4$ . One background picture is obtained with only the fast neutrons of the beam falling on a  $\text{CCl}_4$  cell; the slow neutrons are stopped by a Boron plastic beam shutter. The other background is obtained with full beam and a graphite "equivalent scatterer" target, which scatters as many neutrons as the  $\text{CCl}_4$ , and thus produces as many background gamma rays in the surrounding materials as the  $\text{CCl}_4$ . The data board gives time, date, magnet current, frame number, and has a "pile on" light, as well as a "background" light. Runs on Cl are in progress, having been delayed somewhat by two successive shorts to ground in the Helmholtz coils.

██████████

Pile Oscillator - (H. S. Pomerance). The atomic absorption cross section for thermal neutrons has been measured for several more separated isotopes prepared at Y-12. The results of these experiments are shown in Table 4.

TABLE 4.

|                  |         |   |
|------------------|---------|---|
| Cr <sup>52</sup> | < 0.6 b | Chemical impurities prevent a better value. Using the activation values for Cr <sup>50</sup> and Cr <sup>54</sup> and $\sigma_a$ for normal chromium, there remains about 15-20b for Cr <sup>53</sup> . |
| Cu <sup>63</sup> | 4.3 b   | The isotope values add to 3.6 b for normal Cu.  |
| Cu <sup>65</sup> | 2.1 b   |   |
| Cu               | 3.6 b   |   |
| Ni <sup>58</sup> | 4.3 b   | Supersede the values reported in MonP-368 (1947).   |
| Ni <sup>60</sup> | 2.7 b   | The isotope values add to 4.19 for normal Ni.   |
| Ni <sup>61</sup> | 1.8 b   |   |
| Ni <sup>62</sup> | 14.8 b  |   |
| Ni               | 4.2 b   |   |
| U <sup>238</sup> | 2.86 b  | No impurity could be found in the depleted sample $\left( \frac{25}{28} < \frac{1}{20,000} \right)$ to account for this high value. The accepted value is 2.6 b.  |

Several measurements of natural elements have been made, the results which are shown in Table 5.

TABLE 5.

|    |        |  |
|----|--------|--|
| Mg | 0.06 b | Dow distilled, and a 3% Al alloy, were used. After allowing for the boron impurity, cf ORNL 51 |
| Si | 0.11 b |  |
| Y  | 1.4 b  |  |
| V  | 4.5 b  |  |
| Ru | 2.5 b  |  |
| I  | 6.1 b  |  |

Some service measurements of Ames thorium metal, beryllium metal, and brazed aluminum joints were made for the Technical Division.

Slowing Down Distribution from a Point Source of Fission Neutrons to Indium Resonance Energy in Water - (J. E. Hill, L. D. Roberts, T. E. Fitch, G. McCarmon). In the last two quarterly reports the distribution in water of indium resonance neutrons originating at a point fission source was given in the range of distances from the source  $0 \leq R \leq 92$  cm. The moments of this distribution were not given then for it was known that the indium foils would be activated to some extent by neutrons of energies above 1.44 ev. To correct for this activation by epi-1.44 neutrons, measurements were made using  $B^{10}$  covered foils. In the range 2.28 cm.  $\leq R \leq 7.54$  cm, a disk source 5.08 cm. in diameter and 2.0 mm. thick placed 10 cm. from the bottom of the tank was used. In the range 7.54 cm.  $\leq R \leq 17.60$  cm. this same source was used but was at the bottom of the tank. In the range 17.60 cm.  $\leq R \leq 35$  cm. a source 2.0 mm. thick by 10 cm. square placed on the bottom of the tank was used. Between 2.28 cm. and 17.60 cm. indium detection foils 1 cm square by  $\sim 1.10$  g/cm<sup>2</sup> and covered with 0.337 g/cm<sup>2</sup> of B (90%  $B^{10}$ ) were used, and between 17.60 cm.  $\leq R \leq 35.59$  cm. large indium foils 4 cm x 6.35 cm x  $\sim 0.10$  g/cm<sup>2</sup> of B (90%  $B^{10}$ ) were used. The foils were of the same thickness to within one percent. The amount of boron used was sufficient to essentially completely remove neutrons in the energy range below 10 ev. In the following table, this distribution is given, normalized to the same neutron source strength as the Cd covered data of the distribution to be corrected.

TABLE 6

Curve of  $A_S$  vs. R. for Indium Covered with Boron

| R(cm) | $A_S$ (counts/min) | R(cm) | $A_S$ (counts/min) |
|-------|--------------------|-------|--------------------|
| 2.28  | 399.7              | 10.93 | 27.1               |
| 2.37  | 397.1              | 11.35 | 22.4               |
| 3.65  | 377.3              | 17.60 | 4.56               |
| 3.78  | 303.6              | 19.56 | 3.42               |
| 4.43  | 210.2              | 24.64 | 0.412              |
| 5.29  | 129.4              | 27.17 | 0.357              |
| 6.73  | 98.7               | 29.71 | 0.292              |
| 8.24  | 44.9               | 32.25 | 0.141              |
| 10.23 | 36.3               | 35.59 | 0.0592             |

██████████

In the accompanying graph, Figure III-4, of  $\log_{10} A_S R^2$  vs. R, it is seen that the Boron covered curve is about 3% of the Cd covered curve, and more important, the two curves are almost proportional to each other. This means that the second moment,  $R^2$ , and also the higher moments, will be almost the same for the two curves (within ~ 10%). Because of this small magnitude of the Boron covered indium foil activity and because of the proportionality of the two curves, the correct moments for a 1.44 ev. detection energy will be obtained within a minute error from the Cd covered indium distribution without a correction for a contribution by higher neutron energies. To calculate these moments, the experimental data were extrapolated from 92 cm. to infinity using the function

$$A_S = k \frac{e^{-R/\lambda}}{R^2}, \lambda = 8.786 \text{ cm. and } k = 1.324 \times 10^5$$

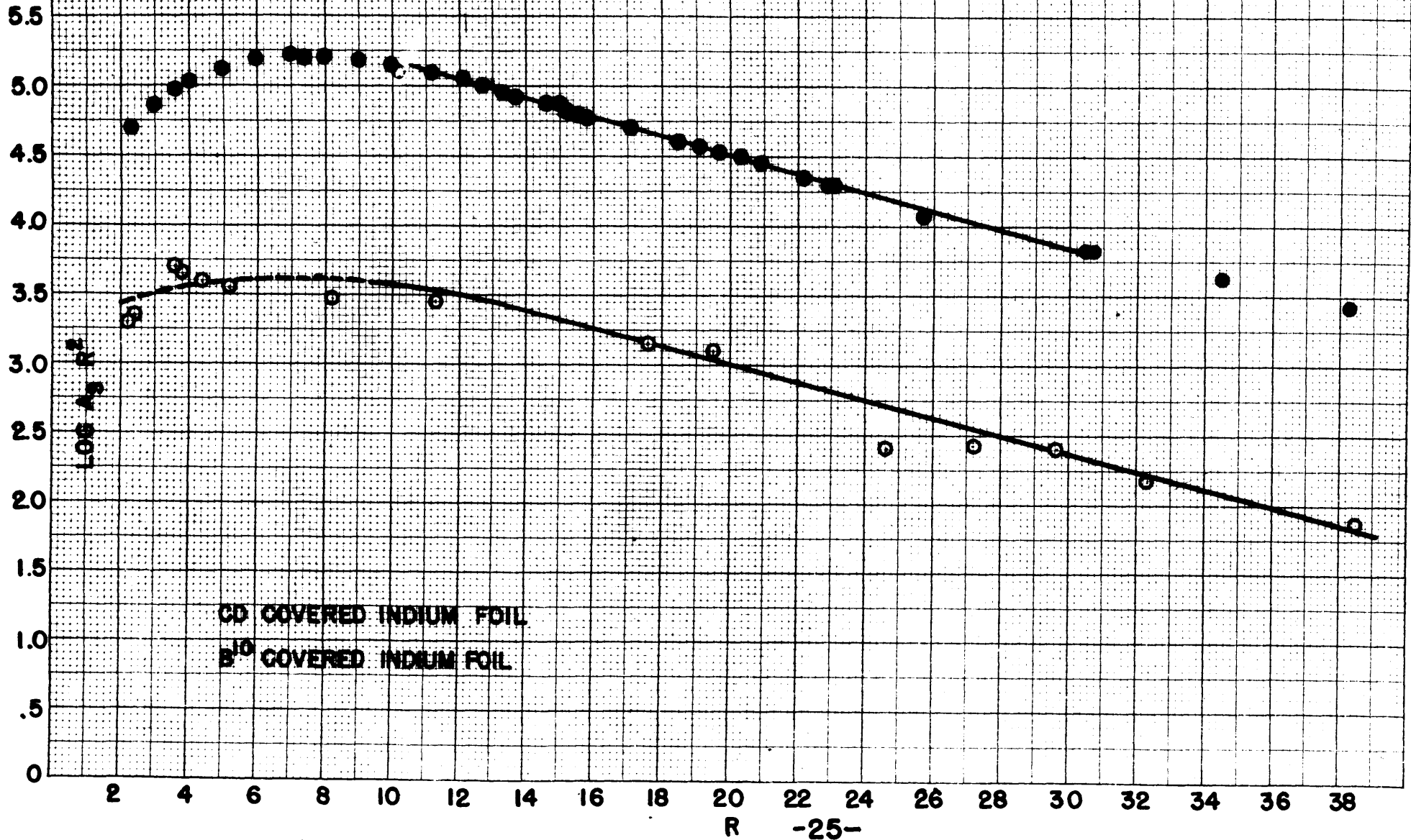
which were the values obtained from the experimental data near 92 cm.

TABLE 7 - The Moments  $\overline{R^n}$  of the Distribution of 1.44 ev. Neutrons from a Point Fission Source in Water

| n  | $I = \int_0^{\infty} A_S R^n dR$ | Fraction of I Extrapolated | Moments<br>$\overline{R^n} = \frac{\int_0^{\infty} A_S R^n dR}{\int_0^{\infty} A_S R^{n-2} dR}$ |
|----|----------------------------------|----------------------------|---|
| 2  | $2.092 \times 10^6$              | $1.40 \times 10^{-5}$      | $R^2 = 184.7 \text{ cm}^2$  |
| 4  | $3.863 \times 10^8$              | $7.95 \times 10^{-4}$      | $R^4 = 1.222 \times 10^5 \text{ cm}^4$  |
| 6  | $2.556 \times 10^{11}$           | 0.0130                     | $R^6 = 2.270 \times 10^8 \text{ cm}^6$  |
| 8  | $4.375 \times 10^{14}$           | 0.0857                     | $R^8 = 8.642 \times 10^{11} \text{ cm}^8$   |
| 10 | $1.357 \times 10^{18}$           | 0.333                      |   |

Dr 6166

FIG. 11) - 4



██████████

Age of Neutrons to In Resonance from a Point Fission Source in a Mixture of Al + H<sub>2</sub>O 1:1 by Volume - (J. E. Hill, L.D. Roberts, T. E. Fitch, and G. McCammon). A tank 5' x 5' x 6' high resting on the X-10 pile thermal column was filled first with 2-S aluminum plates 1/4" thick and spaced 1/4", and next with water. Care was taken to insure that air was completely removed. This gives an aluminum-water mixture 1:1 by volume. The plates were stacked parallel to the bottom of the tank and in such a way that a string of foils could be inserted and removed along the central vertical axis of the tank. In all of the measurements reported below, indium foils 4 cm. x 6.35 cm. x ~ 0.10 g/cm<sup>2</sup> thick were used. They were of the same thickness to within one percent. The foils were enclosed in Cd boxes with a wall 0.320 cm. thick. The fission source was of uranium 235-aluminum alloy of eutectic composition cut in the form of a disk 5.08 cm. in diameter, and 2 mm. thick. This source is one which was previously used in the "age in water" measurements.

In the range of distances from the source  $3.31 \text{ cm} \leq R \leq 26.35 \text{ cm}$ , the source was ~ 20 cm. from the bottom of the tank. For the range  $26.35 \text{ cm.} \leq R \leq 52.69 \text{ cm.}$  the source was on the bottom of the tank. This selection of source positions was based on measurements of age in H<sub>2</sub>O and are such that the measured neutron distribution corresponds to that for a point source in an infinite Al-H<sub>2</sub>O medium. The distribution as measured to date is given below.

| R (cm) | A <sub>S</sub> (c/m)    | R (cm) | A <sub>S</sub> (c/m)    |
|--------|-------------------------|--------|-------------------------|
| 3.31   | 1.522 x 10 <sup>6</sup> | 26.39  | 6.428 x 10 <sup>4</sup> |
| 6.85   | 1.228 x 10 <sup>6</sup> | 30.19  | 3.692 x 10 <sup>4</sup> |
| 10.99  | 7.662 x 10 <sup>5</sup> | 34.39  | 1.638 x 10 <sup>4</sup> |
| 14.45  | 4.748 x 10 <sup>5</sup> | 37.69  | 9.601 x 10 <sup>3</sup> |
| 18.67  | 2.538 x 10 <sup>5</sup> | 41.89  | 4.795 x 10 <sup>3</sup> |
| 22.10  | 1.428 x 10 <sup>5</sup> | 45.19  | 2.822 x 10 <sup>3</sup> |
| 26.35  | 6.842 x 10 <sup>4</sup> | 49.39  | 1.495 x 10 <sup>3</sup> |
|        |                         | 52.69  | 8.259 x 10 <sup>2</sup> |

In measuring A<sub>S</sub>, the foils were counted only on the side close to the source. We will shortly obtain A<sub>S</sub> for other side of the foils and correct the above distribution suitably.

██████████

It is planned to obtain the distribution in a more detailed fashion near the source and carry the measurements out to ~ 90 cm. A preliminary calculation of  $\overline{R^2}$  from these data gives

$$\overline{R^2} = 472.8 \text{ cm}^2, \text{ or } \overline{R^2}/6 = 78.8 \text{ cm}^2.$$

This constant has been calculated by N. M. Dismuke and M. R. Arnette, MonP-219, and their value of  $\frac{\overline{R^2}}{6}$  is 70.0 cm<sup>2</sup> corresponding to

$\overline{R^2}/6 = 31 \text{ cm}^2$  for pure water. Our preliminary value is seen to be about 10% greater than the theoretical value. We prefer to reserve a discussion of this difference, however, until our experiments are completed.

██████████

SECTION IV - PHYSICAL ELECTRONICS

W. H. Jordan, Section Chief

Long Period Delayed Neutrons - (W. H. Jordan). It has already been reported (CNL-35) that observations with a fission chamber in the X-10 pile have shown that for many hours following a pile shut-down the neutron flux is many times that to be expected from spontaneous fission. This has been intensively investigated in an effort to find the source of these neutrons. It now appears that the rate of decay of the neutrons is very similar to that observed by Bernstein (CNL-38) for photoneutrons generated in beryllium by fission product gamma rays. It has been calculated and experimentally checked that the effect could be accounted for by approximately 600 gms. of Be at the pile center, which is equivalent to 1800 gms. distributed throughout the pile.

An analysis of a sample of AGOT graphite by the spectroscopic laboratory indicated no Be in amounts larger than  $3 \times 10^{-8}$  parts. This gives a maximum of 12 gm. of Be in the pile. CC-870 gives an analysis of the uranium slugs and the 25 aluminum used for canning the slugs. The Be in uranium amounts to one part in  $10^7$ . The Be concentration in Al is less than  $10^{-6}$ . This means about 15 gm of Be in the uranium and less than 1 gm in the Al. The pile is used for irradiating a great many substances, but a search through the files has failed to reveal more than a few grams of Be. On the other hand, there is the possibility that someone has put some Be in the pile without informing the operators, or that containers or structural materials containing Be have been overlooked. The fact that the decay curves are characteristic of Be (but not of  $D_2O$ ) leads one to suspect such an explanation.

~~SECRET~~

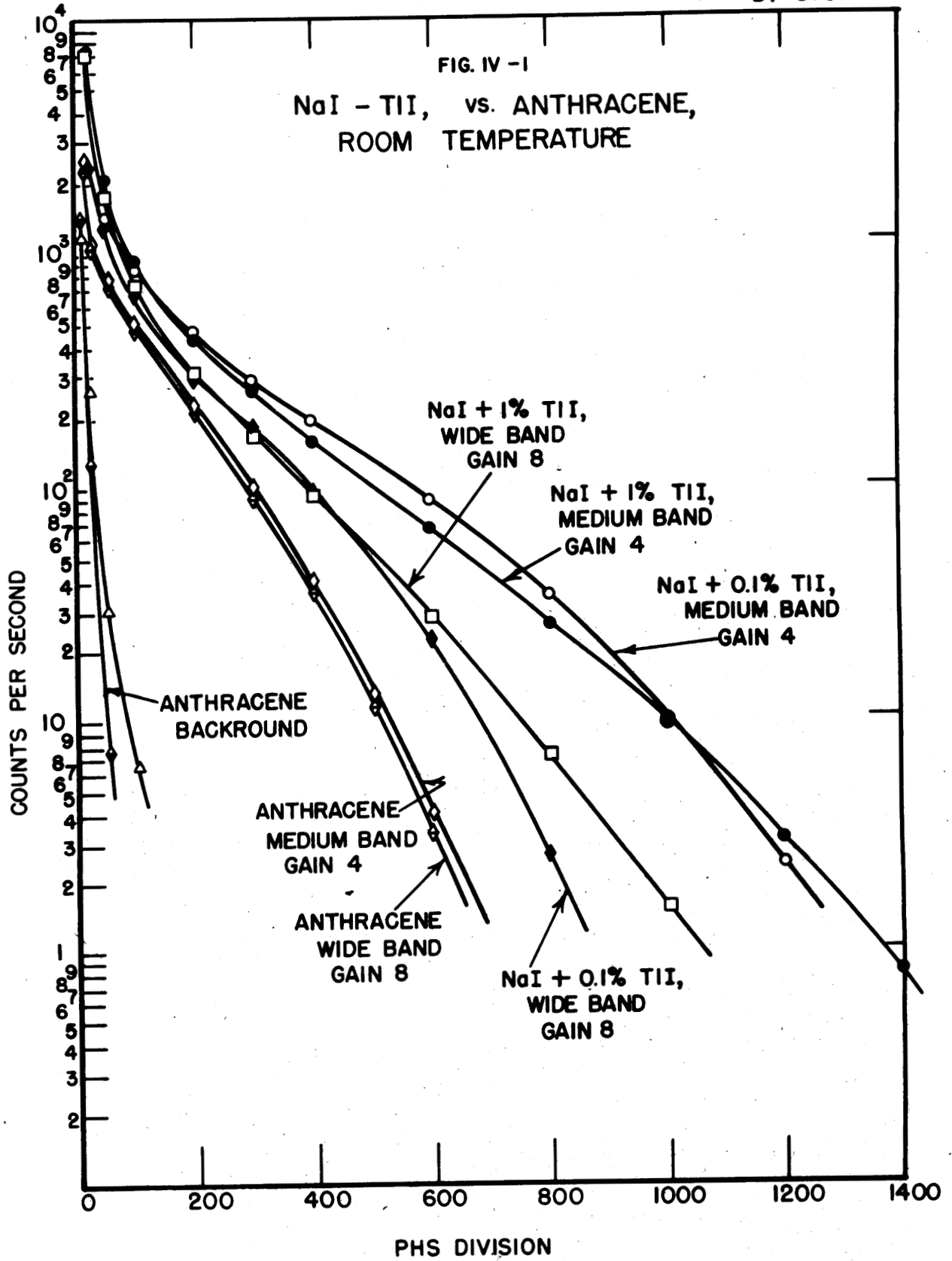
Scintillation Counters - (Bell, Davis). The scintillation work previously reported is being continued. After the report by R. Hofstadter<sup>1</sup> that certain alkali halide crystals activated with a small concentration of thallium halide function as scintillation crystals, several samples of such materials were tried. Sodium iodide was melted with various amounts of thallium iodide. The resulting semitransparent masses were found to produce moderately strong blue fluorescence under ultraviolet light. Counting pulses about twice as large as those from anthracene were obtained for  $\text{Co}^{60}$  gamma rays with the crystal at room temperature. The light flashes, however, were observed to be long. Figure IV-1 shows the results obtained using the wide band (rise time  $0.15 \mu \text{ sec}$ , fall time constant  $\sim 0.17 \mu \text{ sec}$ ) and the medium band (rise time  $0.7 \mu \text{ sec}$ , fall time  $2.0 \mu \text{ sec}$ ) of the A-1 linear amplifier. The curves have been normalized so that the pulse height for anthracene is the same on the two bands. This is justified for anthracene since the light pulse from it has been found to be very short ( $< .03 \mu \text{ sec}$ ). The pulse distribution is smaller for the NaI-TlI on the wide band than on the medium band. A direct oscilloscope examination of the pulses of the wide band showed a rise as rapid as the amplifier would allow ( $0.15 \mu \text{ sec}$ ) and an exponential fall of about  $0.5 \mu \text{ sec}$  period. The pulses were very ragged on the fall due to poor statistics produced by the limited number of photoelectrons from the 1P21 photo-cathode. A long photographic exposure integrating many pulses gave an exponential decay curve, however.

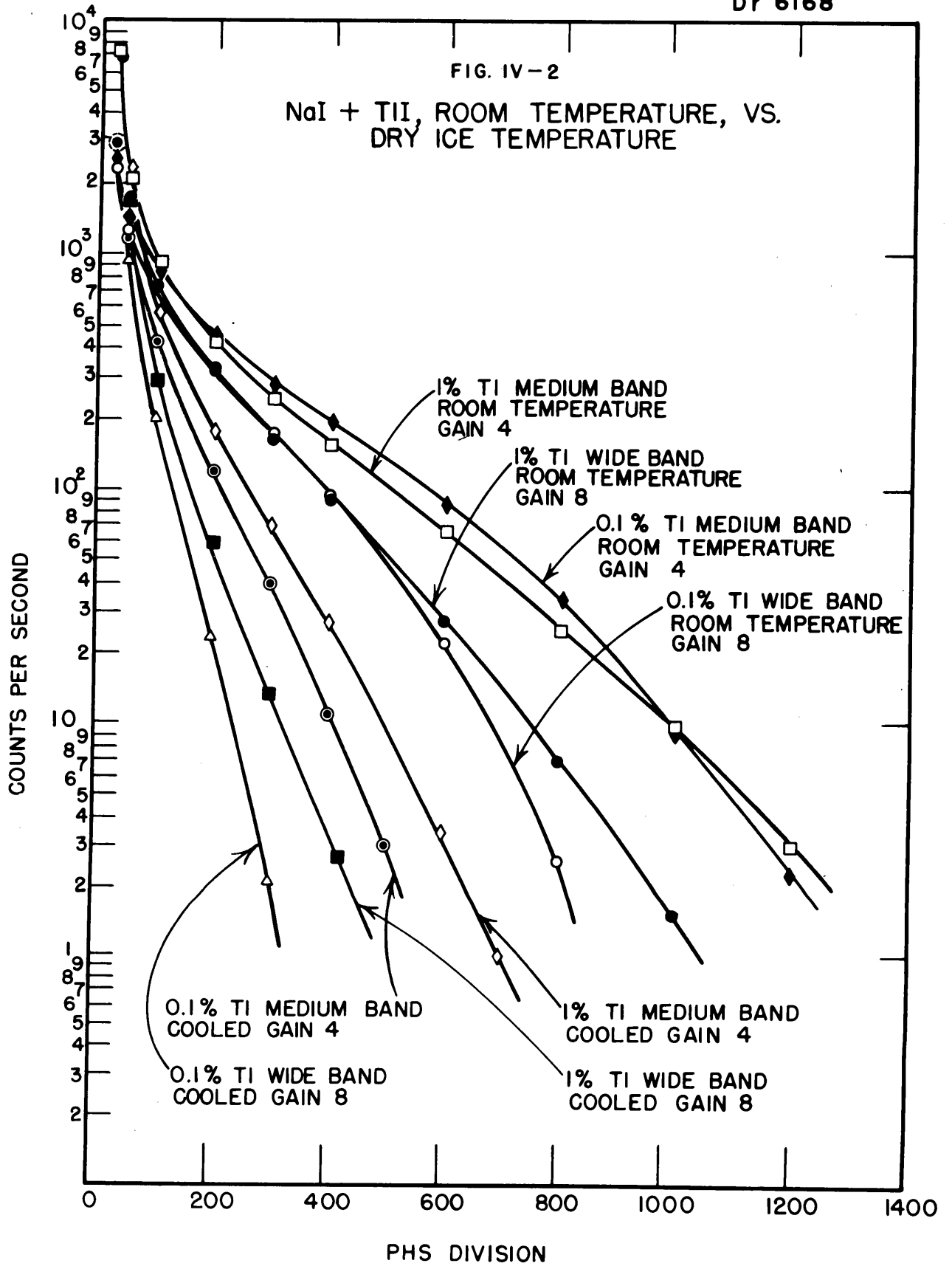
The samples were cooled to near dry ice temperature and a considerable decrease in total light output and a lengthening of the pulse was observed; pulses from anthracene, on the other hand, showed some increase in size. Figure IV-2 shows the results obtained. The data is normalized as in Figure IV-1. Note that these figures are integral plots showing the counting rate of all pulses larger than the value indicated for the pulse height.

Other samples of NaI-TlI crystals have been grown using the method of S. Kyropoulos<sup>2</sup>. This method produces large clear samples

<sup>1</sup>R. Hofstadter, Phys. Rev. **74**, 100 (1948).

<sup>2</sup>S. Kyropoulos, Zeits. f. Physik, **63**, PP. 849-854, 1930.





[REDACTED]

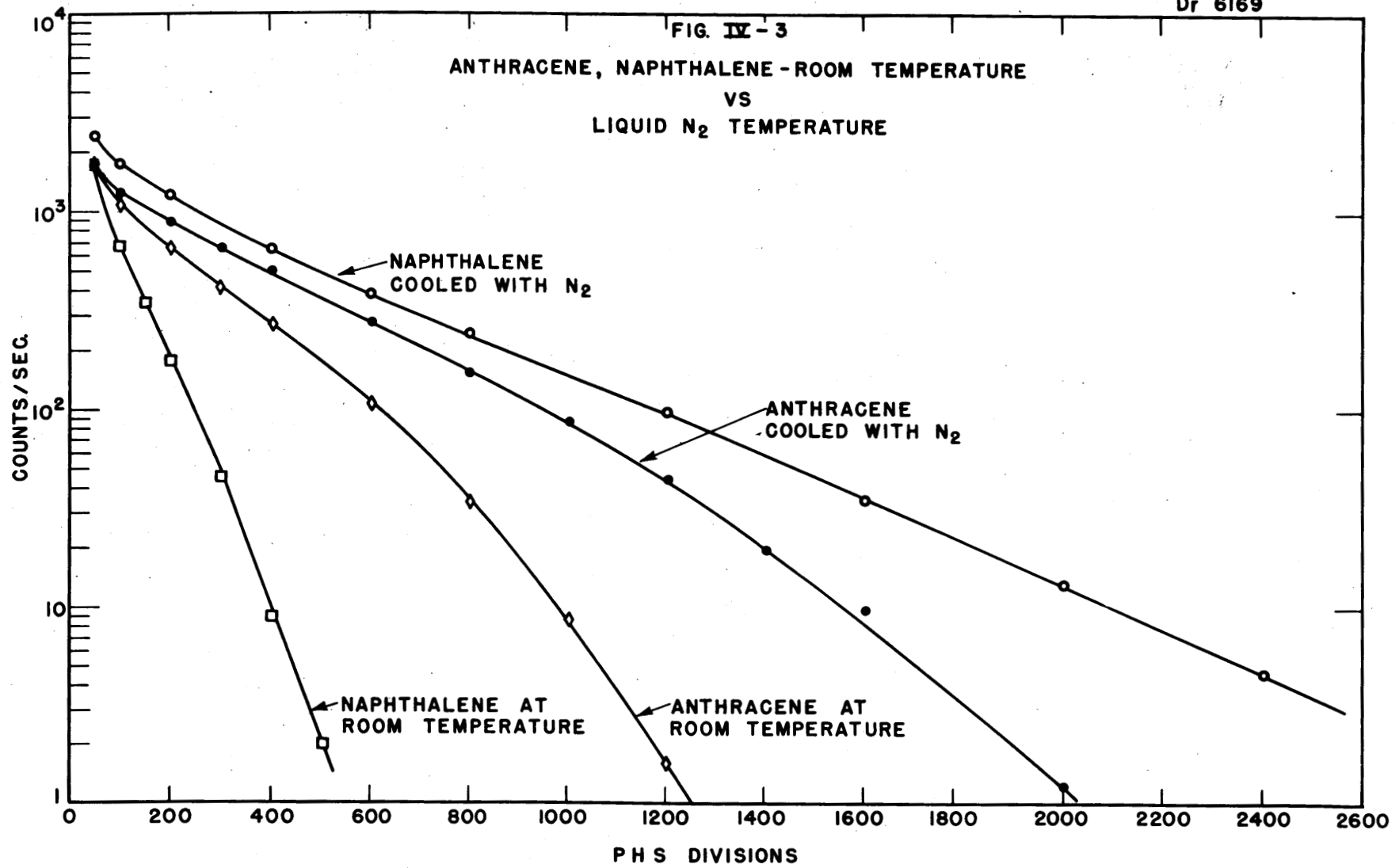
which give substantially the same results as the poly-crystalline masses first used. The material was melted in a porcelain beaker and a stainless steel tube cooled by an internal air blast was inserted in the liquid. After a small lump had grown, it was almost withdrawn from the liquid and a larger mass allowed to form on its end. It has been observed that the surface of these crystals immediately became wet on exposure to air and if then placed in a dry atmosphere show a strongly frosted surface.

We observed some months ago that the pulses from anthracene and naphthalene increased in size when cooled to dry ice temperature. Dr. Frederick Seitz felt that the experiment should be done at still lower temperature, predicting that naphthalene might well show a greater increase in pulse size on strong cooling than would anthracene. Consequently, apparatus for cooling to liquid nitrogen temperature while maintaining electrical shielding and preventing the condensation of water vapor on the insulator surfaces was prepared. The resistors needed for the photomultiplier were maintained at room temperature and only the crystal and photomultiplier were cooled. No change in the gain or efficiency of the photomultiplier was expected upon cooling. At a meeting on fast counters at the University of Rochester, Dr. Alan M. Glover of the Radio Corporation of America, reported that they found less than 2 db change in gain in photomultipliers from +80° to -180° C.

When anthracene was cooled to liquid nitrogen temperature (-196° C) the pulse size increased about 60%. The pulse duration has not yet been examined on the very fast amplifier but at least has not become as long as 0.15  $\mu$  sec. Naphthalene shows a very large increase (about 6 times) and also shows no drastic increase of light pulse duration. Figure IV-3 shows the pulse height distribution found at room temperature and liquid nitrogen temperature.

Small Radiation Instruments - (Bell, Jones). Four small radiation instruments of very simple and rugged design have been under development for about a year. The state of development of these instruments is now such as to allow their general use. One of these instruments is the pocket radiation alarm previously reported\*.

\* Physics Quarterly Report, MonP-314, and 'Pocket Radiation Alarm' by P. R. Bell, Declassified August 19, 1947.



██████████

The second of these instruments, called Raymeter #1 for lack of a better name, is intended to read radiation intensity for  $\alpha$ ,  $\beta$ ,  $\gamma$  or slow neutrons on a linear-logarithmic scale extending from about 10 mr/hr to about 100-200 R/hr of gamma radiation. The instrument is about 2-5/8" wide, 1-1/8" thick and 4" long. The weight is about 136 grams. This includes the weight of the plate and filament batteries contained in it. The RMB-3 filament battery and special plate battery are sufficient for about 100-200 hrs. of continuous use.

The electrometer tube used is a Raytheon CK-571-AX and is used from its floating grid potential up into the electron grid current region. It was expected that tubes used in this region might show considerable changes in performance after being idle for some period but after a few minutes warm up the tubes give reliable results even after a week shutdown. A characteristic of this method of using a tube with an ionization chamber is that at low intensity of radiation the meter motion is slow and takes a considerable fraction of a minute for reading a radiation level near 10 mr/hr, however, the rate of motion becomes more rapid as the radiation intensity increases, requiring only a few tenths of a second to come to a reading near 1 R/hr.

A thin window on the bottom face of the ion chamber allows the entrance of alpha particles and soft beta particles with an effective opening of about 50%; the alpha particle range is reduced by about 1/4 centimeter in air. This window is light tight and conductive and is constructed by cementing two sheets of Dutch leaf (sign painters aluminum foil) one after the other onto a thin open mesh of plastic threads. Figure IV-4 is the circuit diagram of Raymeter #1. The meter used is a modified International Instrument Co. Model 152. A better meter is being obtained from Weston Instrument Co. similar to that used in their photographic light meters.

A thin coat of natural uranium oxide on a nickel foil is used to check the calibration of the instrument and this standard foil may be attached to the upper surface of the instrument or stored

RAYMETER NO. 1

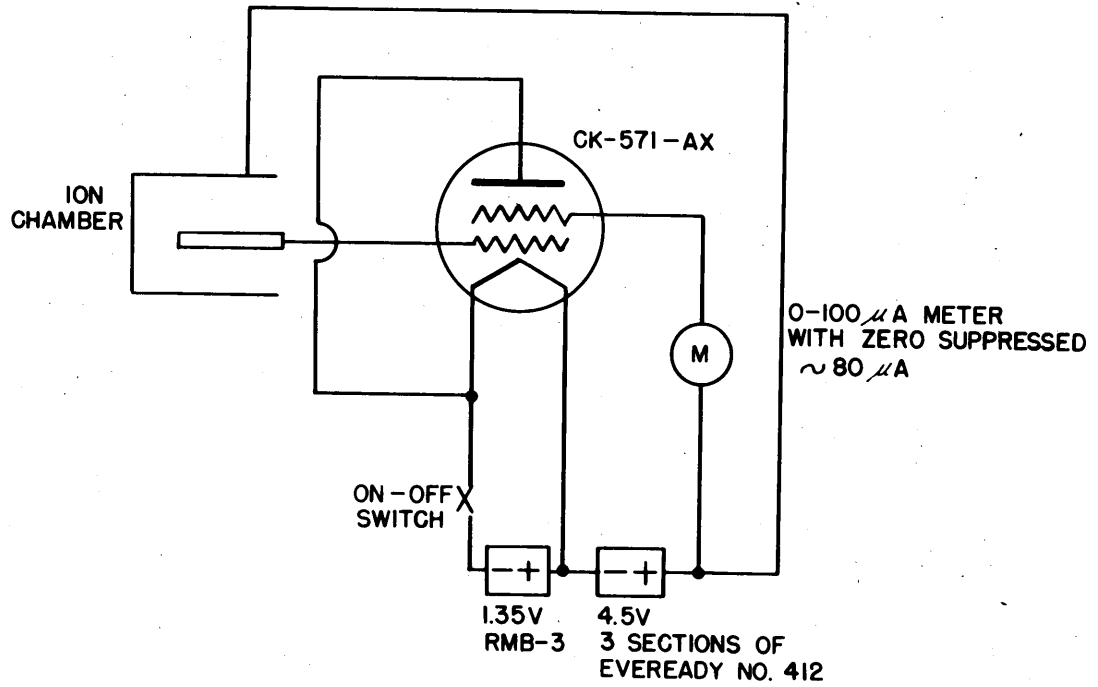
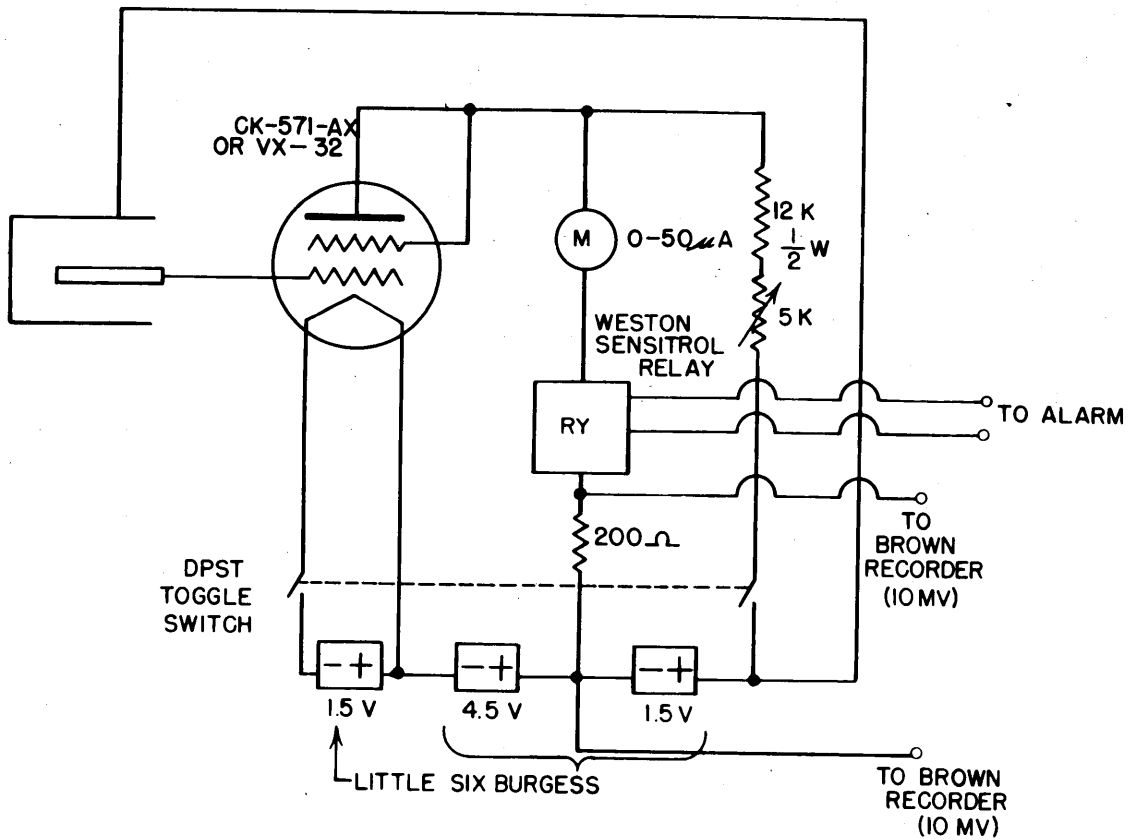


FIG. IV - 5

SMALL MONITRON (RAYMETER NO. 2)



██████████

in the carrying case when not in use.

Raymeter #2 is the third one of these small instruments and uses almost the same circuit as Raymeter #1. This instrument is meant for fixed service on a desk or other place where radiation is to be monitored. The meter is readable from 0.05 mr/hr to 12.5 mr/hr. A pair of leads may be provided to ring an alarm bell at any desired level and remote recording of the radiation level on a Brown recorder can be provided.

The instrument is contained in a six inch cubical box with a 1000 cm<sup>3</sup> cylindrical chamber on top. Batteries for 4-6 months continuous operation are contained in the box. The circuit is shown in Figure IV-5.

Raymeter #3 is a hand survey meter similar to the familiar "cutie-pie" except that it is smaller, lighter and more rugged. It is provided with only a single scale to reduce the likelihood of making an error while using it. The usual scale is 0-100 mr/hr with a linear scale.

The unit somewhat resembles a flare pistol with a cylindrical body about 2½" in diameter and 7" long with the meter face on the rear end. The weight of the complete unit is about 530 g. A very thin window is provided to allow soft β-rays and alpha particles to be measured. The construction of Raymeter #3 is covered by ORNL Drawings D-4354, D-4355, D-4356, C-4400 and Physics letter 48-7-1. It is expected that a number of units of this kind will be made for testing and for service samples.

Mechanisms of Geiger Counter Discharge - (Kelley, Bell, Jordan).  
Variations in the current in a Geiger tube circuit during and after a discharge have been studied in an effort to learn more about the mechanism of discharge. Waveforms obtained indicate that electron collection plays an appreciable part when the counter voltage is well above threshold.

Discharge of a counter represents an energy loss. The

energy may be supplied by a voltage change across the circuit capacity if the charging time constant RC is very long compared to the time of discharge, or directly from the charging source if the time constant is short. See Figure IV-6. In the first case, the voltage variation across the counter is a measure of the integrated energy loss ( $\Delta V = \frac{\epsilon}{CV_T}$ ) and in the second case the series current is a measure of the instantaneous rate of energy loss ( $i = \frac{1}{V_T} \frac{d\epsilon}{dt}$ ). Each of the charged particles resulting from a discharge receives an amount of energy depending on the field through which it must fall. Previously derived equations for the voltage change across a counter have assumed that practically all of the electrons formed during a discharge are formed within a few mean free paths of the central wire and therefore receive a negligible portion of the total energy. When it is assumed that all of the ions are formed at the anode and that therefore the positive ions receive all of the energy in a discharge the following equations hold:

$$\left. \begin{aligned} \epsilon &= \frac{QV_T}{2t_s \ln \frac{b}{a}} \left[ (t+t_0) \ln \frac{t+t_0}{t_0} - t \right] \\ \frac{d\epsilon}{dt} &= \frac{QV_T}{2t_s \ln \frac{b}{a}} \ln \frac{t+t_0}{t_0} \end{aligned} \right\} t \leq t_s \quad (1)$$

$$\left. \begin{aligned} \epsilon &= \frac{QV_T}{2t_s \ln \frac{b}{a}} \left[ (t+t_0) \ln \frac{t+t_0}{t-t_s+t_0} + t_0 \ln \frac{t_0}{t-t_s+t_0} - t_s \right] \\ \frac{d\epsilon}{dt} &= \frac{QV_T}{2t_s \ln \frac{b}{a}} \ln \frac{t+t_0}{t-t_s+t_0} \end{aligned} \right\} t \leq t_s \quad (2)$$

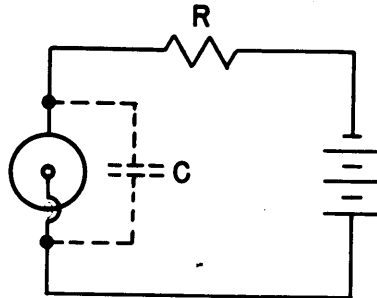


FIG. IV-6

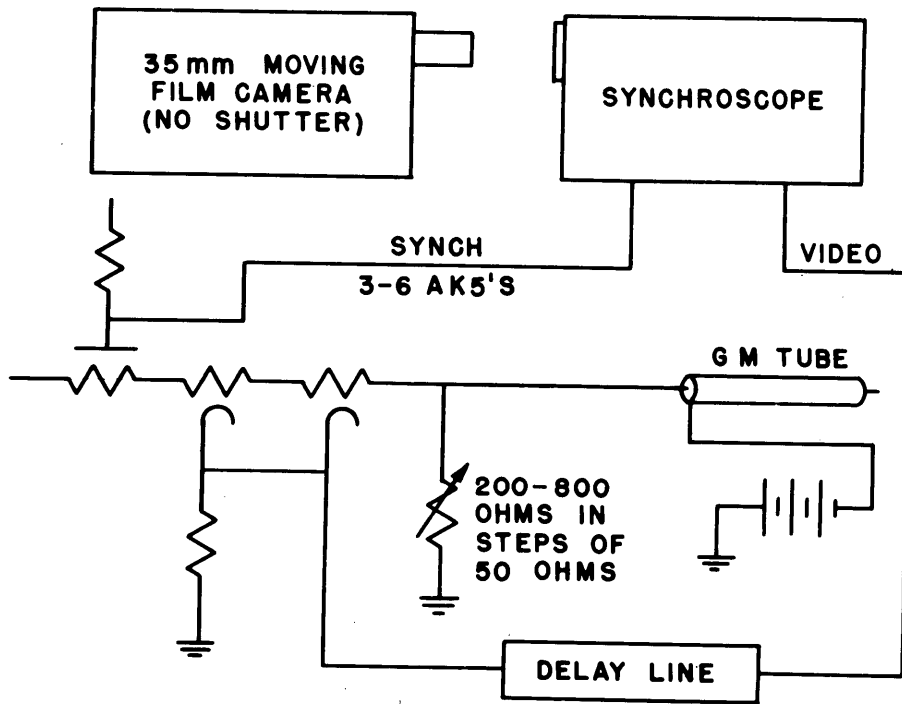


FIG. IV-8

NOT CLASSIFIED

Dr 6172

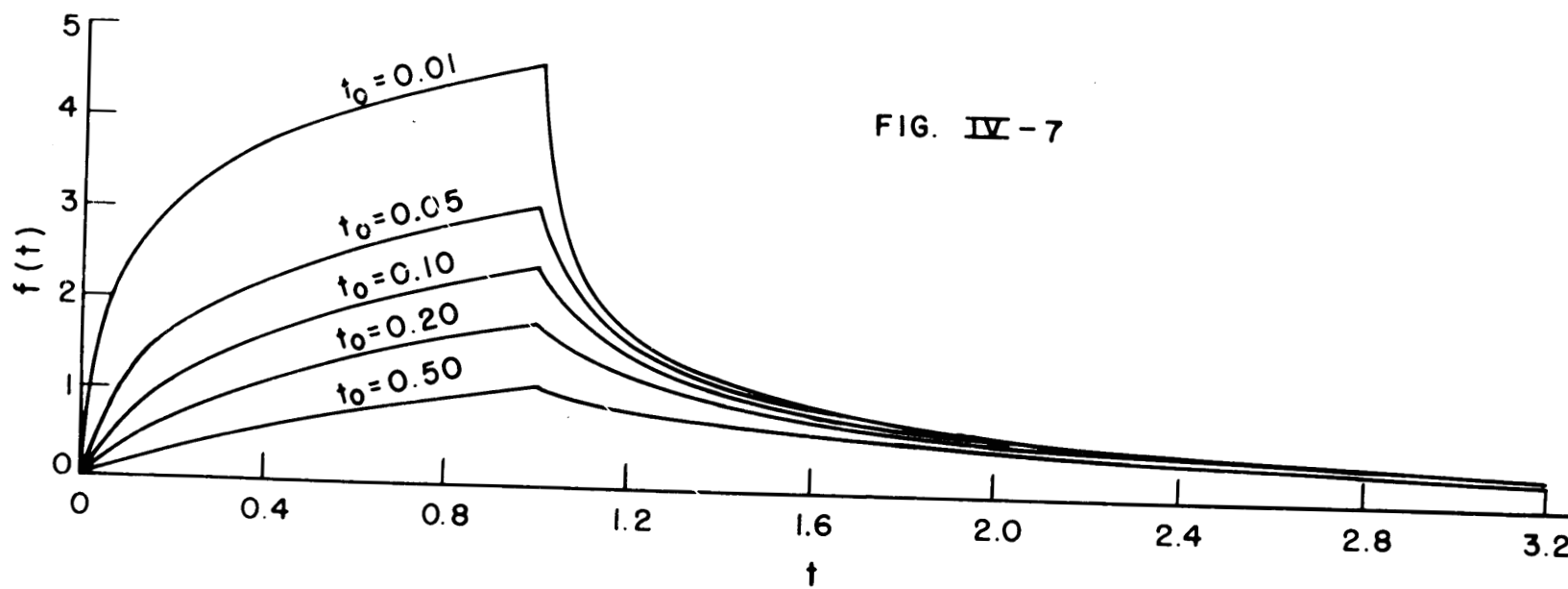


FIG. IV-7

Where  $\epsilon$  = the energy change due to a discharge in joules  
 $Q$  = the total charge produced in coulombs  
 $t_s$  = time for discharge to travel the length of the tube  
 $t_o = \frac{a^2 p \ln \frac{b}{a}}{2 K V_T}$  = time required for ion sheath to move from  
to its actual position at  
 $\frac{K}{p}$  = ion mobility in  $\text{cm}^2/\text{volt sec.}$   
 $b$  = radius of cathode in cm.  
 $a$  = radius of anode in cm.

When a long time constant charging arrangement is used:

$$\Delta V = \frac{Q}{2 C t_s \ln \frac{b}{a}} \left[ (t+t_o) \ln \frac{t+t_o}{t_o} - t \right] \quad t \leq t_s \quad (3)$$

$$\Delta V = \frac{Q}{2 C t_s \ln \frac{b}{a}} \left[ (t+t_o) \ln \frac{t_o}{t-t_s+t_o} - t_s \right] \quad t \geq t_s$$

When a short time constant charging arrangement is used:

$$i = \frac{Q}{2 t_s \ln \frac{b}{a}} \ln \frac{t+t_o}{t_o} \quad t \leq t_s \quad (4)$$

$$i = \frac{Q}{2 t_s \ln \frac{b}{a}} \ln \frac{t+t_o}{t-t_s+t_o} \quad t \geq t_s$$

This last function is plotted in Figure IV-7 for several values of  $t_o$ . Any electron contribution to the current will be in the form of a square pulse lasting only during the actual discharge since electron mobility is so high that the transit time of an electron is almost negligible. Photographs of individual current pulses were taken with the arrangement shown in Figure IV-8 and were compared with theory. It was found that there was an electron contribution for all values of  $V_T$  greater than threshold, increasing

██████████

with the amount of overvoltage. Consideration of this electron contribution led to the following qualitative picture of a discharge. Most of the story is well known and is included only for continuity. A counter containing some poly-atomic vapor (i.e. a self quenching counter) is assumed. An ionizing particle makes at least one ion pair in the previously ion free interior of the counter. The electrons formed fall toward the anode, gaining energy from the field and losing it in inelastic collisions. In the weak field existing everywhere except very close to the center wire the electrons do not gain enough energy between collisions to produce ionization. A field of the order of 5-10 kilovolts per cm. is required, its value varying widely with the gas mixture and pressure in the counter. Ionization occurs at a counter voltage which will produce an average field within one mean free path from the center wire great enough to give an electron sufficient energy between collisions to produce ionization. Greater values of counter voltage cause the electrons formed in this secondary ionization to produce more ions and result in the formation of an electron avalanche. Such values of counter voltage are said to lie in the proportional region. In this region the discharge spreads only about one mm. along the axis of the wire. Light quanta are produced as a result of the collisions and, as the counter voltage is increased toward the Geiger threshold, the number of these quanta that are sufficiently energetic to cause ionization increases. They initiate other avalanches which produce more quanta. The process is limited, however, by the positive ion space charge which builds up in the region close to the wire. The photons responsible for ionization are absorbed very readily by the polyatomic vapor, and below the Geiger threshold the probability is significantly less than unity that a photon will escape from the region in which the field is depressed by space charge far enough to propagate the discharge. At threshold this probability is great enough that practically all discharges spread to the ends of the tube. The spread velocity varies with the overvoltage but is of the order of 20 cm/ $\mu$  sec, while the electrons produced reach the wire within 0.05  $\mu$  sec, most of them arriving sooner. At any instant during the spread, ionization is taking place within two regions about a centimeter long spaced equal distances on either side of the

original avalanche.

During the time that ionization is taking place in any region along the wire, the positive ions left behind by the fast moving electrons remain practically stationary. Their presence decreases the free charge on the wire, the field at  $r = a$ , and the gradient of the field in the region. Consider two regions consisting of thin concentric rings of equal thickness at different distances from the center wire; unless the field is greater in the outer ring, fewer ions will be formed in it than in the inner one, since all electrons formed in the outer ring must fall through the inner one and can produce ionization there. An increase in the number of ions in the inner ring decreases the field in it and increases the field in the outer ring. For this reason, and since at the start of the process the field decreases with increasing  $r$ , the field tends to adjust itself in such a way that the same number of ions is formed in each element of radius. If there were sufficient photons available the field at any point along the wire just after discharge would have a constant value out to a critical radius beyond which there would be no space charge and the field would fall off inversely as the radius. Considering a uniform field in a region just after discharge, the following equations apply:

$$E_k = \frac{V_T}{d \left( \ln \frac{b}{d} + 1 \right) - a}$$

$$Q = \frac{V_T L (d-a)}{d \left( \ln \frac{b}{d} + 1 \right) - a} \times 5.6 \times 10^{-13}$$

$$\frac{\epsilon \text{ elec}}{\epsilon \text{ ion}} = \frac{d \ln \frac{d}{a} - (d-a)}{(d-a) \ln \frac{b}{a}}$$

where  $E_k$  = the uniform field in volts/cm.  
 $d$  = radius of the uniform region in cm.  
 $L$  = length of counter in cm.

How nearly this condition of constant field is achieved in a discharge depends upon the distance outward the high energy photons can reach. Measurement of  $Q$  with an overvoltage of about 150 volts gives a value for  $d$  of about  $0.3 b$  and an electron contribution to the total energy of 60%. Both of these values are too large, indicating that the photons do not bring the field down at all points to the value at which multiplication can just take place.

The equations derived for the ion current on the assumption that all of the positive ions originate at a constant radius also assume that the ions move out in a thin sheath. It was wondered how inaccurate these equations would be in an actual discharge, in which the original sheath is quite thick and spreads as it travels outward. The equations are the result of integration of equations for elemental lengths of the tube. Under the assumptions just mentioned,

$$di = \frac{Qdl}{\ln \frac{b}{a}} \cdot \frac{1}{t+t_0}$$

To compare this theoretical element with that actually obtained the photograph of a current pulse produced in a discharge in which the ionizing particle traveled the length of the tube was used. (Figure IV-9a). The shape of such a pulse should be the same as that produced by an element of length in an ordinary discharge. As may be seen in Figure IV-9b, it fits a curve of the form

$\frac{K}{t+t_0}$  quite well. For this reason it was felt that the assumptions led to an integrated curve differing very little from actuality.

The constant  $t_0$  is interpreted as that for the mean radius of origin of the ions. It may be obtained by fitting the equation for  $i$  to photographs of the current pulses. A study of Figure IV-7 shows that for  $t_s \geq 3t_0$ ,  $\ln \frac{t+t_0}{t-t_s+t_0}$  is practically



FIG. IV-9a

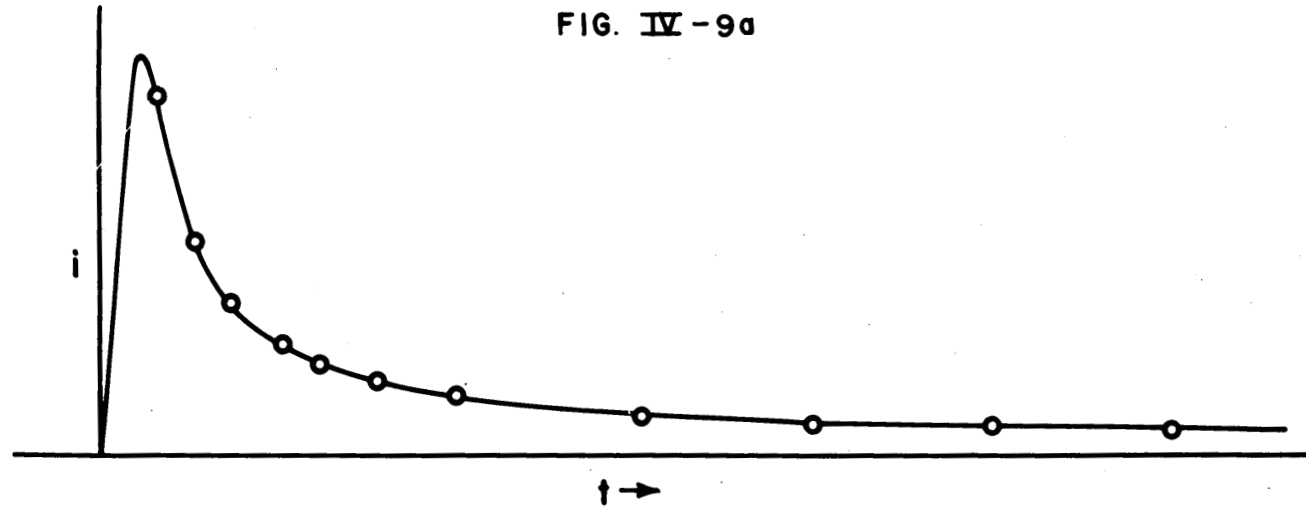


FIG. IV-9b

A TRACING FROM FIG. IV-9a & CALCULATED POINTS

independent of  $t_0$  when  $t > 3 t_s$ , and  $i$  depends on and the constant multiplier. A value of

$$\frac{Q}{2t_s \ln \frac{b}{a}}$$

may be obtained in this manner, or  $Q$  and  $t_s$  may be measured directly. Then  $t_0$  may be determined by selecting a value which produces a fit at a point closer to  $t = t_s$ . Using this method values of  $t_0$  of the order of  $1.5 \times 10^{-7}$  seconds were obtained, the value increasing with the overvoltage. If it were assumed that all the ions originate at the wire,  $t_0$  would be about  $10^{-8}$  seconds.

The photograph of current pulses shown in Figure IV-10a is unusual in that a pulse from an initial avalanche very near the middle of the tube is followed by one from an avalanche near the end of the tube. The second pulse is twice as long as the first and half as high at the time of the end of the first. Figure IV-10b shows the result of fitting ion current equations to the tail of the first pulse. The electron current pulse is the difference between the calculated ion current and the observed pulse. In Figure IV-10c the value of the constant

$$\frac{Q}{2 t_s \ln \frac{b}{a}}$$

in the equation was halved, the value of  $t_s$  doubled and the value of  $t_0$  unchanged. The resulting equation is seen to fit the curve quite well. There is a hump at the beginning of the pulse of electron current due to the fact that the discharge did not start at the end of the tube.

In Figure IV-11 the change in pulse shape with increasing overvoltage is shown. Both the increase in electron current and in  $t_0$  are apparent on inspection.

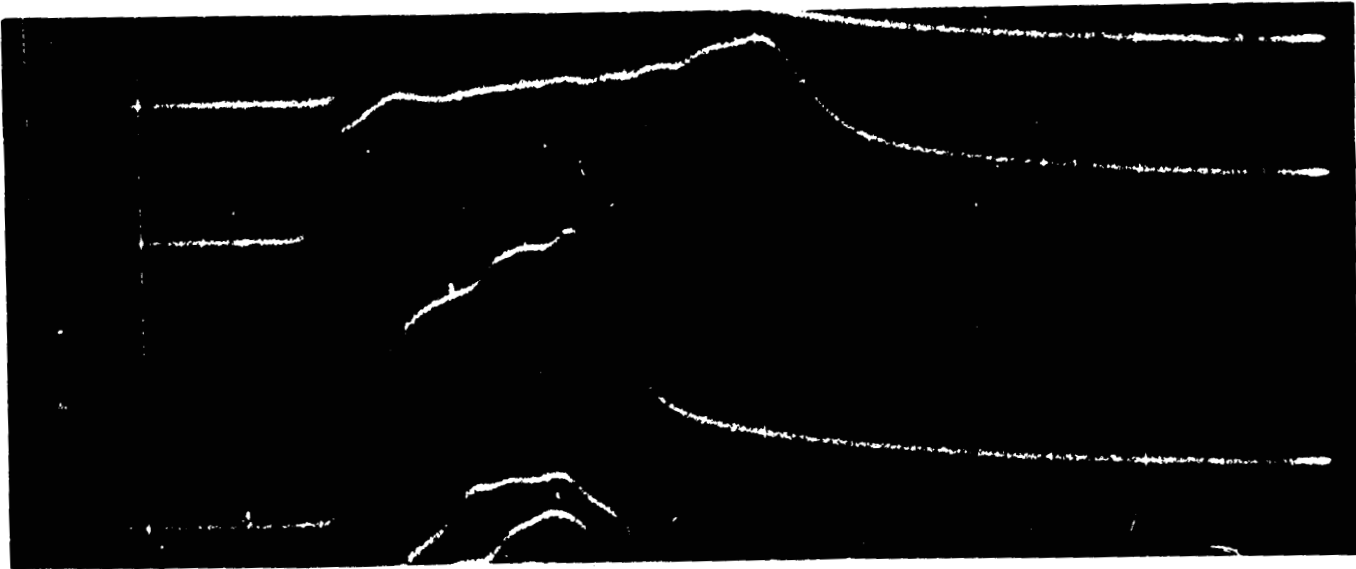


FIG. IV-10a

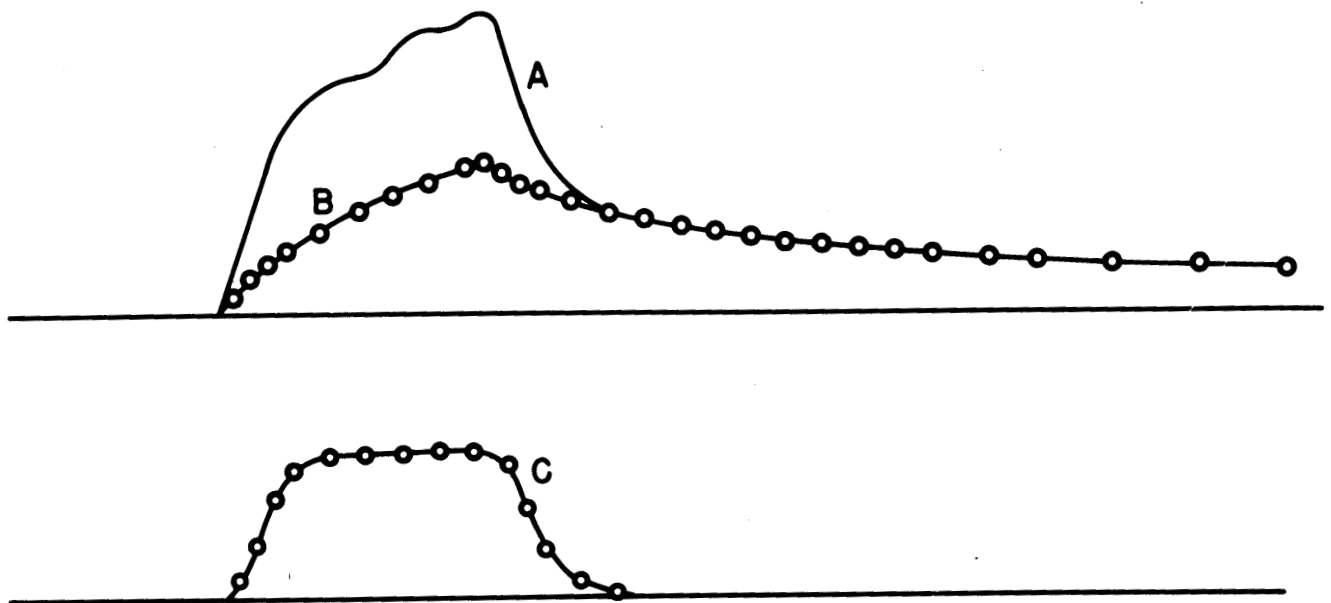


FIG. IV-10b

CURVE A IS A TRACING OF THE SHORTER PULSE SHOWN IN FIG. IV-10a. CURVE B IS THE CALCULATED ION CURRENT FROM EQUATION 4 FOR A VALUE OF  $t_0 = 0.15 \mu$  SEC. CURVE C IS THE DIFFERENCE BETWEEN A & B AND IS THE CURRENT DUE TO ELECTRONS

Dr 6175

NOT CLASSIFIED

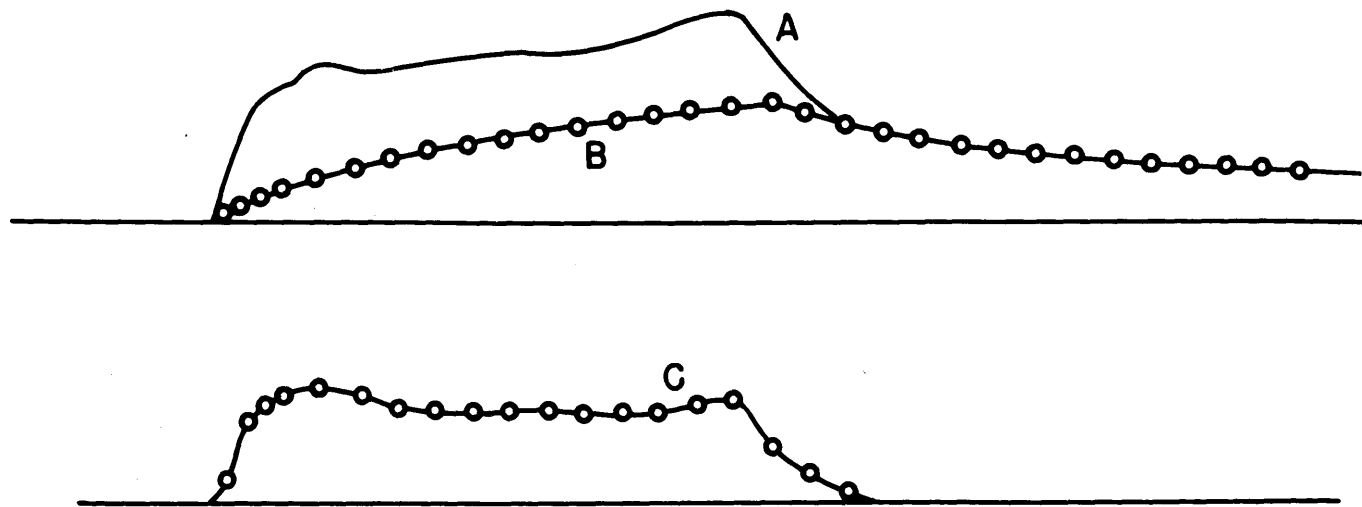


FIG. IV-10c

CURVE A IS A TRACING OF THE LONGER PULSE IN FIG. IV-10a. B & C HAVE SAME MEANING AS PREVIOUS FIG.

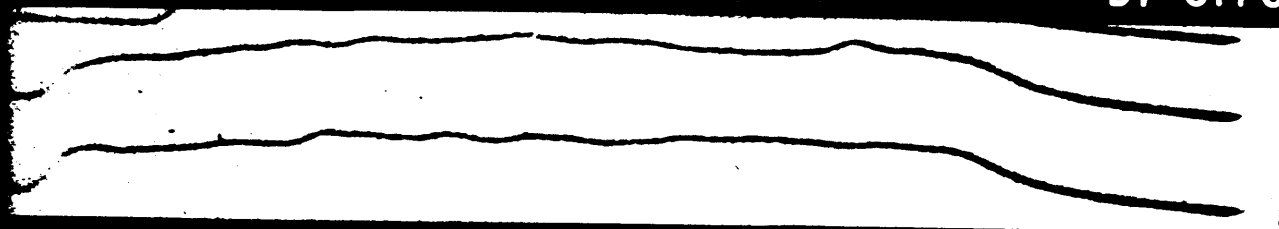


FIG. IV-11a

925 VOLTS



FIG. IV-11b

950 VOLTS

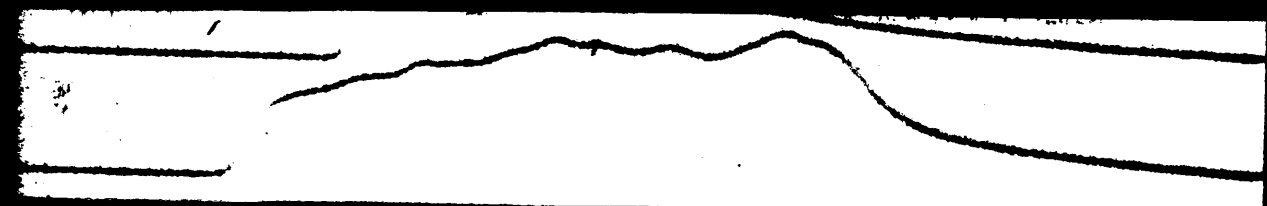


FIG. IV-11c

975 VOLTS

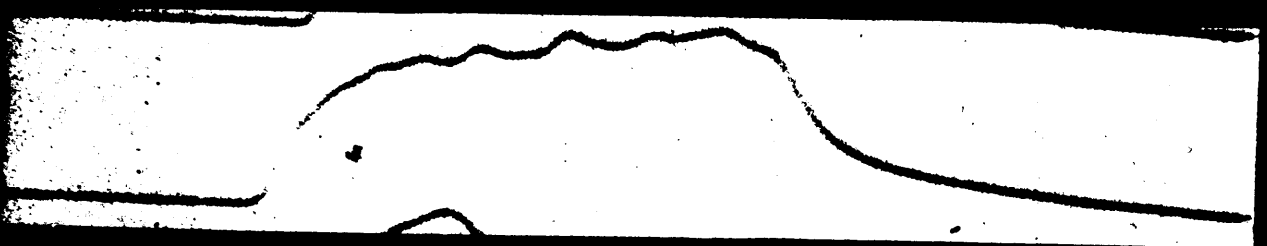


FIG. IV-11d

1000 VOLTS



FIG. IV-11e

1025 VOLTS



FIG. IV-11f

██████████

SECTION V - NUCLEAR STATES AND RADIATIONS

S. DeBenedetti, Section Chief

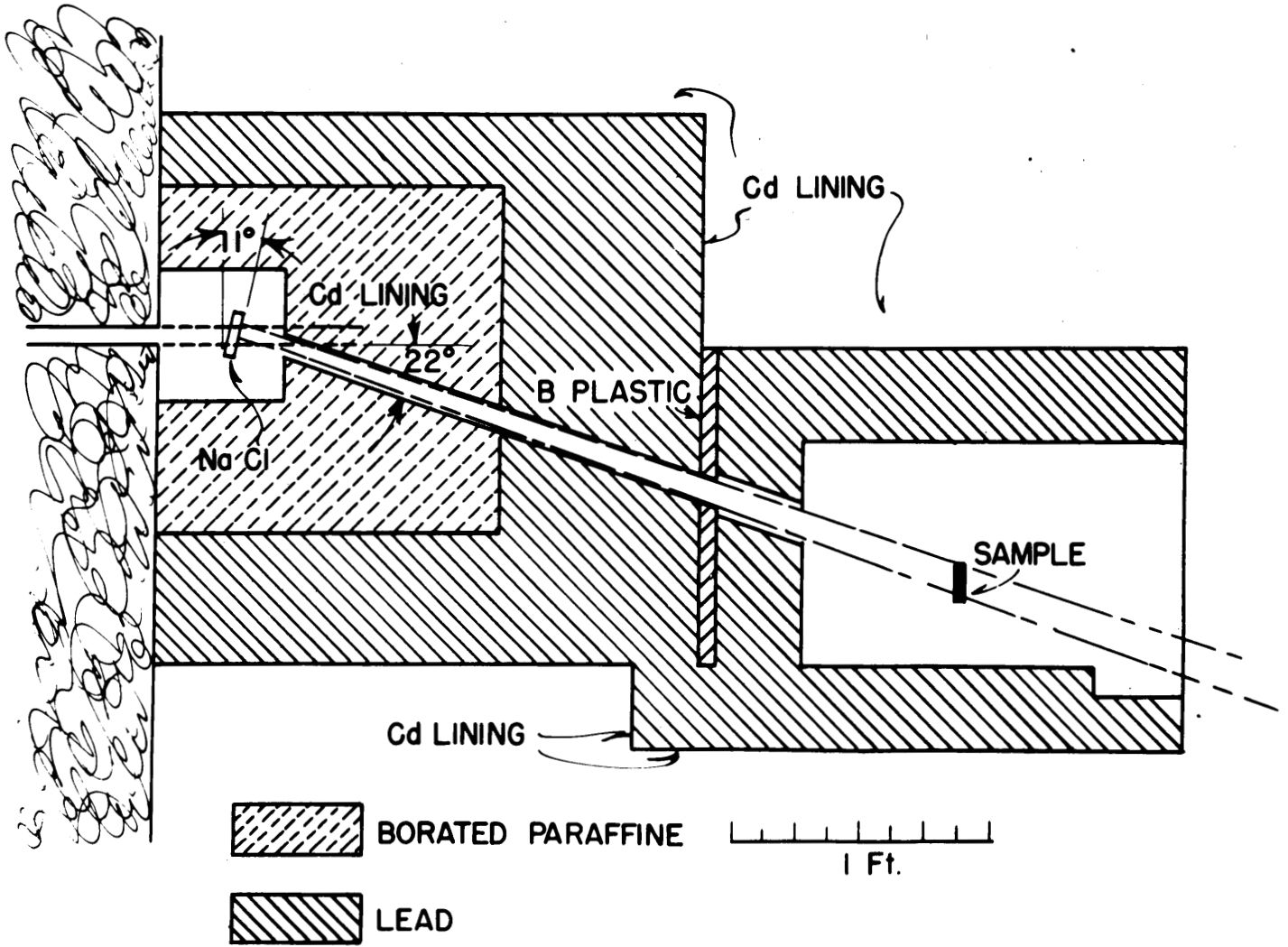
Preliminary Studies on Capture  $\gamma$ -rays with Scintillation Counters-  
(S. DeBenedetti and E. Rodgers). The new technique of scintillation counters was applied to the old problem of capture  $\gamma$ -rays. For this purpose (Figure V.-1) a NaCl crystal was located in front of a hole of the Oak Ridge pile and the diffracted thermal neutrons were directed toward the sample studied. The diffracted beam was canalized through a channel of square cross-section ( $3/8$ "x $3/8$ "") in a heavy shield which absorbed most of the other radiations emerging from the hole in the pile shield. The walls of the collimating channel were heavily borated plastic.

The samples (2.5x2.5 cm) were located in the beam in a position where this had a width (computed from the geometry of the collimator) of  $\sim 2$ x2cm. At a distance of  $\sim 3$  cm from the center of the beam, an anthracene crystal was placed. The scintillation pulses were revealed with a photomultiplier, amplified and counted in a conventional way. Sample and anthracene were inclosed in a second heavy shield of lead and cadmium to protect the anthracene from the radiation from the other holes of the pile. This shield had an opening through which the beam could emerge.

The background of the instrument consisted of photomultiplier noise, and radiation background. The photomultiplier noise was measured with the pile off and, for typical amplifier setting, was found to be  $\sim 30$  c/m; the radiation background contributed  $\sim 300$  c/m at the same setting and seemed to be due mostly to radiation from other holes of the pile.

When samples of large capture cross section (like Cd) were placed in the beam the counting rate (at the same amplifier setting) was  $\sim 1300$  c/m. If the diffracted neutron beam was removed only the background counts were recorded.

FIG. V - 1



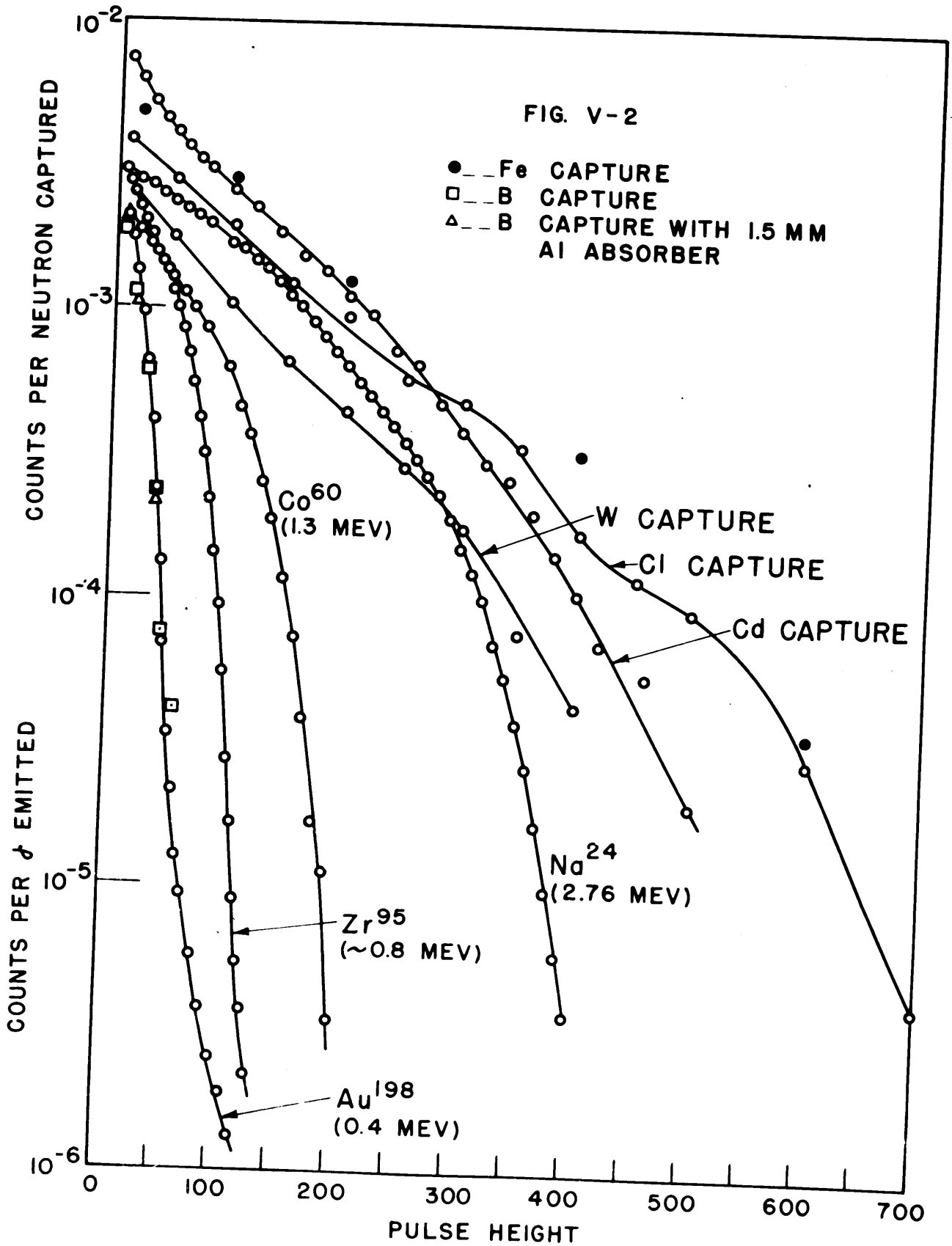
SECRET

In order to study the energy of the capture  $\gamma$  rays, the distribution in height of the pulses was measured by varying the pulse height selector setting of the amplifier. For comparison, similar pulse height distribution curves were recorded using calibrated radioactive sources emitting  $\gamma$  rays of known energy. These sources were located in the same position as the capturing samples; however, because of their different shape the geometry was not quite the same.

The results are plotted in Figure V -2. In this figure the abscissae are the settings of the pulse height selector, and the ordinates the counts recorded, divided by the number of neutrons captured (for the capture  $\gamma$  ray curves) or by the number of  $\gamma$  rays emitted (for the calibration curves). Radioactive sources of Au<sup>198</sup>, Co<sup>60</sup>, Zr<sup>95</sup>, and Na<sup>24</sup> were used in the calibration. Since Na<sup>24</sup> is known to give off the two  $\gamma$  rays of energies 1.38 and 2.76 Mev in equal numbers, it was possible, by assuming the 1.38 Mev component to behave as the 1.3 Mev  $\gamma$  ray of Co<sup>60</sup>, to compute the contribution of the 2.76 Mev component.

It will be noted that the points obtained with B as capturing sample fall almost on the curve for radioactive gold. This is to be expected since B is supposed to emit 0.42 Mev  $\gamma$  rays after neutron capture. Three of the readings with B as sample were repeated with 1.5 mm of Al as absorber between the sample and the crystal. This was done to eliminate the possibility that the counts from B might be due to conversion electrons. The close agreement of corresponding points with Au and B indicates the emission of approximately one  $\gamma$  ray for each neutron captured by the B.

With the exception of B, all samples used for capture indicated the emission of rather hard  $\gamma$  ray components. Unfortunately the portions of the curves at large pulse height settings are not very good statistically, and this is the region which probably gives the best indication of the hard  $\gamma$  ray energies. More work is needed before much can be said about these energies.



████████

The striking feature of these curves is their parallel shape and the apparent scarcity of soft components.

Search for Short-Lived Isomers - (S. DeBenedetti, J. E. Francis, F. K. McGowan and H. Schweinler). During the last quarter the efforts of the group have been concentrated on attempting to develop an instrument capable of measuring time intervals of the order  $10^{-8}$  sec. We have to report, however, that our efforts have not yet been successful.

A number of circuits were built and tested, some following the principle of self-delayed coincidences, others using the straight delayed coincidence technique. In all these circuits the multipliers were used at high voltage (1500 to 2000 V) with the purpose of reducing the required amplifier gain to a minimum and thereby minimizing the difficulties in electronic design.

The pulse from the 1P21 multipliers was studied with the fast oscilloscope using a video amplifier of  $.025 \mu$  sec. rise time. It was found that the apparent width of the pulse is  $\sim 0.05 \mu$  sec; though part of this width is due to the time constant of the amplifier and to distortions caused by the delay line used in the experiment, it was apparent that the actual duration of the pulses contributed to the observed width. We concluded that the duration of the pulse is considerably smaller than one-tenth microsecond, and could be as short as a few hundredths of a microsecond.

It should be possible, in principle, to use these pulses directly on a self-delayed coincidence circuit. The scheme was tried, but it failed for the following reasons: in order to obtain directly from the multiplier high enough pulses to operate the coincidence circuit, one was obliged to use such high voltage that the background was very large; since the pulses have a wide distribution in height, the resolving time was not constant; some difficulties were experienced which were attributed to attenuation of the pulse in delay line.

We thought that these difficulties could be overcome by

██████████

using two photomultipliers at lower voltage, some stages of amplification, and pulse forming tubes to produce short equalized pulses to be fed to a delayed coincidence circuit. Instruments working on this principle were built. In these instruments the delay line was inserted in the amplifier before the pulse forming tube in order to overcome the possible attenuation of the pulse. It was found that in order to obtain prompt and equalized pulses from the pulse forming tubes they had to be started with large signals. The large signals were produced with non-linear amplifier designed to give the fastest raise of voltage at the output in volts per  $\mu$  sec, but a pulse of relatively long duration. With this amplifier most of the pulses were large enough to strongly saturate the output in a very short time; a few of the pulses, however, were small enough not to produce saturation and their maximum did not occur promptly, introducing false delayed coincidences.

We also tried a coincidence scheme for the elimination of noise. Four photomultipliers were used, each pair of them being connected in coincidence and exposed to the radiation of an anthracene detector. The coincidence circuit used for this purpose consisted of two IN34 crystal rectifiers directly attached to the photomultipliers plate. This single circuit permits the use of the photomultipliers at high voltage virtually eliminating the noise. However, when two such circuits were fed to amplifiers, pulse forming tubes and delayed coincidence circuit (similar to the one described) it was found that the improvement was not yet sufficient.

Some of our circuits were partially successful since we could eliminate 95% of the immediate coincidences with delays of  $0.04 \mu$  sec. The remaining 5%, however, were distributed over delays up to  $0.4 \mu$  sec and made the instrument worthless for our purpose.

In the immediate future we plan, together with P. R. Bell, to attack the problem by using two coincidence circuits of the kind described for the suppression of noise, and two fast video amplifiers. It is hoped that this arrangement will prove more successful than the ones tried thus far.

██████████

The Radiations from 24.1 hr W<sup>187</sup> - (Paul W. Levy). The attempt to ascertain the energy and intensity of all of the radiations from 24.1 hr W<sup>187</sup> has continued. An endeavor to improve the photo-electron technique by utilizing coincidence counters, as described in the last Quarterly Report, and reducing the source dimensions to reduce the half width of the photo-electron lines met with some, but not complete, success. A pronounced reduction in the counter background was obtained but there was no appreciable reduction in the half width of the photo-electron line, nor in the photo-electron to Compton electron ratio. It may be that the size of the radiator foil was reduced too severely and an optimum size foil could be determined by a more careful study. Also, the absorption in the wall of the additional counter materially reduced the total counting rates in the low energy region. It appears, at the moment, that while no outstanding improvement in the ability to detect low energy photoelectrons (those < 200 Kev) was obtained, a considerable improvement was accomplished in the region above 400 Kev.

The continuous beta-ray spectrum was determined again with a source  $\sim 10$  mg/cm<sup>2</sup> while in the previous run a source of  $\sim 30$  mg/cm<sup>2</sup> was used. Essentially the same results were obtained. The maximum energy of the high energy spectrum is 1.32 Mev. If one proceeds in a straightforward manner to separate the spectrum obtained into "allowed type" spectra (those with essentially straight Kurie plots) one obtains a second component with maximum energy between .614 and .632 Mev, these limits being the maximum and minimum values permitted by various extrapolations of the Kurie plot. In addition one can obtain a low intensity component of  $\sim .35$  Mev. This component could be real, it can come entirely from back scattering by the thick source, or it could be attributed to the 78 day neutron induced period in Tungsten. This latter alternative will be tested as soon as the 24.1 hr activity has completely died away. Should this latter component exist, a complete decay scheme could be obtained. Approximately 25% of the beta-ray transitions are in the high energy spectrum, the remaining 75% of the betas being in the low energy component, or components.

The conversion electron studies in the region from 1.2 to

.018 Mev have been completed. In all, 13 conversion lines have been detected. (A summary of the conversion line results are contained in Table I). These can be attributed to 6 gamma rays. While most of these lines have been reported previously as definitely existing, only inconclusive evidence for the existence of a gamma ray of .767 Mev had been obtained. Since we now observe both photoelectrons and conversion electrons from this gamma ray, we feel it definitely exists.

TABLE I

Conversion Electrons and Gamma-rays in 24.1 hr  $W^{187}$

| Gamma-ray | Conversion Lines Observed | Estimated Intensity of Conversion Lines | Energy of Conversion Lines (Mev) | Best value gamma-ray Energy (Mev) |
|-----------|---------------------------|---|----------------------------------|-----------------------------------|
| 1         | K                         | Very strong                             | .062                             | .133                              |
|           | L                         | Strong                                  | .121                             |                                   |
|           | M                         | Medium                                  | .130                             |                                   |
| 2         | K                         | Medium                                  | .133                             | .204                              |
|           | L                         | Faint                                   | .191                             |                                   |
| 3         | K                         | Strong                                  | .407                             | .478                              |
|           | L                         | Weak                                    | .465                             |                                   |
|           | M                         | Faint                                   | .477                             |                                   |
| 4         | K                         | Medium                                  | .541                             | .615                              |
| 5         | K                         | Weak                                    | .609                             | .680                              |
|           | L                         | Faint                                   | .670                             |                                   |
| 6         | K                         | Very Weak                               | .696                             | .767                              |
|           | L                         | Very Faint                              | .754                             |                                   |

██████████

Scattering of Polarized Gamma-Rays in Magnetized Iron - (Eric Rodgers). Recently the writer observed at the University of Alabama an anomalous effect in X-ray scattering. X-rays from a 200 K.V. machine were observed after having been scattered twice at  $90^\circ$ . First, they were scattered by carbon, the purpose being to polarize the rays. The polarized rays were then scattered by a strip of iron which could be magnetized by a current in a coil through which the iron strip passed. The rays scattered at  $90^\circ$  by the iron were then observed in directions parallel and perpendicular to the direction of the primary beam. A G-M counter was used to compare intensities of the twice scattered rays when the iron was magnetized in various ways, with the intensities when the iron was unmagnetized. It was found that no change took place in the scattered intensity when direct current was passed through the coil. On the other hand a change was observed when 60 cycle alternating current was used. For a direction of observation perpendicular to the primary beam, the current in the coil caused an increase of from 2% to 3% in the scattered intensity. In a direction parallel to the primary beam, the increase was very much smaller, amounting to about 0.30%.

It was felt desirable to repeat these experiments by using gamma-rays instead of X-rays. There were several reasons for this. In the first place, no really sound theoretical explanation has been found to explain the effect, although it can be predicted on a somewhat artificial semi-classical basis. In the second place, it was felt that the changes of experimental error would be less with a steady gamma ray source than with X-rays from a machine operating on the same A-C line as the counter circuit.

In attempting to do the experiments with gamma rays, great difficulties were encountered. Even with the strong gamma ray source used, (about 30 curies of  $\text{Au}^{198}$ ) the intensity at the position of the first scatterer was some hundred times smaller than that obtainable from the X-ray machine. This difficulty was partly overcome by (1) using thick samples as scatterers and substituting aluminum for carbon as the first scatterer, (2) using larger cross sections of the beam, and (3) using an anthracene scintillation counter instead of a G-M counter.

██████████

Another difficulty which was never overcome in a satisfactory manner was due to the effect of the alternating magnetic field on the photomultiplier. It was found that the field reduced the number of counts recorded. Several things were done in an effort to correct this. The multiplier was surrounded by two concentric cylinders of soft iron, and a large sheet of soft iron was placed between the magnet and the multiplier. This greatly reduced the effect and would have proved satisfactory if the effect of the field had remained consistent. In making tests to detect the effect of the field, gamma rays from another gold source were scattered twice by aluminum blocks and allowed to strike the crystal. The multiplier and magnet were left in the same position as when the magnet itself served as the second scatterer. Several tests showed a small but definite decrease in counting rate when the field was turned on while other tests showed no detectable change. In no instance was an increase observed. It must be said, however, that this effect does place a question mark after the results obtained.

In spite of the difficulties, some data were obtained which lend support to the results obtained with X-rays. In view of the fact that the background count with the aluminum scatterer removed was usually about two-thirds the rate with the scatterer in place, considerable time was required to get a statistically sound set of data. The procedure was to measure counts of one minute duration with the field alternately off and on. The background is determined at the beginning and at the end of each experiment. Also at the end of two experiments a test was made by substituting aluminum for the iron as the second scatterer. One of them showed a decrease in counting rate but the other did not. No reason can be given for this except that it might possibly be due to the fact that the photomultiplier had been removed between the two experiments, and possibly was in slightly different position. Another rather long test (experiment 6 in the table) failed to show any significant change. Before the iron shielding was placed around the photomultiplier, as much as 5% decrease in counting rate was observed. A summary of the results obtained after shielding the photomultiplier is given in the following table.

| Exp. No. | Max. Flux Density in Iron (Gauss) | Voltage on Multiplier | Pulse Height Setting | Second Scatterer | Number of Trials | Percent Change over Background |
|----------|-----------------------------------|-----------------------|----------------------|------------------|------------------|--------------------------------|
| 1        | $10 \times 10^3$                  | 630                   | 14                   | Iron             | 25               | 1.77±.39 Increase              |
| 2        | $5 \times 10^3$                   | 585                   | 10                   | Iron             | 41               | 1.48±.29 Increase              |
| 3        | $5 \times 10^3$                   | 585                   | 10                   | Aluminum         | 41               | 1.34±.30 Decrease              |
| 4        | $5 \times 10^3$                   | 540                   | 6                    | Iron             | 40               | 1.55±.26 Increase              |
| 5        | $5 \times 10^3$                   | 540                   | 6                    | Aluminum         | 13               | No change                      |
| 6        | $15 \times 10^3$                  | 630                   | 12.5                 | Aluminum         | 49               | No change                      |
| 7        | $15 \times 10^3$                  | 675                   | 26                   | Iron             | 28               | 0.18±.44 Increase              |

██████████

As will be noted, some inconsistencies appear in the table. Experiment 3 was done immediately after experiment 2 and showed a definite decrease when aluminum was used as the second scatterer. Experiment 5 was done immediately after experiment 4 and showed no change at all. Experiment 6 with aluminum used as the second scatterer also showed no change, although conditions were different from those in experiment 5. The result in experiment 7 is also puzzling. The current through the magnetizing coil was three times as great during this experiment as during experiments 2, 3, 4 and 5 but was the same as in experiment 6 in which no change was observed with the aluminum as the second scatterer. However, experiments 6 and 7 were done on different days and the photomultiplier had been removed in the meantime due to electronic troubles. Another thing which might be significant is the fact that the counting rate slowly decreased all the way through experiment 7, being about 7% slower at the end than at the beginning. This trouble was encountered in most of the experiments. The only experiments in which no change occurred in counting rate were experiments 4 and 5.

It is difficult to draw any conclusion from the results. About all that can be said is that during steady operation of the counting circuits, there is an indication of an increase when the polarized rays are scattered by the iron magnetized with alternating current. More work is needed. Especially is it desirable to find a way to eliminate all possible effects of the alternating magnetic field on the multiplier directly. Also the necessary adjustment should be made to insure that the counting rate does not drift during an experiment.

[REDACTED]

## SECTION VII - CRITICAL EXPERIMENTS

M. M. Mann, Section Chief

A. B. Martin

J. K. Bair (on loan from NEPA)

A. L. Preston

R. V. McCord

A. H. Toepfer

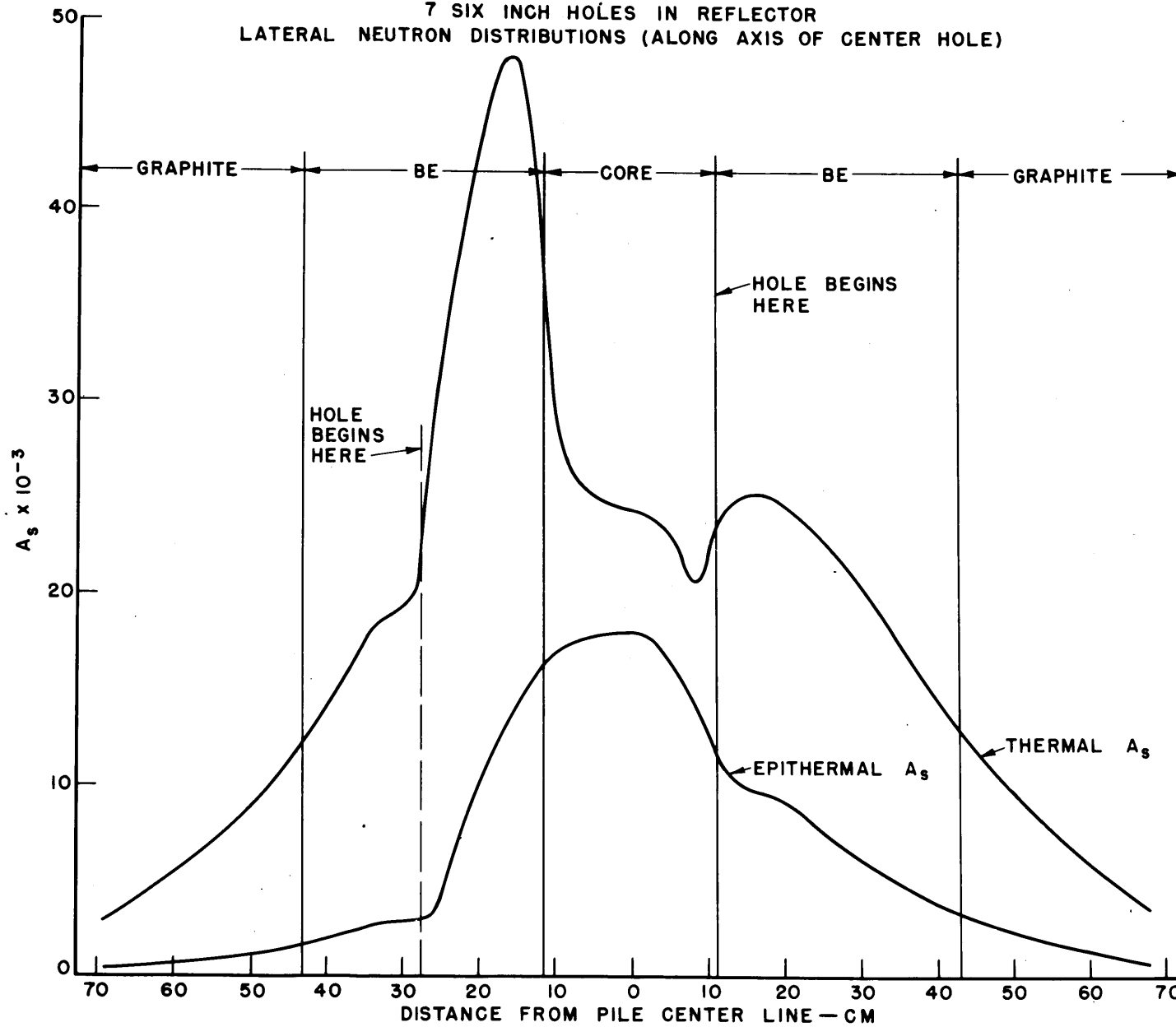
### Introduction

During the past quarter a considerable amount of time has been devoted to completion of a number of miscellaneous experiments of interest to the high flux reactor design, namely, the evaluation of Cd and Th control rods, the measurement of neutron flux between two adjacent rods, the measurement of gamma ray heat production along the edge of one of the experimental holes in the reflector, fast neutron ( $E > 1$  mev) flux measurements, and an experiment to ascertain the feasibility of obtaining a high thermal flux in a Beryllium block placed in the core of the high flux reactor in place of a fuel assembly.

In addition, a graphite reflected assembly has been built and various spatial neutron flux distributions in this reactor have been measured.

I. Spatial Neutron Flux Distributions in the 3.95 Kg Mock-up of the High Flux Pile. In order to present a clearer picture of the neutron flux distributions in the various experimental holes in the high flux pile, we show, in Figures VII-1, VII-2 and VII-3, composite curves, made up from data previously reported, which represent complete Indium foil traverses taken along the axes of the large experimental holes. These data are repeated here because it is believed that the composite representation offers a better perspective of the spatial variation of thermal and epithermal (Indium resonance) neutron flux in the high flux reactor than has heretofore been presented.

FIG. VII-1  
 4 Kg SLAB PILE (71 x 22.5 x 66 CM)  
 7 SIX INCH HOLES IN REFLECTOR  
 LATERAL NEUTRON DISTRIBUTIONS (ALONG AXIS OF CENTER HOLE)



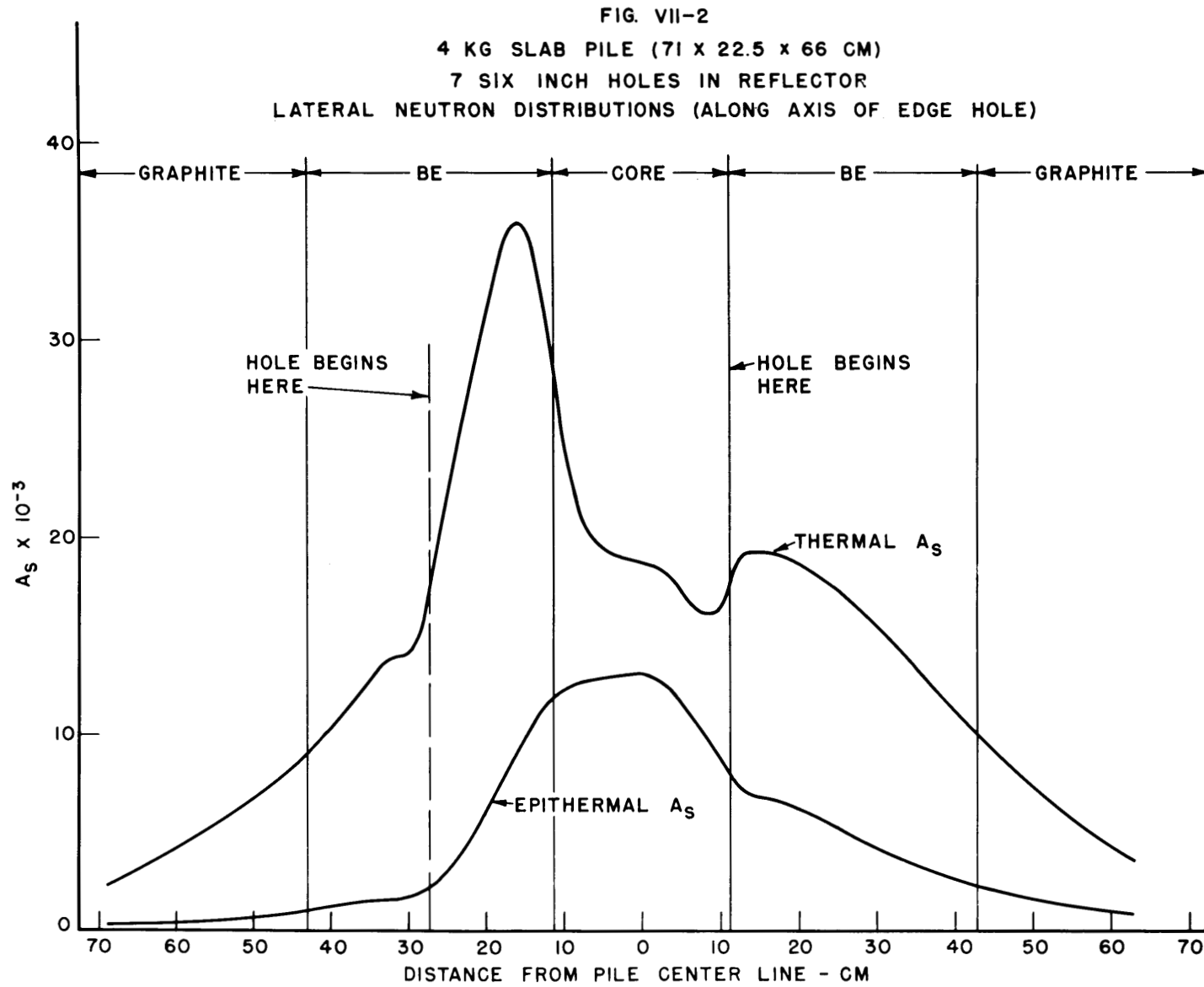
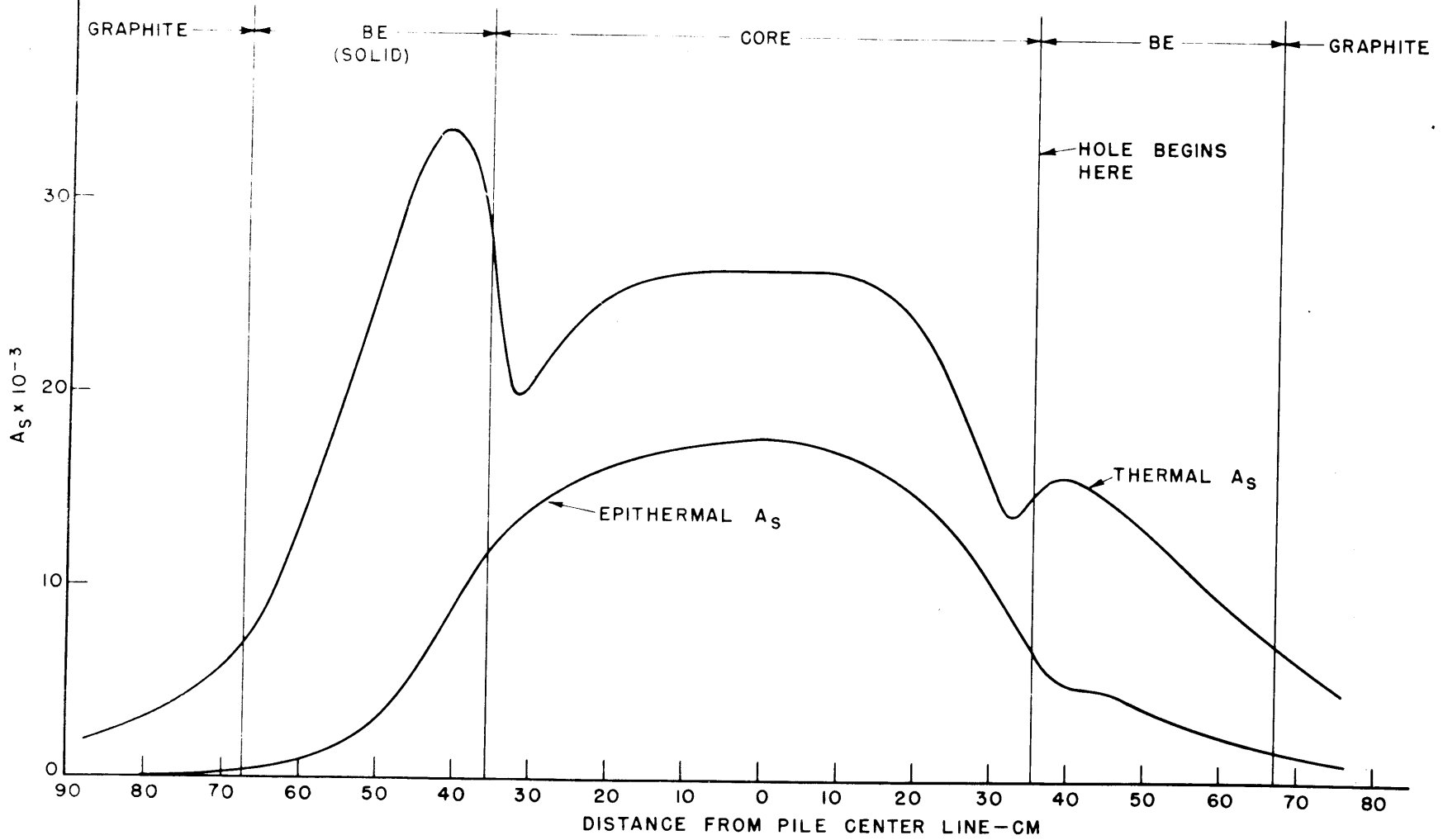


FIG. VII-3  
4 Kg SLAB PILE (71 x 22.5 x 66 CM)  
7 SIX INCH HOLES IN REFLECTOR  
LONGITUDINAL NEUTRON DISTRIBUTIONS (ALONG AXIS OF END HOLE)



Also, in Figure VII-4, we show the thermal and epithermal neutron flux measured (1) along the axis of the deep center hole, and (2) along the edge of the same hole.

II. Control Rod Experiments. A number of experiments have been carried out to study the effectiveness of control rods of various sizes in the 4 Kgm. mock-up of the high flux reactor. The experiments are performed in the following way: the uniform poison in the "clean" core (before the control rod is inserted) is adjusted until the assembly is just critical. The control rod is inserted and the amount of uniformly distributed poison in the core is reduced until the assembly is again just critical. When the experiment involves no change in the amount or concentration of fuel in the core, the percentage change in  $k$ ,  $(\Delta k/k)$ , is given simply by  $\Delta\Sigma/\Sigma$  where  $\Delta\Sigma$  is the change in uniform poison and  $\Sigma$  is the total cross-section of the core after the rod is inserted. In experiments which entail the removal of fuel and the insertion of a control rod, the  $k$  of the clean core ( $k_1$ ) is calculated, the  $k$  of the active portion of the core after insertion of the rod ( $k_2$ ) is calculated and  $\Delta k/k$  is then given directly by  $\frac{k_1 - k_2}{k_2}$ .

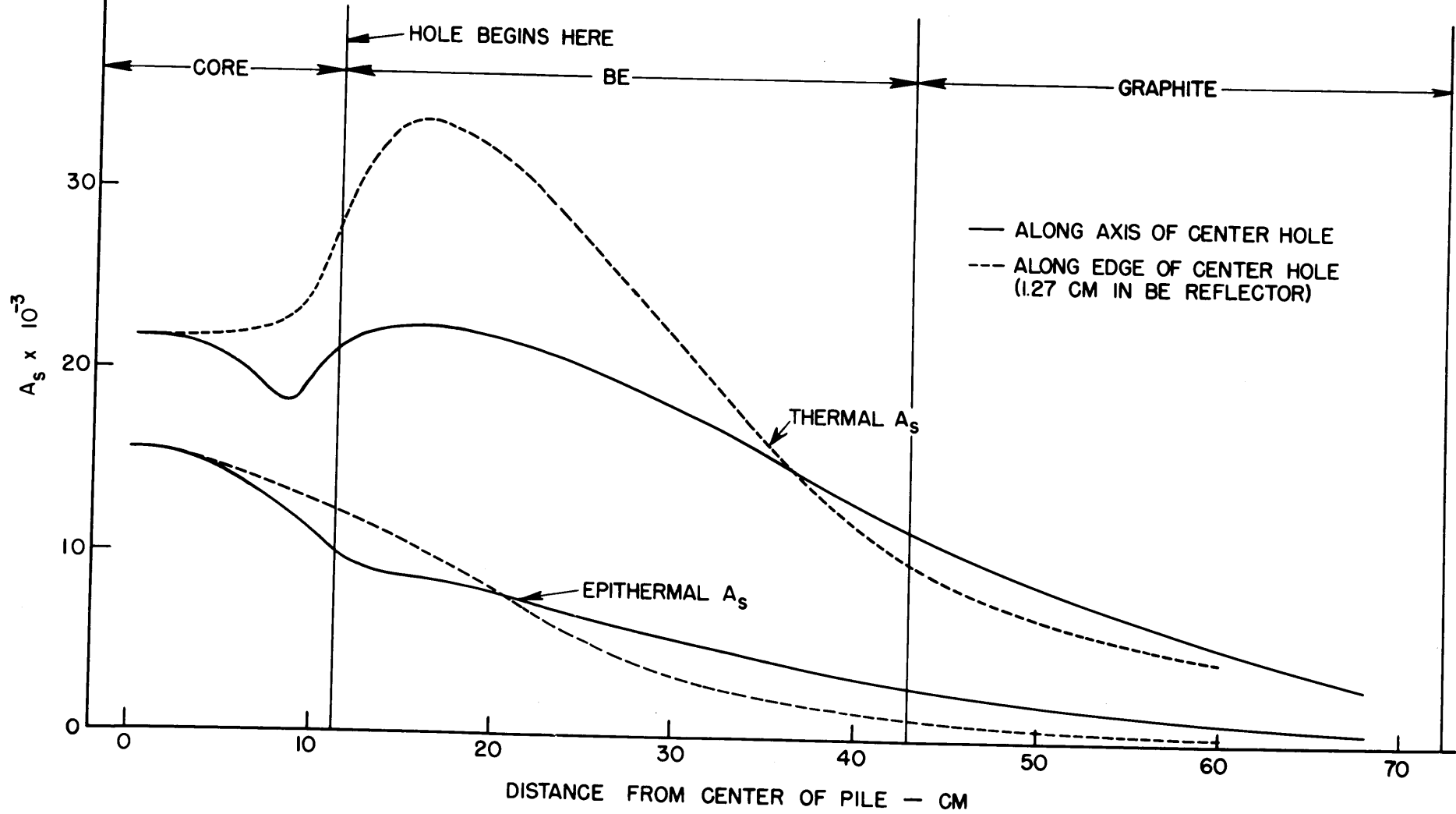
Figure VII-5 is a horizontal section through the core of the 4 Kgm. mock-up Be assembly, showing the positions at which control rods were inserted for study. Our standard 3/4 inch square Cd control rods which are normally located at a and b were replaced by fuel tubes for these studies, so that the rods to be tested were inserted in clean fuel.

The Cd control rods tested in these experiments were essentially replicas of those designed for the high flux reactor insofar as dimensions and compositions are concerned. They were in the form of hollow cylinders of square cross-section ( $3\frac{1}{4}$ "x  $3\frac{1}{4}$ "x 26" in length) and were filled with water to duplicate the conditions that will obtain in the case of the high flux reactor.

The Th rods for the high flux reactor are made up of

FIG. VII - 4

NEUTRON DISTRIBUTIONS IN 4 Kg PILE





██████████

several plates, stacked in a sandwich-like assembly, with spaces between plates for the passage of cooling water. In our experiments Fe was used instead of Th for reasons of availability and ease of fabrication, the amount of Fe being adjusted to give the same total thermal cross-section as that provided by the current design of Th rod. The test rod then consisted of a rectangular sandwich of Fe and lucite plates having the same dimensions as the Cd rods described above.

For use in the high flux reactor, it is planned that these rods be attached at one end to fuel assemblies, so that as a rod is withdrawn fuel is inserted in its place and vice versa. Therefore, the measurement of interest is the effect of the rod vs. fuel in the same position. The percentage changes in reactivity of the active portion of the core when these rods were inserted in place of fuel at positions A and B of Figure VII-5 were as follows:

|                    | $\Delta k/k$ |
|--------------------|--------------|
| Cd Rod at A        | 7.3%         |
| Cd Rods at A and B | 20.7%        |
| Th Rod at A        | 4.2%         |
| Th Rods at A and B | 9.0%         |

It was also observed that the reactivity change due to the removal of 120 grams of fuel (9 tubes or a  $3\frac{1}{4}$  inch by  $3\frac{1}{4}$  inch section) from a central position such as A amounted to about 3%.

At first glance, a comparison of the effect of a single rod at A with the effect of rods at both A and B indicates that the effect of a rod at B (a position of relatively low statistical weight) is greater than the effect of the similar rod at A (a position of relatively high statistical weight). It is apparent, however, that this anomaly comes about as a result of the drastic change in neutron flux distributions caused

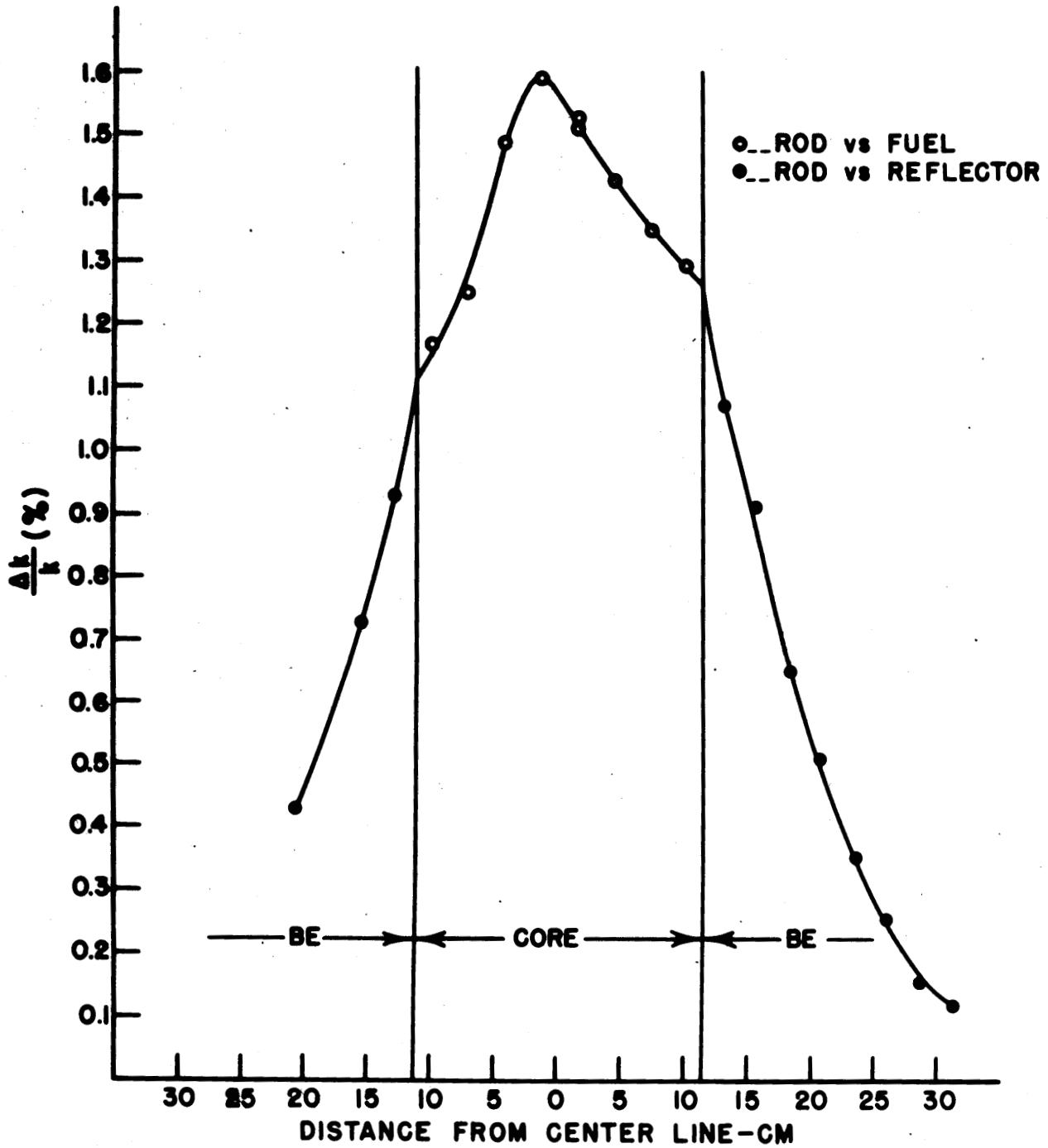
██████████

by the introduction of the first rod at A. The neutron flux is depressed in this region and the statistical weight distribution in the core is shifted in such a way that the maximum is now in the vicinity of position B. Hence it is true that the second control rod, introduced at B, has a greater effect on the asymmetrical core than the control rod at A has on the clean pile. Also, this anomaly is more pronounced in the case of the Cd rods than in the case of the Th rods, as one would expect, since the depression in the neutron distribution and the asymmetry caused in the statistical weight distribution are considerably greater in the case of Cd. Also the statistical weight at A is reduced by a small amount due to the presence of the large experimental hole through the end reflector on the A end of the reactor.

In order to determine the effectiveness of control rods as a function of position in the reactor, a traverse was made along the line indicated by C-D in Figure VII-5 with one of our standard 3/4 inch square Cd rods. In the core the rod replaces one fuel tube (20 grams of fuel) and in the reflector the rod replaces a 1 inch x 1 inch x 26 inch column of Be. Figure VII-6 shows the data obtained from this experiment. The marked asymmetry in the statistical weight distribution is due to the presence of the large experimental holes which extend completely through the reflector on one side of the reactor and begin 15 cm. out in the Be on the opposite side.

III. Neutron Flux Measurements Between Two Thorium Rods. In order to determine the extent of the depression in the thermal neutron flux between two Thorium rods closely spaced, a traverse was taken with Indium foils along a line midway between two 3 1/4" square Thorium rods placed in the core of the 4 kg. mock-up assembly and separated by a distance of about 3-5/8" between inner edges, or about 6-7/8" between centers. The results are shown in Figure VII-7, where the thermal neutron flux between the two rods is compared to the thermal flux observed in the clean assembly with solid reflector and also with thermal flux obtained along the same line after the seven large experimental holes have been introduced through the reflector. For this comparison the three flux distributions have been normalized at the edge of the core since this is the point of maximum heat production

FIG. VII-6  
 STATISTICAL WEIGHT TRAVERSE  
 WITH 3/4" SQUARE CD CONTROL  
 ROD ALONG LINE C-D OF FIG. VII-5

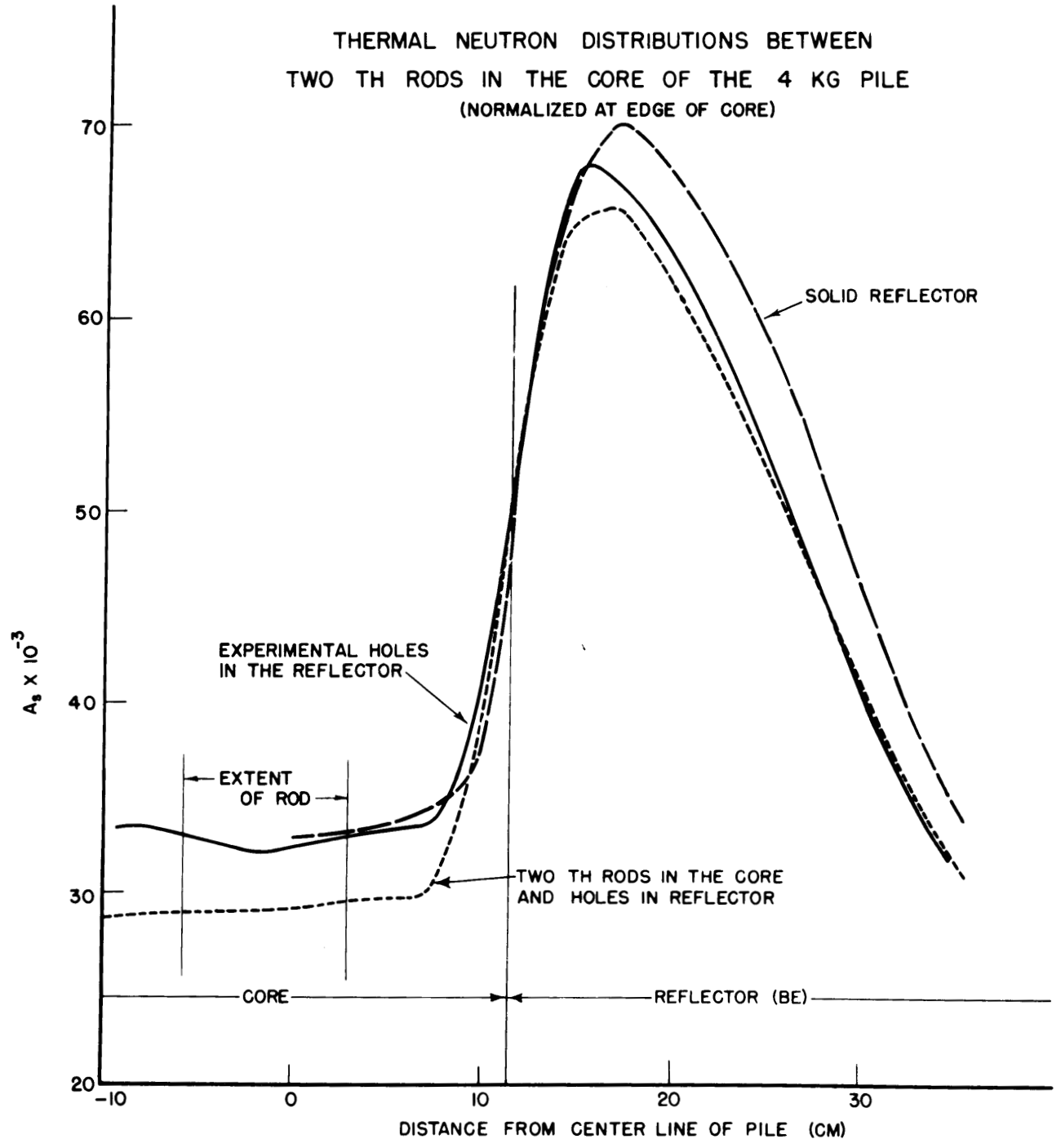


~~SECRET~~

Dr 6085

FIG. VII-7

THERMAL NEUTRON DISTRIBUTIONS BETWEEN  
TWO TH RODS IN THE CORE OF THE 4 KG PILE  
(NORMALIZED AT EDGE OF CORE)



~~SECRET~~

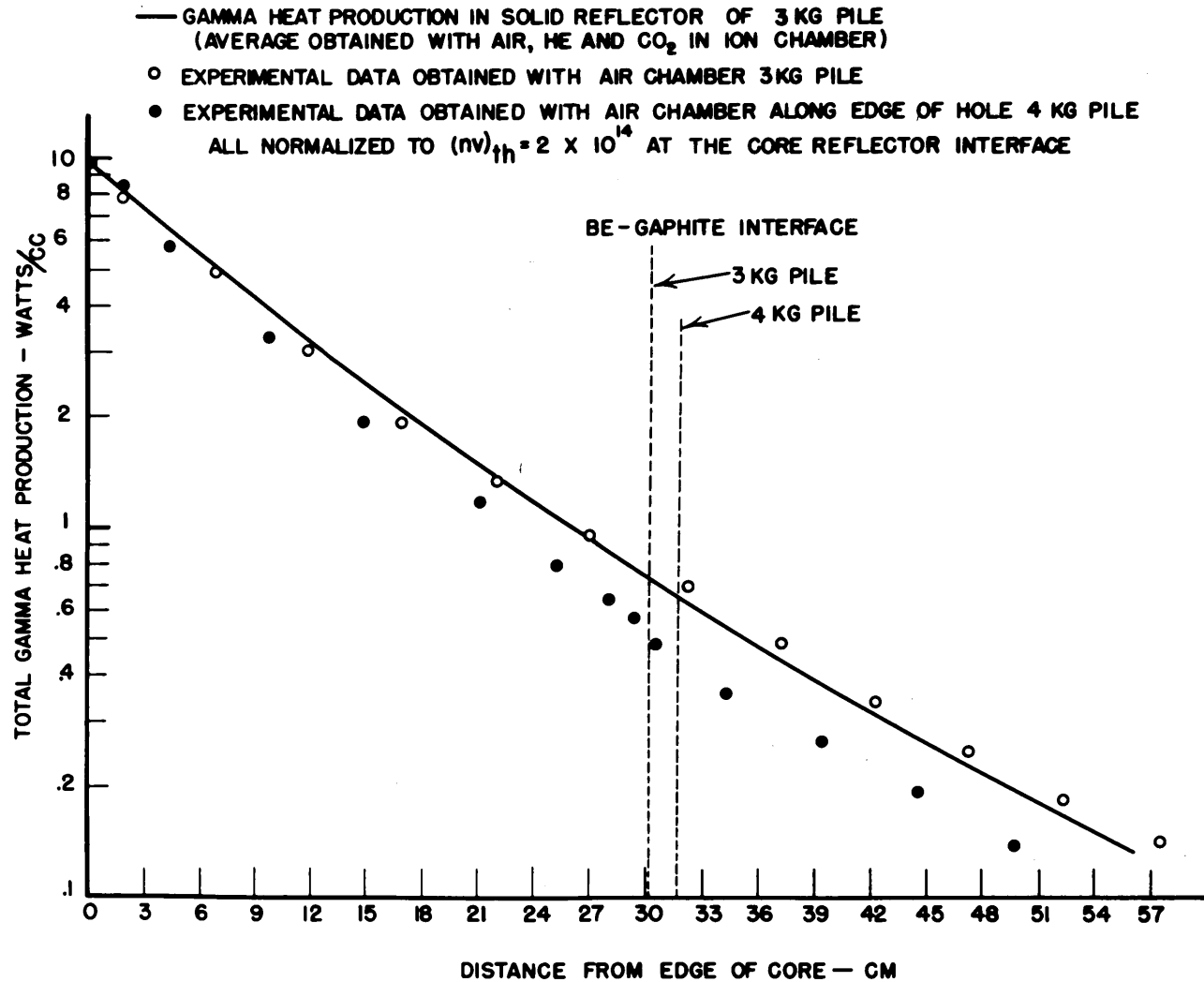
in the reactor.

IV. Gamma Ray Heat Production Along the Edge of an Experimental Hole. It has been suggested that the heat production in graphite due to gamma ray absorption might be increased at points along the edges of the experimental holes due to the streaming of gamma rays from the core through these holes. The concept was essentially that a considerable intensity of soft gamma radiation, which in the case of a solid Be-graphite reflector is strongly attenuated in the Be layer, could stream through an experimental hole and add to the gamma ray intensity in the portion of graphite adjacent to the hole. Since the gamma heat production in graphite measured and reported previously for the solid reflector (see ORNL-51) was somewhat higher than the calculated value, it appeared worthwhile to examine the possibility of increased heating along the edge of a hole.

The measurements were made with the same graphite ion chambers which were used to study gamma heating in the solid reflector. In the present experiment the 10 cc and 200 cc chambers were used and the filling gas was air at atmospheric pressure. Corrections were made as before for the ionization due to protons from the nitrogen (n,p) process. The measurements were made along the edge of the deep center hole, the chamber being placed as near the edge of the hole as practicable. In the case of the Be portion of the reflector, the 10 cc chamber was used and the center of the chamber was in the Be, 0.5 inches from the actual edge of the hole; through the graphite portion of the reflector, the 200 cc chamber was used and the center of the chamber was in the graphite, 1.0 inches from the edge of the hole.

The results of the measurements are shown in Figure VII-8, where the heat production along the edge of the hole, in watts per cc, is compared to: (1) the average gamma heat production in the solid Be-graphite reflector as measured with air, helium and CO<sub>2</sub> fillings in the ion chamber, and (2) the data obtained with the air-

FIG. VII-8  
GAMMA HEAT PRODUCTION



██████████

filled chamber alone in the solid reflector. It is seen that gamma heat production falls off more rapidly along the edge of the hole than it does in the solid reflector. The interpretation of these results is not straightforward, however, because in taking the measurements along the edge of the hole, the ionization chamber was backed on only three sides by reflector. On the fourth side, only the  $\frac{1}{2}$  inch aluminum wall of the hole and the  $\frac{1}{8}$  inch graphite wall of the chamber were effective in absorbing gamma rays, and therefore the Bragg-Gray criteria for the determination of gamma ray energy loss by measurements of this type were not fulfilled to the same degree as in the case of the data taken in the solid reflector.

V. Fast Neutron Flux ( $E > 1$  Mev.) Distribution in the 4 Kg. Be Assembly Mock-up. In order to study the distribution of neutrons having energies greater than 1 mev. a threshold type fission chamber was constructed, using a 145 mg. sample of uranium, supplied by the K-25 laboratory, which is depleted in U-235 content to about one part in 100,000. The uranium metal is coated uniformly on the inner surface of a 12 inch long nickel cylinder which has a .020 inch wall thickness and 1 inch O. D. This cylinder is used as the outer conductor of an Argon filled ion chamber; the ionization collected on the central wire is fed to an A-1 amplifier.

In a preliminary series of experiments the fission chamber was placed in a graphite column containing an Sb-Be neutron source, and also at several different points in the Be reflector of the 4 Kg. mock-up assembly, and the counting rate was observed both when the chamber was bare and when it was completely surrounded by 20 mils of Cd. The thermal neutron flux and the Cd ratio were known in each case from standard Indium foil measurements. From the data obtained in the Sb-Be graphite column, it was determined that 93% of the fissions in U-235 were caused by neutrons having energies below the Cd-cut-off, at a position where the Cd ratio was 3.70. The results of the bare and Cd-covered exposures in the reflector of the Be critical assembly indicated that the U-235 content of the uranium sample was one part in 97,000, in good agreement with

██████████

the depletion figure given by K-25 analysis. The information gained from these experiments enables one to correct the total counting rate of the fission chamber for the counts due to fissions of U-235.

The chamber has been used to investigate the spatial distribution of fast neutrons in the 4 Kg. Be mock-up assembly as shown in Figures VII-9 and VII-10. Figure VII-9 shows a comparison of the fast neutron flux and the Indium resonance flux along a line midway between two of the large experimental holes that extend completely through the reflector, and Figure VII-10 shows a similar comparison along the edge of one of the experimental holes. At the center of the core the  $(nv)_{fast}$  is 40% of  $(nv)_{thermal}$ , in reasonably good agreement with the calculated value of 60% given in MonP-272.

VI. Thermal Flux in a Beryllium Block Placed in the Core of the Mock-up Assembly. It was suggested by Henry Newson that it might be possible to establish a thermal flux considerably greater than that attained at the maximum of the thermal distribution in the reflector by replacing a fuel assembly near the center of the core of the high flux pile by a block of Beryllium. It was reasoned that the pile-up of thermals observed in the Be reflector should take place from each side of the Be block and hence the flux at the center of the block should be increased by perhaps two or three-fold over the maximum on any one side of the reflector. Since such a block would require water cooling if inserted in the high flux pile, the block investigated was made up of 1 inch x 1 inch Be columns, 26 inches long, separated by 1/8 inch strips of lucite. The ratio of Be to lucite by volume was therefore 6/1, and this was estimated to be the optimum ratio to produce the pile-up of thermals at the center of the block. The thermal neutron flux was measured through the center of the block by the use of Indium foils and Figure VII-11 shows the distribution obtained, compared to the thermal distribution measured along the same line with the Be block not present in the core. It is seen that the gain in thermals at the center of the block over the maximum in the reflector is not appreciable.

FIG.VII-9

TRAVERSE TAKEN BETWEEN TWO DEEP HOLES  
AT MIDGEIGHT OF PILE

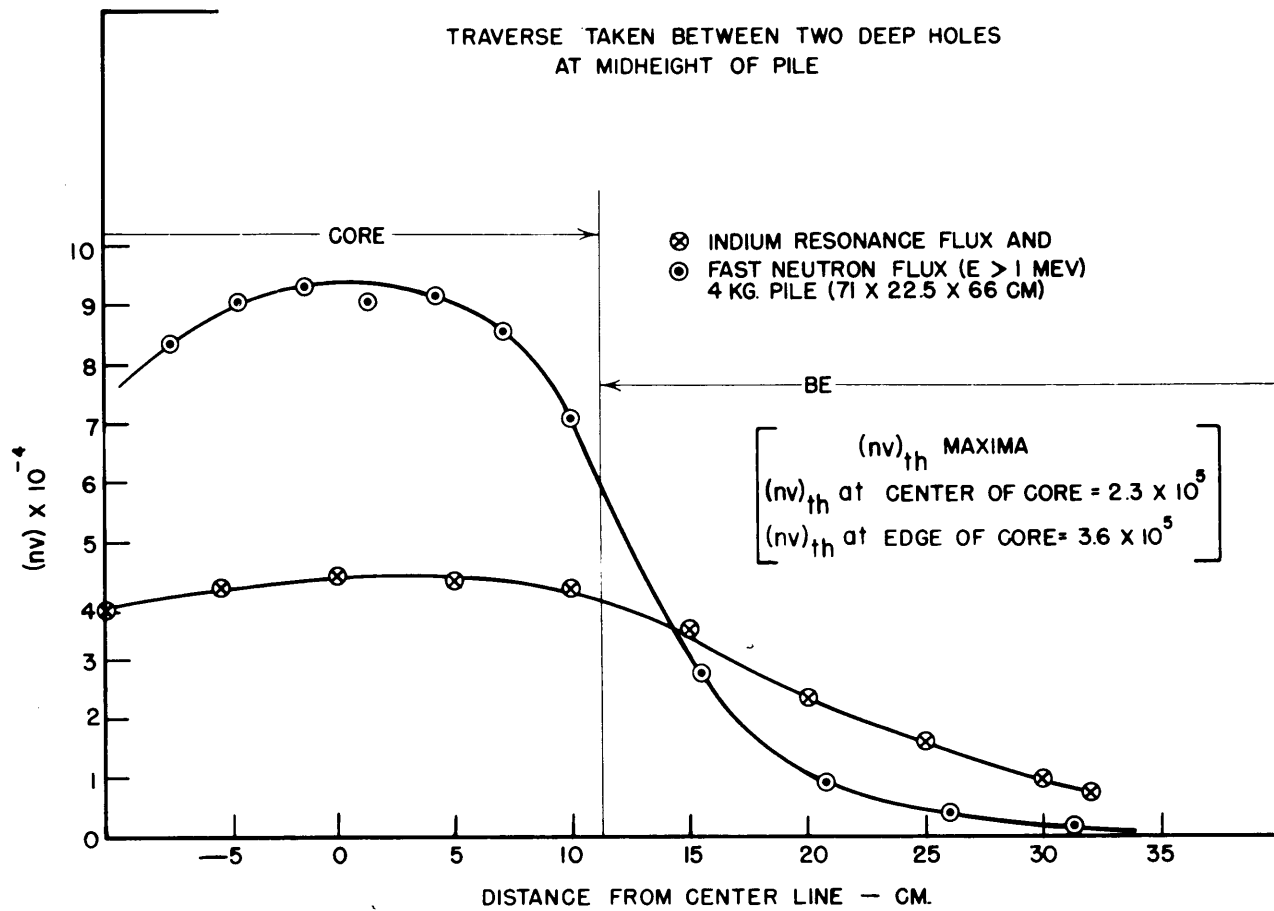


FIG. VII-10  
 4 KG PILE (71 x 22.5 x 66 CM)  
 TRAVERSE TAKEN ALONG EDGE OF  
 CENTER HOLE (IN FIRST INCH OF BE)

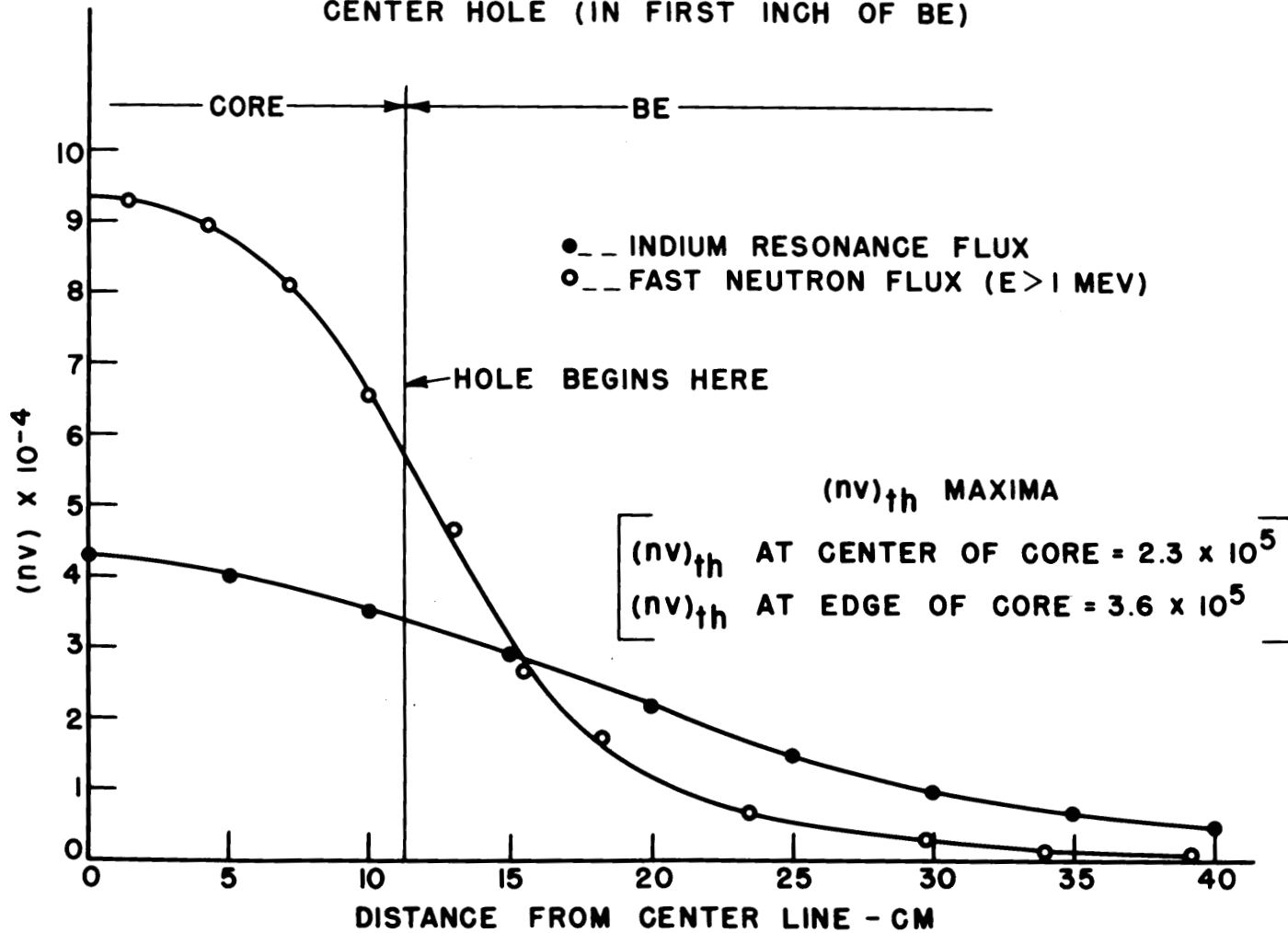
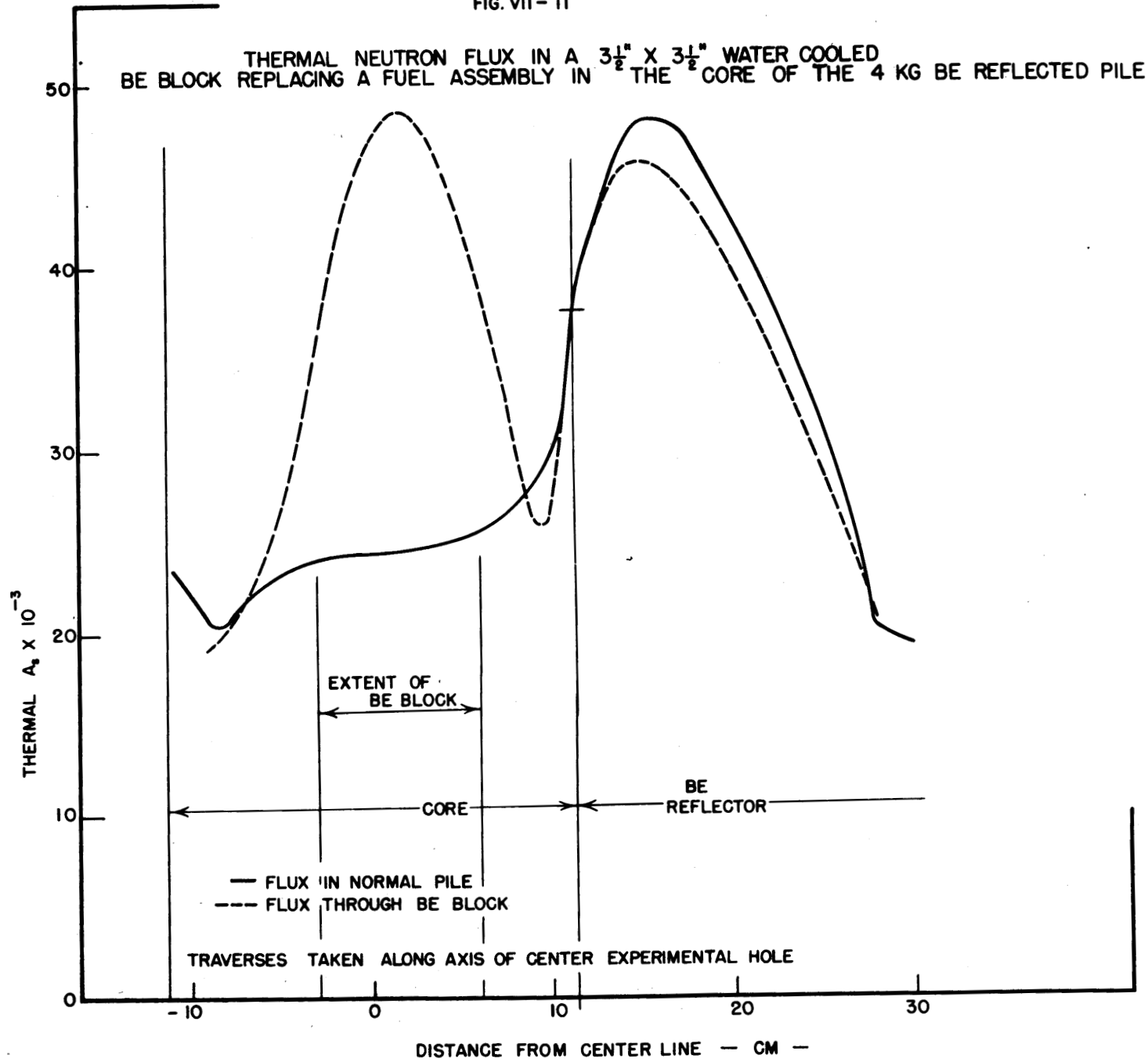


FIG. VII - 11



██████████

VII. Graphite-Reflected Critical Assembly. A graphite-reflected assembly having the standard U-Al-H<sub>2</sub>O core has been constructed and brought up to criticality. The core contains 37.1 gms of U-235 per liter of core and the volume ratio of Al to H<sub>2</sub>O is 0.65. The core volume was laid out to be approximately square in cross-section (10 tubes by 11 tubes) and is reflected on all sides by 61 cm of type FAB-AGHT - Batch 16 graphite. There is no reflector top or bottom.

At a loading of 2.16 kgm. this assembly requires 90 uniformly distributed 30 mil diameter gold wires, totaling 171 cm<sup>2</sup>, to hold it just critical with all control rods withdrawn. The minimum critical mass, corrected for distributed poison and for control rod ports, is 1.8 ± 0.1 kgm., in good agreement with the value calculated by Spinrad (1.82 kgm.).

The spatial distributions of thermal, Indium resonance and fast neutrons in this assembly have been measured. Figure VII-12 shows the thermal and epithermal distributions measured along the perpendicular bisector of one side of the core, at the midheight of the pile. Figure VII-13 compares the Indium resonance flux and the fast (E > 1 mev.) flux along the same line.

FIG. VII-12

NEUTRON DISTRIBUTIONS IN GRAPHITE-REFLECTED ASSEMBLY  
 CORE DIMENSIONS 28.3 X 31.2 X 66 CM. - 61 CM REFLECTOR  
 AL-H<sub>2</sub>O VOL-RATIO = 0.65 FUEL CONCENTRATION 37.1 gms 25/LITER

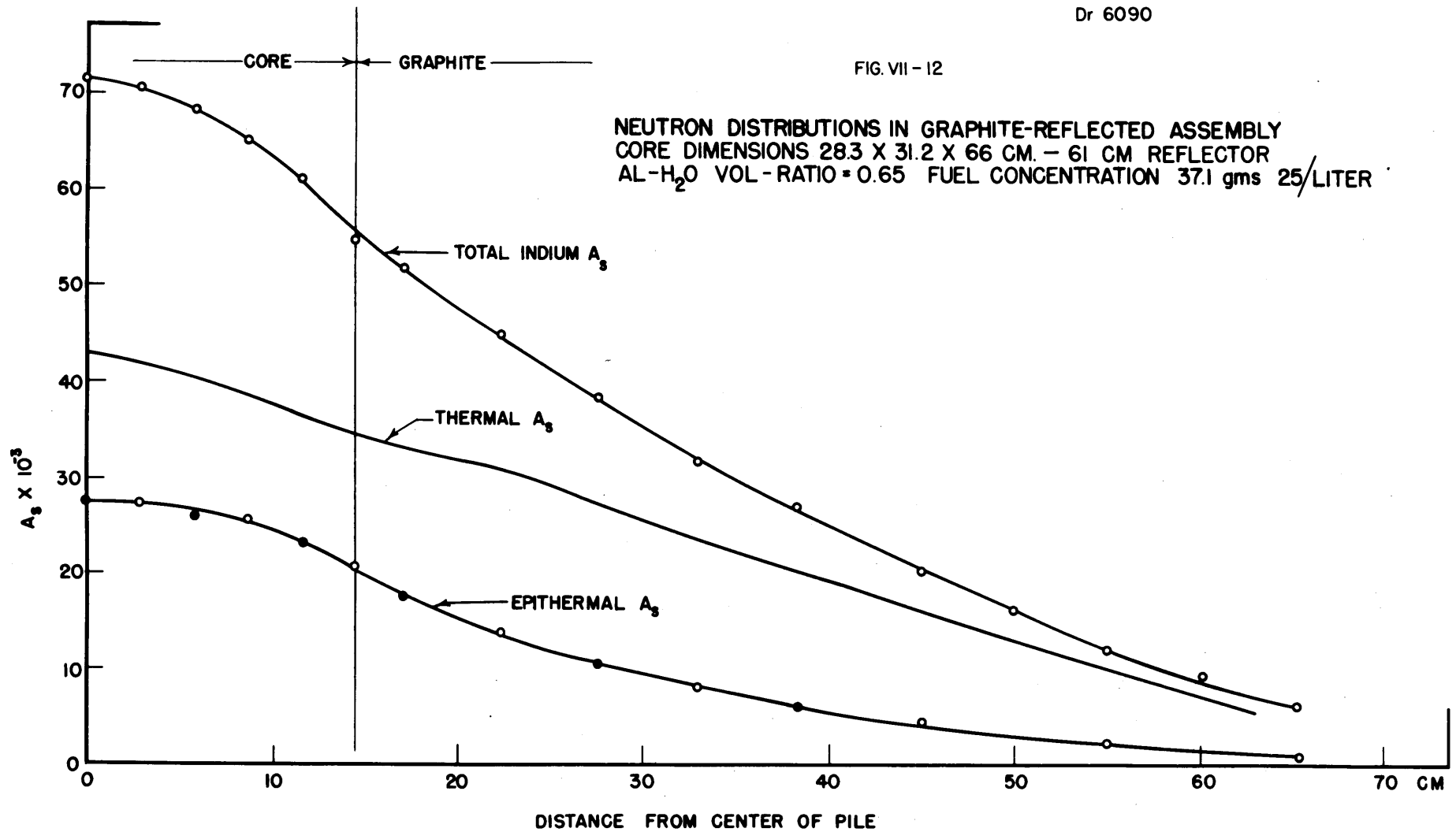
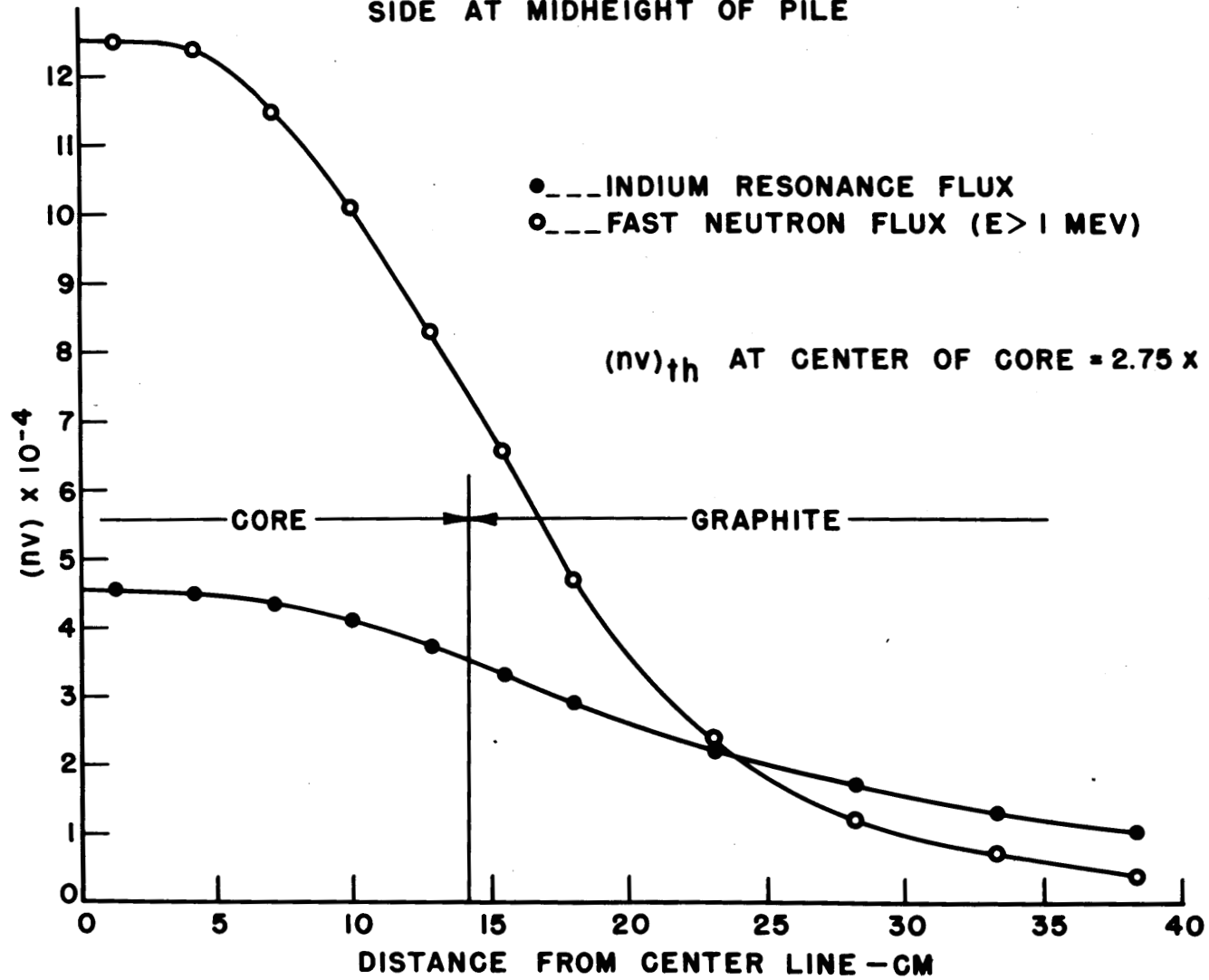


FIG. VII-13  
 GRAPHITE REFLECTED PILE  
 TRAVERSE ALONG BISECTOR OF ONE  
 SIDE AT MIDHEIGHT OF PILE



SECTION VIII - PHYSICS OF SOLIDS

S. Siegel, Section Chief

|                  |                                    |
|------------------|------------------------------------|
| D. S. Billington | H. M. James (on leave from Purdue) |
| W. E. Johnson    | J. A. Barker (on leave from USN)   |
| R. P. Metcalf    | E. E. Conrad (on leave from USN)   |
| F. T. Rogers     | E. B. Roth (on leave from USN)     |
| T. A. Read       | W. Yatchmenoff (on leave from USN) |
| D. K. Stevens    | R. W. Coyle (NEPA)                 |
| S. E. Dismuke    | R. H. Kernohan (NEPA)              |
| M. R. Goodman    |                                    |
| F. A. Sherrill   |                                    |
| M. J. Valentine  |                                    |

Al-U Alloys - (Siegel, L. B. Reynolds, Comdr. Conrad). A series of experiments has been started, with the aid of Dr. M. B. Reynolds, of KAPL, on the release of radioactive gas from the irradiated samples during anneals at various temperatures from 200°C to 500°C. The gas studied is presumably Kr<sup>85</sup> with a half life of 9.5 days. It is released at a maximum rate near 250°C. The effects of these successively higher temperature anneals in reducing the increases in hardness and electrical resistivity produced by irradiation are also being studied.

Uranium Single Crystals - (Read, Sherrill). Uranium single crystals are needed for a variety of studies of the properties of uranium such as investigations of dimensional stability when irradiated or thermally cycled and of the mechanisms of plastic deformation of uranium. Accordingly, attempts are being made to prepare uranium single crystals in wire or rod form. The usual methods of metal single crystal preparation, that is, the Bridgman method of slow solidification from the melt and the strain-anneal method of re-crystallizing critically strained material, do not appear attractive in the case of uranium. The Bridgman method is complicated by the fact that uranium undergoes two phase changes on cooling to room temperature. The strain-anneal method has been applied to uranium by others, particularly A. R. Kaufmann of M. I. T., without success,

██████████

possibly because the marked anisotropy of thermal expansion of uranium makes it impossible to obtain a sufficiently uniform plastic strain in the metal sample.

Two other crystal-growing techniques have been tried here. The first of these consisted of slow recrystallization of a severely cold-worked uranium wire in a steep temperature gradient. This method was quickly abandoned as it failed to produce even a coarse grain size. The second method consisted of slow heating and cooling of the uranium sample through the  $\alpha$ - $\beta$  transformation temperature, again in a steep temperature gradient. This was accomplished by lowering a sealed-off quartz tube containing the sample at the rate of 2 inches per hour into a furnace maintained at 725°C and withdrawing it at the same rate. By this method crystals as long as two inches have been obtained, but none of these have extended completely across the cross-section of the sample. Attempts are now being made to grow larger crystals by other choices of rate of lowering and of the furnace temperature.

Relaxation of Strains in U - (Read, Goodman). As discussed in the previous Quarterly Progress Report, it appears that the blistering of uranium slugs produced by pile exposure results from some original structural inhomogeneity in the uranium such as a variation in type or degree of preferred orientation from one part of the slug to another. These inhomogeneities are being studied through measurements of the dimensional changes of local areas of a slug as the temperature is changed. Non-uniform dimensional changes are to be expected as a consequence of the pronounced anisotropy of thermal expansion of uranium. The experimental method consists of measurements of the change in resistance of wire strain gages cemented to the uranium slug. The results obtained to date have revealed a definite variation in behavior from one part of the slug to another but have also shown that rather large dimensional changes occur at constant temperature after the temperature of the uranium sample has been abruptly changed. This relaxation effect is of considerable interest as it may provide a new method of studying the dimensional instability of uranium. It is therefore

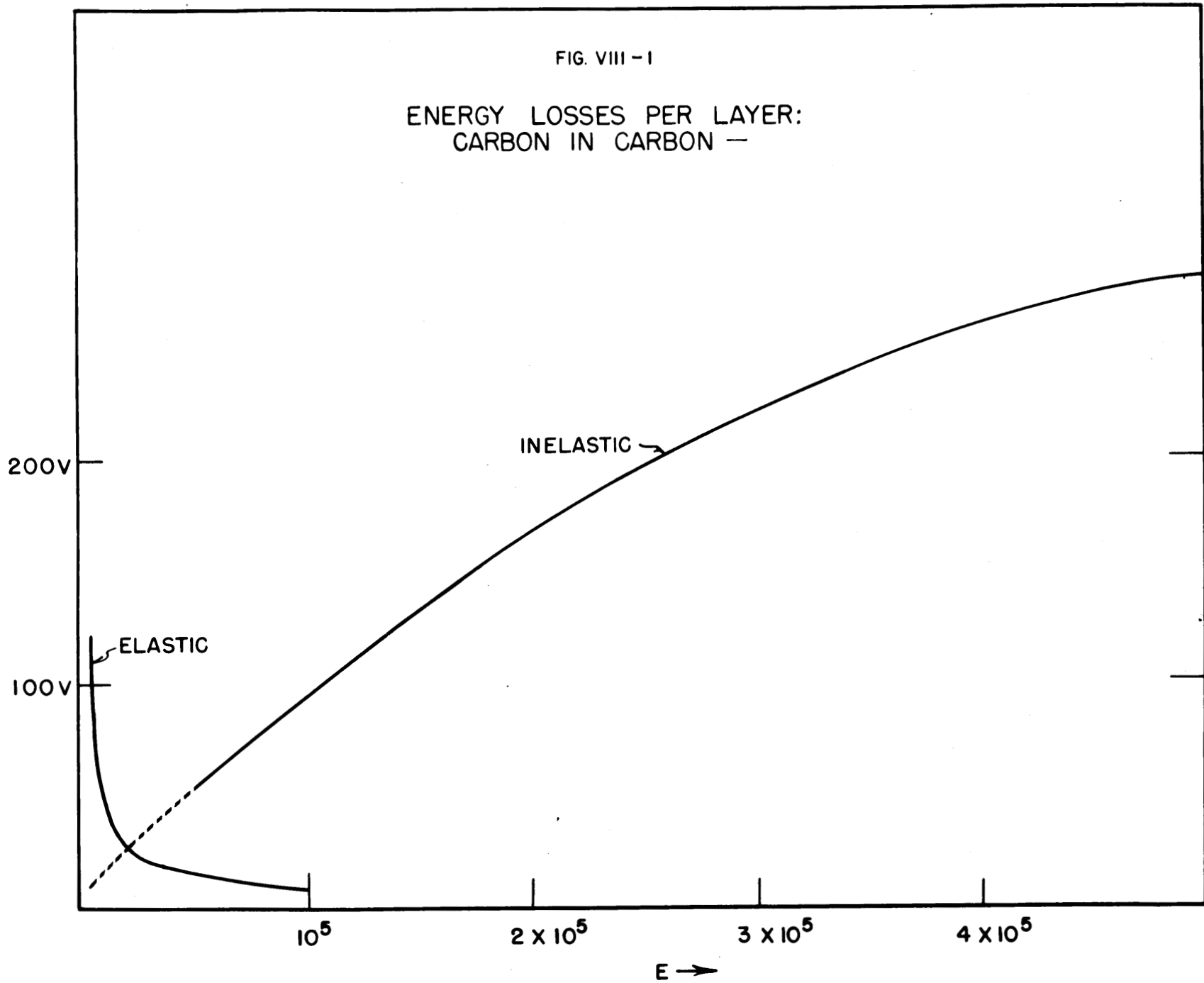
~~SECRET~~

being studied further. Preliminary results indicate that most of the time-dependent strain disappears at constant temperature with a relaxation time of a few hours. This is followed by another relaxation process with a relaxation time of several days. In order to establish whether these relaxation effects are characteristic of the uranium or of the strain gages being used, measurements have been made both with gages bonded with Duco cement directly to the uranium and with gages bonded with Bakelite cement to a thin (0.001 inch) layer of Al-Si alloy on the surface of the uranium. In the latter case the gage could not be bonded directly to the uranium because, at the required baking temperature of 150°C, sufficient oxidation of the uranium underneath the gage occurred to destroy the adhesion. The similarity of the results obtained by these rather different experimental methods indicates that the relaxation effects observed are characteristic of the uranium rather than of the gages.

Theory of Production of Displaced Atoms in Graphite - (James).

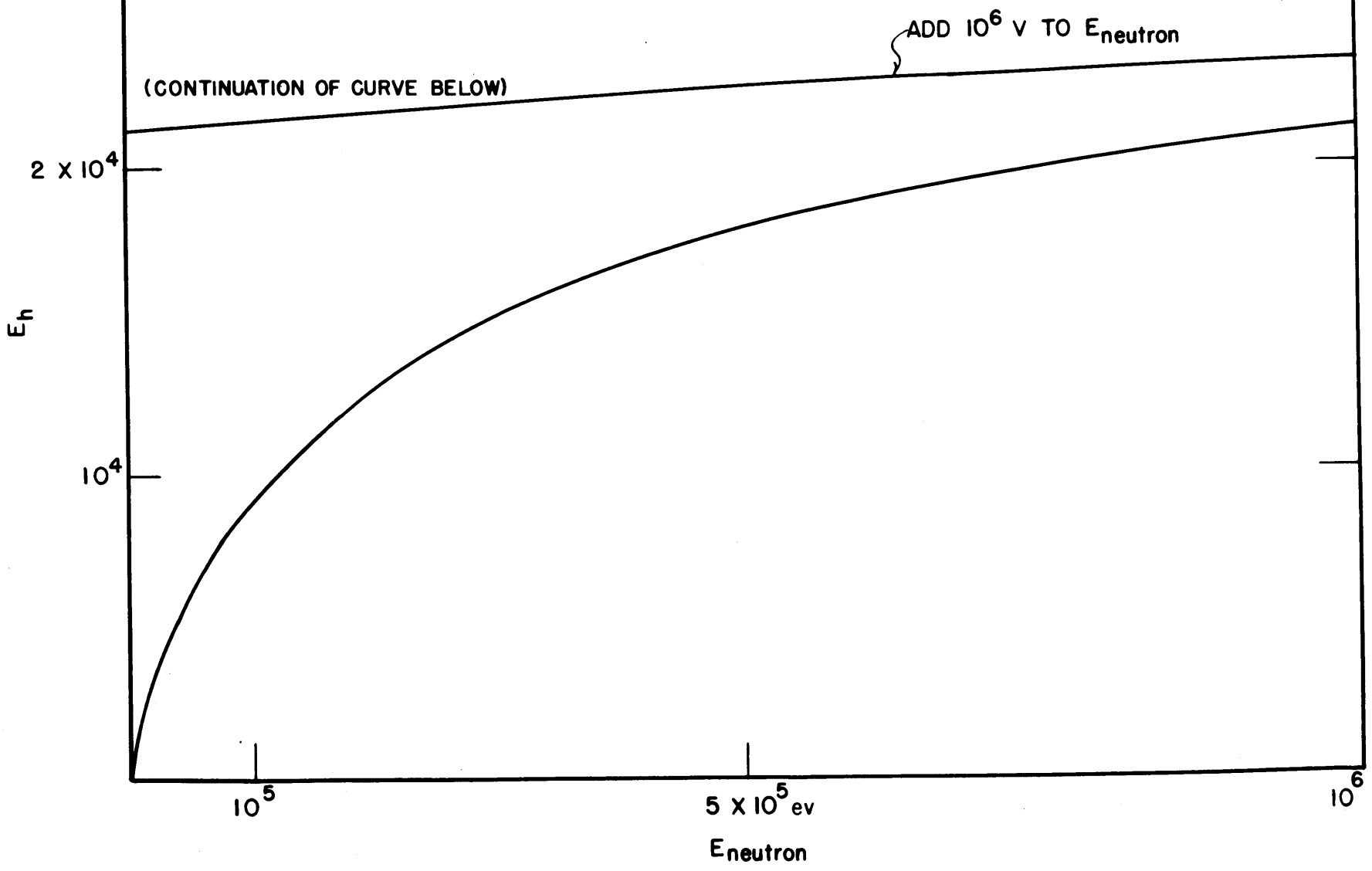
A calculation of the rates of energy loss from a fast recoil C atom by various processes has been made. The energy loss per atomic layer by elastic and by inelastic (excitation and ionization) processes is plotted in Figure VIII-1, against the energy  $E$  of the fast C recoil. The total energy dissipated in producing holes in the lattice is plotted in Figure VIII-2, against the initial energy  $E_i$  of the primary C recoil. It is evident that the major portion of the damage to the graphite lattice occurs during the latter portion of the range of the C recoil. The energy used up in damaging the lattice depends only weakly on the initial energy of the C recoil. Thus a 250 kev, C recoil uses up 25 kev in making holes in the graphite, while a recoil of only 50 kev still uses up 18 kev in damaging the graphite.

FIG. VIII - I

ENERGY LOSSES PER LAYER:  
CARBON IN CARBON -

E →

FIG. VIII - 2  
ENERGY INTO HOLES / NEUTRON COLLISION



██████████

Effects of Radiation on Various Metals - (Billington, Siegel, Read, Valentine). Two general progress reports have been written dealing with this topic, ORNL-115 and ORNL-138, to be issued shortly. Changes in hardness, electrical resistivity, and width and intensity of X-ray diffraction pattern lines have been studied for various alloys and pure metals. Changes are found in many cases; generally it is found that initially soft annealed alloys and pure metals exhibit changes, except for the light pure metals Al, Mg and Be. Metals and alloys in cold worked or hardened conditions also show changed properties in many instances, but a concordant interpretation of the data is not yet clear.

A replica method of studying the metallographic structure of irradiated samples has been developed. Indium metal is used for the replica, the "hot" sample being pressed against it. The method gives adequate detail up to about 500 x magnifications, but does not work well above that.

The disordering of the ordered alloy  $\text{Cu}_3\text{Au}$  by pile irradiation has been described in the previous Progress Report. A test has now been made on the ordered alloy  $\text{CuZn}$  (beta brass). Electrical resistivity measurements were carried out over a period of four weeks on a sample of this alloy in a doughnut hole of the Clinton Pile. No change was found although a change of 0.25 per cent could have been detected. Interpretation of this result is somewhat uncertain, however, for the electrical resistivity of disordered beta brass at room temperature is not known. The relaxation time for the establishment of order in the alloy on cooling through the critical temperature is so short that previous investigators have failed to retain disorder at room temperature by rapid cooling.

Low Temperature Exposure Tube - (Metcalf). Development work has continued on the apparatus for keeping materials at a temperature in the neighborhood of  $100^\circ\text{K}$  while they are irradiated in the pile.

During the last quarter, tests outside the pile have been made of the operation of the cryostat proper. With dry ice in the

~~SECRET~~

cooling tank and with cooling air flowing at the maximum rate for which the apparatus was designed, a temperature of  $-68^{\circ}\text{C}$  was attained in the experimental region of the cryostat. This is considered a satisfactory performance. However, the vacuum jacket developed a leak while the cryostat was cooling down; this may indicate faulty design.

The automatic temperature control was tested. It comprises a thermocouple located in the experimental region of the cryostat, a Leeds and Northrup "Speedomax" controller, and a motor-driven valve on the compressed air supply line. Its performance appeared to be adequate.

One of the cooling tanks is being modified to permit testing the apparatus using liquid nitrogen as the cooling agent.

Semi-Conductors - (Johnson). Survey experiments to determine the effects of pile irradiation on semi-conductors have been continued. In particular resistivity measurements as a function of irradiation time have been made for samples of P type tellurium, P type selenium, P type cuprous oxide and N and P type silicon. In all cases the resistivity has increased with irradiation, and cuprous oxide samples begin to increase immediately upon irradiation. However, with selenium the resistance remains relatively constant for a period of ten to fifteen days and then increases rapidly. This increase probably is not due to the formation of impurities, since the most abundant impurity formed, bromine, tends to decrease the resistance of pure selenium. A possible explanation for the increase of resistance of silicon was thought to be the formation of silicon oxides during irradiation due to the presence of ozone in the pile. This was ruled out by exposing a silicon sample enclosed in an evacuated tube. The resistance of the enclosed sample behaved similarly to the previous exposed samples.

The conductivity  $\sigma$  of a simple semi-conductor is given by

$$\sigma = neb$$

██████████

when  $n$  is the number of carriers and  $b$  the mobility of the carriers. The Hall coefficient  $R$  for a simple semi-conductor is given by

$$R = - \frac{3\pi}{8ne}.$$

Hence by simultaneously measuring the conductivity and the Hall coefficients for a given sample, it is possible to determine the number and type of carrier, and the mobility of the carrier.

Equipment has now been assembled for making these measurements on samples before and after irradiation. Design of equipment for making these measurements during irradiation is nearing completion. This equipment should enable the determination of the relative roles of the number of carriers, and of the mobility of the carrier in causing the observed resistance changes.

The work reported above and that reported in the previous Quarterly report has been done on the bulk properties of semi-conductors, i.e., either on small plates of material or in the case of crystal rectifiers at high enough voltage to make the rectifying barrier ineffective. Measurements have now been made on the forward resistance of the germanium 1N38 at 0.1 and 3 volts alternately, as a function of irradiation time. The measurements at 0.1 volt give the sum of the barrier resistance and the bulk resistance while those at 3 volts give the bulk resistance alone. The results of such measurements show that the barrier resistance decreases while the bulk resistance increases. The two curves meet at the maximum of the bulk resistance curve and then decrease together. Hence the effect of irradiation is to destroy the rectifying barrier between germanium and the tungsten cat-whisker. A similar experiment carried out on a silicon 1N21 does not show the same effect. Both the forward and back resistance increase continuously as a function of time of irradiation.

Effect of Neutron Bombardment on Internal Friction - (Read, Dismuke)

As part of the general program of study of the effects of irradiation on the plastic properties of solids, internal friction measurements are being made on metal single crystals mounted in front of a

[REDACTED]

pile beam hole. This method of irradiation was chosen for the first experiments of this type because it permits the maximum precision of measurements of internal friction insofar as irradiation induced changes are concerned. The internal friction of metal single crystals is so extraordinarily structure-sensitive that measurable changes in it might well be produced by an irradiation which is too small to affect detectably other physical properties.

Physics of Solids Seminar. During the past quarter a weekly seminar was started. An experimental and theoretical description of the properties of semi-conductor rectifiers was presented by W. E. Johnson, a series of talks on "Electronic States in Perturbed Periodic Systems" has been presented by H. M. James.

~~SECRET~~

Section IX - Mathematics and Computing

A. S. Householder, Section Chief

Stochastic Estimates of Age in Water - (G. Goertzel, B. I. Spinrad, E. A. Forbes, P. O. Levy, M. K. Hullings, M. R. Arnette, A. S. Householder)

As a pilot study, 100 neutrons were followed by hand computations from 10 mev slowing down in water to 1 ev. Methods of computation were essentially as outlined for the IBM in an informal memorandum by Goertzel and Householder.

When the population was collected statistics were computed on  $z$  and on  $u = \log (E_0/E)$ , as follows. For the  $z$ -statistics energy levels at integral powers of 10 were selected. For any given energy level, record was made for each neutron of the  $z$ -value at the collision which first carried it to an energy below this level. The moments about the mean were then calculated for this distribution. Moments were taken about the mean instead of about the origin, since these are statistically preferable. Computations were made by taking between 15 and 20 class-intervals and then applying Sheppard's corrections.

The results are as follows:

Moments in  $z$

|         | $10^6$            | $10^5$            | $10^4$             | $10^3$             | $10^2$             | 10                 | 1                  |
|---------|-------------------|-------------------|--------------------|--------------------|--------------------|--------------------|--------------------|
| $\mu_2$ | $1.0 \times 10^2$ | $4.4 \times 10^2$ | $4.5 \times 10^2$  | $4.6 \times 10^2$  | $4.6 \times 10^2$  | $4.5 \times 10^2$  | $4.6 \times 10^2$  |
| $\mu_3$ | $5.2 \times 10^2$ | $9.1 \times 10^3$ | $9.3 \times 10^3$  | $9.4 \times 10^3$  | $9.5 \times 10^3$  | $9.5 \times 10^3$  | $9.3 \times 10^3$  |
| $\mu_4$ | $5.6 \times 10^4$ | $9.1 \times 10^5$ | $1.02 \times 10^6$ | $1.01 \times 10^6$ | $1.01 \times 10^6$ | $1.01 \times 10^6$ | $1.00 \times 10^6$ |

All units are powers of a centimeter.

These results are somewhat paradoxical in that the greater increase occurs between energies  $10^6$  and  $10^5$ , whereas one would expect it to occur above  $10^6$ . The explanation appears to be

that the small sample of 100 is not adequate for any high degree of precision -- a fact that was, of course, recognized in advance.

Moments in the distribution in the lethargy  $u = \log (10^7/E)$  were computed about the mean after the first collision, the second collision, etc. These moments, and the positions of the means, are given in the following table, along with the values of skewness and kurtosis.

MEAN AND MOMENTS ABOUT THE MEAN, SKEWNESS AND KURTOSIS IN  $\mu$

| Col. | $\bar{u}$ | $\mu_2$ | $\mu_3$ | $\mu_4$ | sk   | kur  | N   |
|------|-----------|---------|---------|---------|------|------|-----|
| 1    | 0.78      | 1.00    | 2.29    | 8.84    | 2.29 | 5.84 | 100 |
| 2    | 1.58      | 1.85    | 3.17    | 17.71   | 1.26 | 2.18 | 100 |
| 3    | 2.55      | 3.16    | 5.52    | 40.77   | .98  | 1.08 | 100 |
| 4    | 3.32      | 4.32    | 7.85    | 70.66   | .87  | .79  | 100 |
| 5    | 4.16      | 6.46    | 14.47   | 156.23  | .88  | .74  | 100 |
| 6    | 5.07      | 6.56    | 10.92   | 131.44  | .65  | .06  | 100 |
| 7    | 6.07      | 8.34    | 13.88   | 205.40  | .58  | -.05 | 100 |
| 8    | 6.83      | 9.26    | 13.49   | 222.81  | .48  | -.40 | 100 |
| 9    | 7.51      | 10.37   | 13.92   | 269.05  | .42  | -.50 | 100 |
| 10   | 8.21      | 10.20   | 8.31    | 247.50  | .26  | -.62 | 98  |
| 11   | 8.73      | 10.01   | 5.27    | 222.72  | .17  | -.78 | 95  |
| 12   | 9.31      | 9.23    | -0.51   | 204.20  | -.02 | -.60 | 90  |
| 13   | 10.02     | 8.69    | -8.13   | 180.27  | -.32 | -.61 | 88  |
| 14   | 10.87     | 8.63    | -9.09   | 170.94  | -.36 | -.70 | 87  |
| 15   | 11.48     | 8.36    | -13.53  | 189.48  | -.56 | -.29 | 82  |

After 15 collisions the number of epithermal neutrons was diminishing rapidly and no further moments were computed.

~~SECRET~~

Members of the Section have also participated in the following projects:

Project ARUU (R. R. Coveyou) for Health Physics Division.

Computations on the  $\beta$  spectrum of gold (F. O. Levy) for Paul Levy.

Least-square curve fitting to some biological data (P. O. Levy) for Dr. R. F. Kimball of the Biology Division.

Calculations of inverse Laplace transforms (R. Crook) for Henry Straus.

Least-square curve fitting (R. Crook) for W. M. Good.

Computations of  $\phi_j(\alpha)$  for various values of  $j$  and  $\alpha$  (M. R. Arnette) for M. E. Rose.

Solution of a transcendental equation for various values of relevant parameters (M. R. Arnette) for F. H. Murray.

Computation of photo-disintegration cross-sections (E. A. Forbes) for A. E. Snell.

Computation and plotting Inhour formula for rising and falling activities from most recent data on delayed neutron fractions and periods (E. A. Forbes) for A. B. Martin.

Computation of counting rates from experimental records (M. K. Hullings) for E. C. Campbell.

Computations of atomic positions in ice (M. K. Hullings) for E. O. Wollan.

[REDACTED]

R. R. Coveyou is back at work; H. L. Garabedian has left to work for the AEC in Washington, D. C.; B. I. Spinrad and Nancy Dismuke are working with the Section.

Greatest activity has related to stochastic methods of solving integral and differential equations and to machine computations. A general survey will be given first, and then some of the individual problems will be described in detail.

Work on programming the computations for the internal conversion problem (cf. the previous Quarterly Report and the discussion below) is proceeding under the direction of B. I. Spinrad. This computation is to be done either on the SSEC by the International Business Machines Corporation, or on the Automatic Sequence Controlled Calculator at Harvard.

Arrangements have been made with Dr. C. C. Hurd and Mr. F. C. Uffelman whereby a series of computations will be performed on standard IBM equipment, some at K-25 and some at Y-12. At K-25 an elaborate set of statistical regression equations are being set up for Dr. J. S. Felton of the Health Division with the collaboration of members of this Section. At the same time, plans are being made for solving certain two-dimensional pile equations on the installation at K-25, using a Gauss-Seidel iterative procedure. This method is a precursor of the popular relaxation methods, the latter being unsuited for mechanization in view of the choices required.

At Y-12 the problems are to be chiefly stochastic. Ruth Arnette and Mrs. Hullings are now spending their full time there and will continue to do so while X-10 problems are being run. It is hoped that this will permit the completion at an early date of the stochastic estimate of neutron age in water that was started some time previously.

Other stochastic problems under consideration for solution at Y-12 are the following. The first is the age from high initial

██████████

energies in a mixture of H, O, N and C simulating tissue. This problem has been discussed with members of the Health Physics Division and would be set up and analyzed with their collaboration. The IBM routines would be almost identical with those employed for the current computation of age in pure water from a low-energy monochromatic source. There has been some discussion of the advisability of performing a stochastic estimate of age in graphite to compare with the data of Hill and Roberts. This computation would be similar, though somewhat simpler in its details, but would require a great many more collisions for completion, and probably a great many more individual particles for adequate precision.

The next likely problem is that of the energy distribution of neutrons in natural uranium. This might be performed as a matrix iteration, though the stochastic estimate seems most feasible. In the problem as conceived, spatial distributions will not be considered. Neutrons following an appropriate initial distribution in energy will be slowed down, and will be absorbed either with or without fission. This leads to a gradual change in the overall distribution of energies with possibly an asymptotically stable form

A proposed long-range series of stochastic estimates would involve the distribution of neutrons undergoing collision near thermal energies with monoatomic substances of various types, including crystals.

Preliminary results of stochastic estimation are described below. In addition to these and the problems just mentioned, investigation is being made of the possibility of obtaining stochastic estimates of the solutions of partial differential equations. For this, two possibilities are at once apparent. One may make the special assumptions which yield the diffusion equations as a special case of the Boltzmann equation and set up the stochastic process accordingly. In this case one encounters deviations at the boundaries of the same character exactly as those encountered in the attempt to represent the distribution of neutrons by the

██████████

diffusion equation. Or else one may follow the lines of the now classical discussions of Brownian movement. In this event the boundaries present no problem in principle, and furthermore the process is the simplest possible. The difficulty is that an inordinate number of steps may be required. Nevertheless the extreme simplicity of the individual steps adapts the method admirably to machine methods. Moreover it is possible to build up a standard population of collisions that is independent of the character of the boundary, of the nature of the source, and even of the number of dimensions. Thus if the boundaries are not too complex, the utilization of this population for the solution of different boundary problems involves principally a change in sorting techniques.

Solution of Milne Problem - (G. Goertzel, B. I. Spinrad, T. W. Mulliken, R. R. Coveyou, M. R. Arnette, A. S. Householder).

This problem was proposed by Drs. W. S. Snyder and J. Neufeld of the Health Physics Division for purposes of estimating the density of collisions of thermal neutrons as a function depth within a slab of tissue. A parallel entering beam of neutrons was assumed and the equation taken in the form

$$f(x) = e^{-x} - 0.4961 \int_0^{10} E_1(|t-x|) f(t) dt.$$

The coefficient of the integral

$$0.4961 = \lambda/2$$

represents an assumed probability of

$$1 - \lambda = .0078$$

of an absorption at any collision; the exponential term outside the integral represents the distributions of depths of first collisions; and the function  $E_1$  represents the distribution of changes in depth between successive collisions.

SECRET

By means of an alignment chart devised by Spinrad it was possible to accumulate a population quite rapidly. A total of 100 neutrons were followed. The first random number for any neutron gave the depth of the first collision; thereafter consecutive random numbers gave locations on the alignment chart from which consecutive collisions could be located in depth. The neutron was dropped when it escaped from either boundary or was absorbed.

These neutrons yielded something over 1800 collisions and the resulting distribution was used as a trial function for an iterative solution of the integral equation by numerical integration. It turned out that the second iteration provided almost negligibly small corrections and the process was stopped. It appeared further that the resulting curve could be represented with considerable accuracy by

$$f(x) = 2.98 (x + 0.806) e^{-0.464x}$$

A noteworthy feature of the curve and the distribution is the occurrence of a maximum a short distance from the incident boundary.

The iteration required for the improvement of the stochastic estimate is in this problem particularly simple. Since this is not always possible or feasible it appeared to be of some interest to examine further the result of the unimproved stochastic estimate. For this purpose a function of the same form was fitted by least squares to the stochastic data, points being weighted by the reciprocal of the observed ordinate. Two such fits were made, one using 10 and the other using 20 class-intervals. The histogram for this latter case was quite irregular, giving evidence of considerable statistical fluctuation. The resulting curves in the two cases came out to be

$$4.93 (x + 0.234) e^{-0.544x} \quad (10 \text{ intervals}),$$

$$4.19 (x + 0.416) e^{-0.526x} \quad (20 \text{ intervals}).$$

[REDACTED]

These parameters differ substantially from those obtained after iterative improvement of the stochastic estimate. However, two points must be noted in this connection. The first is that although the functional form employed for representing the result gives a fairly close fit, it is nevertheless not theoretically correct. But second, and more significant, is the fact that the 1800 collisions are not statistically independent. One must conclude that the 100 neutrons are not sufficient for a precise estimate of the collision densities.

As this work was going on it was realized that by very slight changes in the procedure it would be possible to develop a population for estimating collision densities in slabs of any thickness whatever. Instead of recording at each step the depth of the collision one merely records the change in depth,  $\Delta z$ , between collisions. One thus develops a population of  $\Delta z$ 's with no consideration of the location of boundaries. Now, given boundaries in any position, one adds  $\Delta z$ 's until one boundary or the other is transgressed, after which the next  $\Delta z$  is taken to start a new neutron. This is one of the striking advantages of the stochastic method, that the same basic population can be used for an entire class of problems.

Such a population is now being collected and about 4000  $\Delta z$ 's have been recorded. One of the first uses to be made of these is to obtain collision densities from an isotropic source in slabs of several thicknesses.

This work will all be described in greater detail in reports to be prepared later.

Gauss-Seidel Iteration - (B. I. Spinrad) In conjunction with Mr. Buford Carter of K-25, and in accordance with the suggestion made by Mr. Goertzel, a procedure for solving two dimensional relaxation problems by a Gauss-Seidel iteration procedure on standard IBM equipment has been worked out. The procedure consists of replacing the differential

██████████

equation to be solved by a difference equation over a finite lattice, assuming a set of values of the function whose solution is to be determined, and iteratively correcting each value in terms of its neighbors. Boundary conditions are set numerically. Each lattice point is represented by an IBM card, on which is punched the value of the function at the lattice point and at the four nearest neighboring points in a square lattice. A correction is then made on each point, new values punched, and the process repeated until a convergent set is obtained.

The sample problem being considered is that of a square pile, 32 cm per side, in a square reflector 32 cm thick. Constants of the regions have been arbitrarily chosen to be in the same order of magnitude as many pile problems. This problem is being done according to the one group picture, and is complicated by the necessity for determining a critical buckling. However, the contemplated detailed procedure will correct the buckling and test for convergence simultaneously, and consequently the critical condition does not require any extra time.

The octant which is being treated in the problem (symmetry conditions reduce it to a single octant rather than the full square) has 91 lattice points with a spacing of 4 cm. between points. Mr. Carter estimates that a single iteration for this number of points should take between  $\frac{1}{2}$  and 1 hour on the K-25 machine.

Internal Conversion Calculation - (G. Goertzel, B. I. Spinrad, N. Dismuke, M. K. Hullings, T. W. Mulliken). The computation of internal conversion of  $\gamma$  radiation in the K shell has reached the final stages of preparation for machine coding. This computation uses a reduced formulation derived from the formulae given in MonP-426.

There is considerable manual computation necessary before the problem can conveniently be started on a machine. The extent of this hand computation is, however, dependent upon the final decision as to which machine is to be used for the

██████████

calculation. This is due to the fact that because there are many operations indicated (raising a complex number to a complex power and interpolating  $\Gamma$  functions of complex argument are the two most troublesome) which, while favorable on a time comparison for machine computation, require the use of a large extra amount of tabular data and order sequencing. The cost of the extra machine time involved has not yet been estimated.

A listing of the problems auxiliary to the internal conversion calculation follows:

I. Preparation of a Flow Sheet. The first step in any preparation of a problem for machine computation is the representation in a diagrammatic form of the sequence of operations required to get the answer. This "flow sheet" gives an overall view of the problem, tracing out the intermediate steps, and outlining in a general way the linear sequence of operations required and the contents of the storage position as the operation proceeds.

II. Decision as to Which Cases are to be Computed. The particular representation of the hypergeometric series which we have chosen as most useful is convergent only for the case  $|\zeta| > 1/2$ . Since the hypergeometric series evaluation is the largest part of the calculation, and since the convergence of the hypergeometric series is roughly as is the geometric series, and hence slow for  $|\zeta|$  near  $1/2$ , we have decided to keep  $|\zeta| > 1$  as much as possible. This is one limitation on the points to be computed at present, and corresponds to a lower  $\gamma$  energy bound for given  $Z$  (atomic number).

Classical formulae predict that the internal conversion coefficients will vary roughly with  $Z^3$  and  $1/k$  ( $k = \gamma$ -energy). We have used this as a spacing criterion for points in  $Z$ - $k$  space, distributing them proportionately to  $Z^3$  and  $1/k$  so that interpolation may most conveniently be performed on the answers.

Messrs. Stoughton, Rose, and DeBenedetti were consulted to determine whether the points chosen were useful insofar as they corresponded to regions of the Z-k plane in which  $\gamma$ -radiation is known to exist. It was found that some of the more important regions corresponded to points for which  $1/2 < \zeta < 1$ . Consequently, a few points in this "slowly converging" region were added.

Lastly, the k used for a given Z were so chosen as to yield values of  $\beta$  which were even 1/20 integral values. This was done so as to avoid as much as possible two-dimensional interpolation of  $\Gamma$  functions for which  $\beta$  is the imaginary part of the argument. The computation of these k and  $\beta$  was done by Mrs. Hullings.

A table of points tentatively chosen is given below. Points marked with an asterisk are in the region of poor convergence of the hypergeometric series. k's are given in  $m c^2$  units.

TABLE I

z:

| 40       |                           | 54       |                           | 64       |                           | 72       |                           |
|----------|---------------------------|----------|---------------------------|----------|---------------------------|----------|---------------------------|
| <u>k</u> | <u><math>\beta</math></u> | <u>k</u> | <u><math>\beta</math></u> | <u>k</u> | <u><math>\beta</math></u> | <u>k</u> | <u><math>\beta</math></u> |
| .275251  | .5                        | .290869  | .7                        | *.285625 | .9                        | *.324481 | 1.0                       |
| .506194  | .4                        | .407051  | .6                        | .458297  | .7                        | .475295  | .8                        |
| .856017  | .35                       | .673072  | .5                        | .708771  | .6                        | 1.220333 | .6                        |
| 3.378036 | .3                        | 4.911961 | .4                        | 1.916893 | .5                        | 2.532825 | .55                       |

| 78       |                           | 83       |                           | 88       |                           | 92       |                           | 96       |                           |
|----------|---------------------------|----------|---------------------------|----------|---------------------------|----------|---------------------------|----------|---------------------------|
| <u>k</u> | <u><math>\beta</math></u> |
| *.313742 | 1.2                       | *.461086 | 1.0                       | *.538018 | 1.0                       | *.465400 | 1.2                       | *.518121 | 1.2                       |
| .468819  | .9                        | .900035  | .75                       | .910399  | .8                        | 1.097898 | .8                        | .879927  | .9                        |
| .895946  | .7                        |          |                           | 1.746539 | .7                        | 2.792598 | .7                        | 2.087521 | .75                       |
| 2.340498 | .6                        |          |                           |          |                           |          |                           |          |                           |

██████████

Points of higher energies can be added with not too much difficulty, if one uses a less restricted condition on the  $\beta$ . For the present, these are being neglected until a comparison of lower energy points with non-relativistic results has been obtained.

III. Check on Procedure by Preliminary Coding and Time Estimate on a Sample Problem. In order to check the validity of the procedure outlined in the flow sheet, and to obtain a reasonable time estimate for the procedure, it is necessary to do a manual computation on a single case from a coding derived from the flow sheet. A simple three-address code was devised, and the flow sheet converted into a coding by Mrs. Dismuke. A sample card, with explanation, is given below:

#1

| <u>No In</u> | <u>Open With</u> | <u>Operation</u> | <u>Store At</u>                  |
|--------------|------------------|------------------|----------------------------------|
| 24           | 34               | ÷                | 13                               |
| 13           | 34               | +                | 23                               |
| 23           | 80               | x                | 23                               |
| 13           | 34               | -                | 13                               |
| 23           |                  |                  | 34                               |
| 13           | 70               | -                | If + go to # 1<br>If - go to M S |

This card is an iterative square rooting sequence (sequence #1). The numbers in the first, second, and fourth columns refer to addresses in the internal memory, by which the numbers (signed, or with sign modified as in the bottom line) may be identified. The first column gives a number which is to be operated on arithmetically by the number in the address given by the second column according to the operation in the third column. The fourth column gives the address in which the result is stored. A typical transfer order, as in the next bottom line above, simply shifts a number, without operation, to another storage position. The end of a sequence is indicated by a written order, telling which

[REDACTED]

sequence to proceed to. In this case, the number whose root is wanted is located in position 24, and the root found, after convergence, in 34. The number in 80 is  $1/2$ , and the number in 70 is a convergence limit (in this case,  $10^6$ ) for the operation.

The storage spaces have been set up on a blackboard, and the coding completed. Mrs. Dismuke and Mr. Mulliken are now engaged in going through a sample case. Present indications are that the flow sheet is essentially correct, and that previous estimates as to machine time are probably high. This computation should take about two weeks. Mrs. Hullings has also participated in this work.

It has been found that the machine coding scheme is feasible. The procedure requires two people, one reading the orders and working a Friden calculator (the analogs, respectively, of the order tapes and the arithmetic organs of a sequence computer), and one functioning as a memory recorder and interpreter.

The computation is being done for the case  $Z = 40$ ,  $k = .275251$ . It is hoped that the answers will check non-relativistic formulations sufficiently well that the remaining calculations for  $Z = 40$  will not need to be performed.

IV. Computation of Preliminary Constants. Mrs. Hullings has computed many of the simple constants which are functions of  $Z$ ,  $k$ , and  $J$  for the cases we intend to do. If it is decided not to use machine table look up, considerable hand interpolation of  $\Gamma$ -functions and of fractional and complex powers of numbers is required.

██████████

## SHIELDING PROGRAM

E. P. Blizard, Physics Division, Leader  
T. Rockwell, Technical Division, Associate Leader

The Physics Division's Shielding Program has been merged with the Technical Division's Shielding Program. Identical reports of the work are included in both Divisions' Quarterly Reports.

Additional personnel have been obtained, test facilities are being expanded, and more space for the making up of test samples is being provided. It is expected that an increased amount of engineering data can be produced and attenuation measurements will be more clean-cut.

Shielding Symposium - (Rockwell) . Plans are being made for a classified Shielding symposium to be held at Oak Ridge National Laboratory September 27 through 30, 1948. Invitations have been sent to persons at nearly fifty different locations. Indications are that over a hundred persons will attend the symposium.

The purposes of the symposium are to cover as completely as possible the field of shielding. Some of the items to be discussed are:

1. The problems of reactors, stationary and mobile; bomb protection; isotope shipping; accelerator shielding, etc.
2. Organizations with shielding problems, but not necessarily shielding programs, U. S. Navy Bureau of Yards and Docks, NACA; et al.
3. Organizations with programs or facilities potentially useful to shielding research, but not necessarily with shielding problems, e.g. Battelle, Fansteel, et al.
4. Presentation of what data have so far been accumulated.

██████████

All of the talks will be written up in advance and bound into a single reference book to be distributed to the visitors before the symposium. In addition, each organization has agreed to make up an information sheet outlining what manpower and facilities it has which might be of use to the shielding program. To round out the reference book, a great many topics which will not be discussed formally will be written up and included in the reference book.

The national shielding committee, proposed by Dr. J. B. Fisk, is being organized under the guidance of Drs. Weil and Garabedian and will hold its first meeting during the symposium.

Core Holes Through Oak Ridge Pile Shield - (Rockwell, J. Goodman, DiRito). Three cores have been drilled completely through the shield of the Oak Ridge pile with a standard water-lubricated diamond-lined gasoline-driven core drill. The cores from each hole are three different diameters to give a stepped hole, and concrete-filled steel pipe plugs have been placed in the holes, providing three additional test holes in the pile shield. The purposes of the tests were:

1. To check the strength of the Oak Ridge shield and to see whether it is becoming dangerously weak.
2. To determine the effect of five years' radiation on the inside face of the concrete; or more precisely, to plot such criteria as strength, chemical composition, specific gravity, against distance from the inside face.
3. To obtain accurate chemical composition data on the special concrete of the shield, particularly its water content. This information will allow evaluation of the permanence of the mechanically bound water in the haydite part of the shield, and will provide precise data for attempting to explain theoretically the measured attenuation through the shield. This in turn will help to evaluate the effect of streaming of neutrons into the shielding samples in the testing hole.

██████████

The results indicate:

1. The radiation has had no effect on the concrete back of the first six inches, and probably little effect in the first six inches.

2. The haydite cement has lost considerable water at the outer faces next to the bituminous seal. This seal seems to be in good condition, but apparently has not prevented the escape of water.

3. The strength of the regular concrete on the inside and outside layers of the shield is quite low, although not dangerously so -- around 2000 psi.

4. The density of the haydite shield is below specifications, about 2.2, but the strength is consistently within specifications, about 2600 psi. These are preliminary data, and are subject to modification as the work is completed. Several of the cores will be ball-milled and samples taken to provide an accurate picture of the chemical composition. A complete report will be written on these tests.

Oak Ridge Pile Shield Test - (Shor, Cassidy). Attenuation tests have been run on the Oak Ridge Pile Shield, using one of the above core drillings. Concrete cores were fitted with foils for neutron detection and placed in the hole. Interstices were filled with water. The shield absorbed considerable water from the test hole, so that the results were not truly characteristic of the shield in its present dry state. During the tests, the density of the shield increased 3.3% due to water absorption. The effect on neutron attenuation is shown in figures 1 and 2.

Tests of MO Concrete

Attenuation Tests with Fission Source- (Blizard, Clifford, Sleeper, Cassidy, T. Arnette). As a result of discussions with Gale Young and others it was decided to measure the attenuation of MO concrete,

FIG. 1

Dr 6098

NEUTRON ATTENUATION THROUGH 4 5/8" HOLE  
IN OAK RIDGE SHIELD —  
CADMIUM COVERED INDIUM

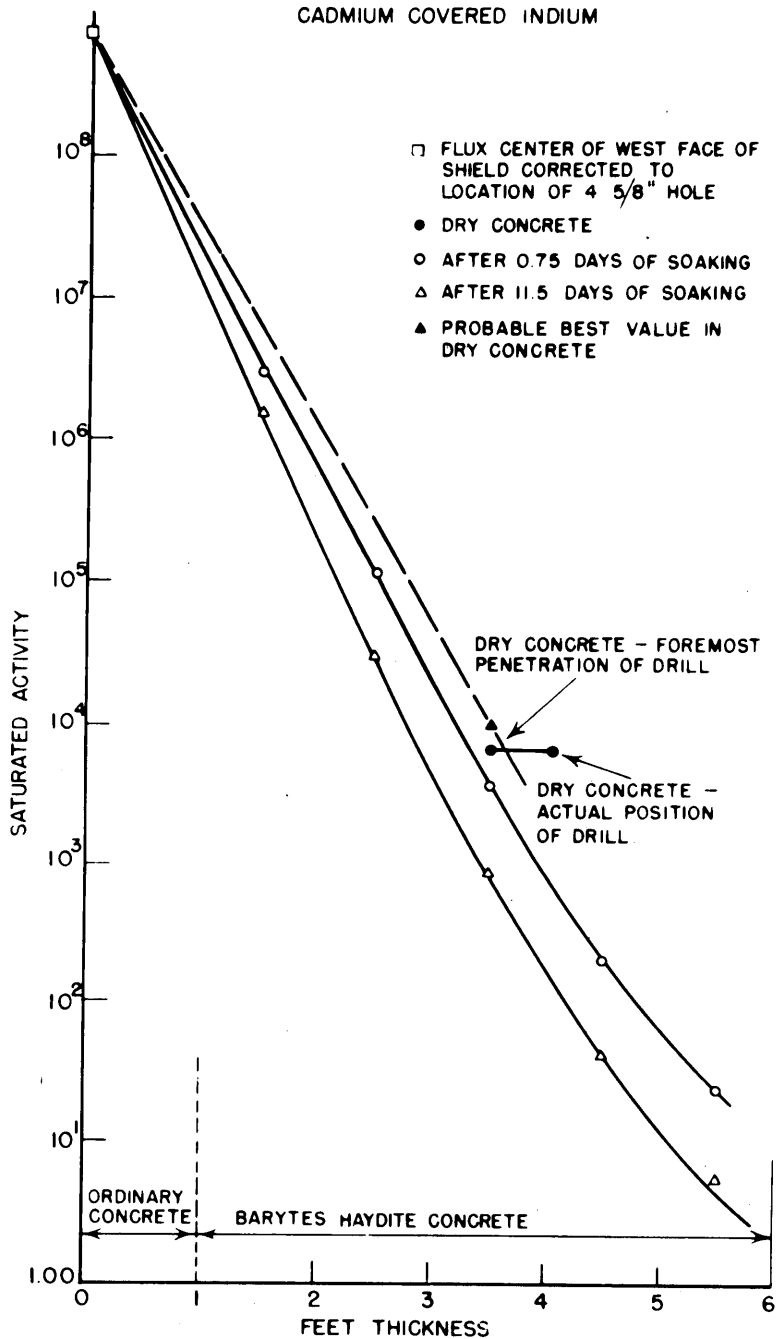
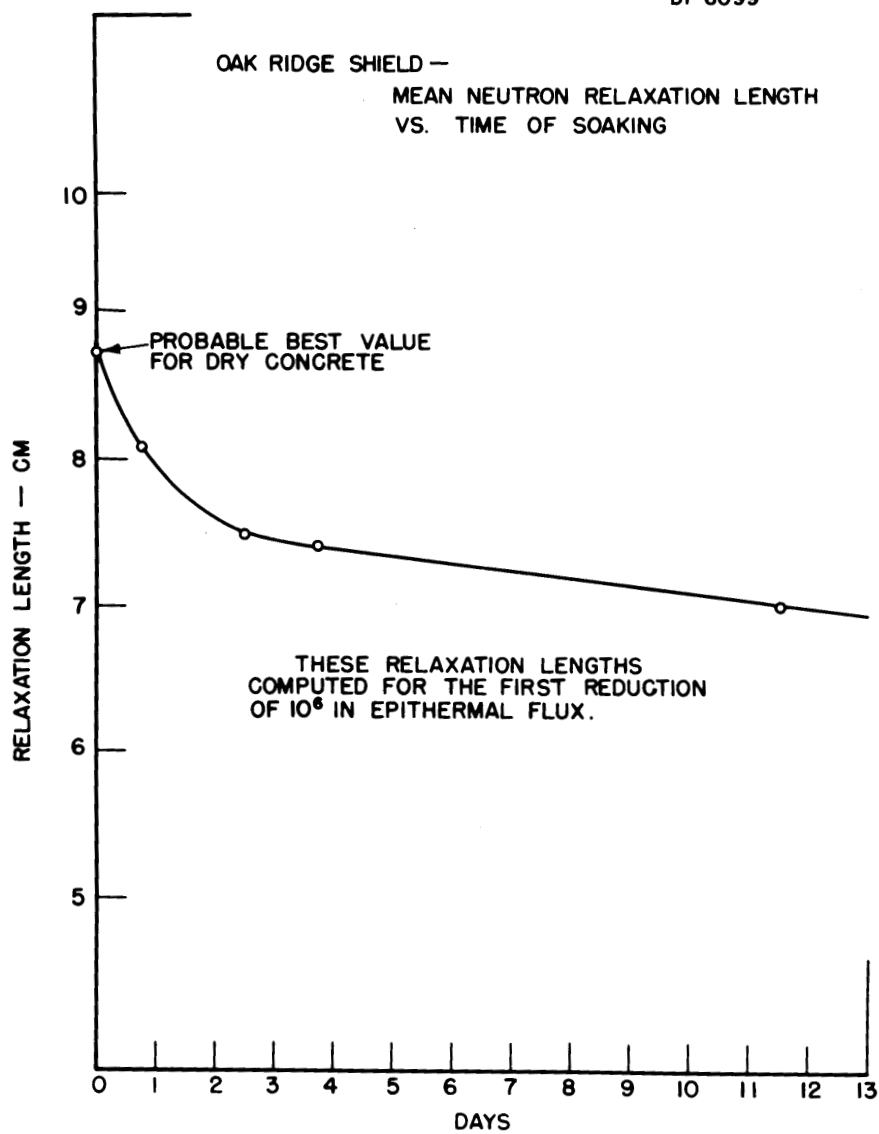


FIG. 2

Dr 6099



SECRET

(see ORNL-17; 32, for details of this material) for a more nearly pure fission spectrum. Accordingly, two tests have been run in the west face core hole, one with a plate of natural uranium at the pile face of the Mo sample, Run 30, the other without, Run 31. The arrangements are shown in Figure 3. The difference in flux for the two runs should be directly attributable to the fission source. The uranium was introduced in the form of cylindrical slugs, about 4" long, by 1.1" diameter, all held in place by lead cast around them. The lead had a dual purpose. It served to hold the slugs in the desired array, and also served as protection to personnel when the radioactive plate was removed from the pile.

In the second run, Run 31, the uranium and lead plate were replaced by a 2" thick lead plate, to simulate the effect of the source plate on the pile radiations. The simulation was not perfect. The lead will attenuate gammas less than uranium, the effect being approximately proportional to the two densities. The density ratio is 1.16, Pb + U to Pb. The uranium will, of course, absorb a large fraction of the thermal neutrons from the pile. To simulate this absorption, the 2" of Pb was coated with B<sub>4</sub>C on the face away from the pile.

To detect thermal neutron flux thin gold foils were wrapped around selected slugs, others were fastened on front and back of the 2" slabs, and still others were distributed throughout the MO concrete as described in ORNL-32. Thermal neutrons were also observed on a boron-filled ion chamber located at the core hole exit.

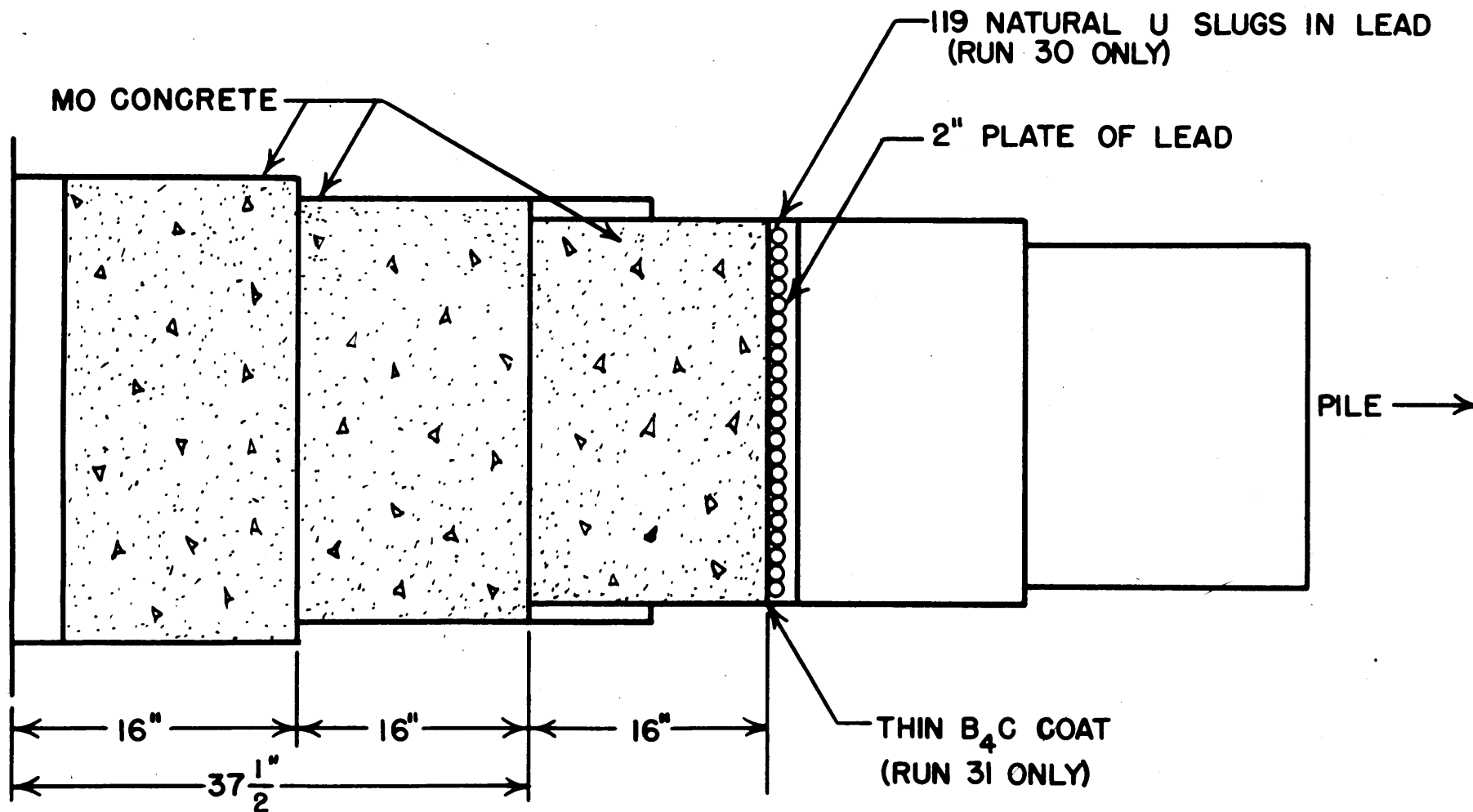
Fast neutron flux was observed by means of small indium foils in B<sup>10</sup> holders. The 4.1 hr. activity is induced by fast neutrons, above about 0.5 mev. Only a few of these readings were taken.

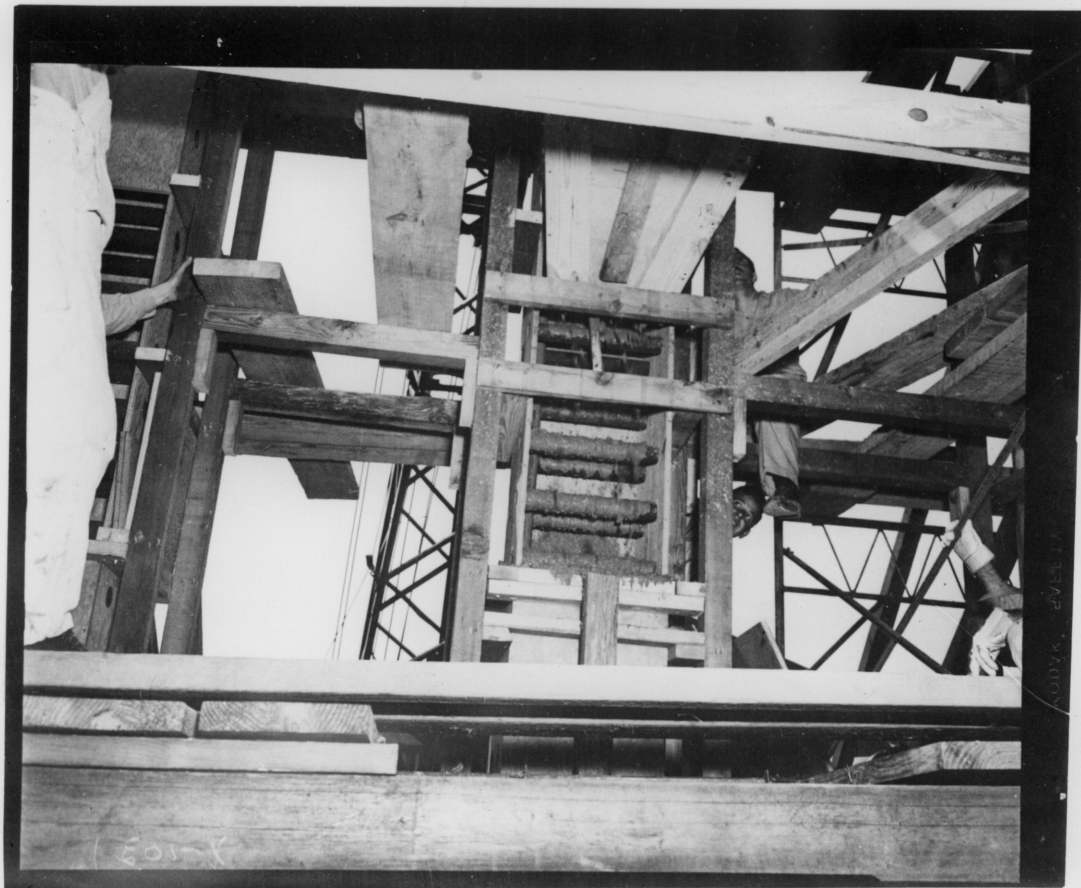
Gamma intensity was observed by film exposure, by Geiger counter measurements behind successive shield blocks, as described in ORNL-32, and by an air-filled ionization chamber located at the core hole exit.

FIG. 3

Dr 6100

ARRANGEMENT OF MO SHIELDING  
FOR ATTENUATION TEST





MO CONCRETE POURING TESTS

Figure 4  
111



MO CONCRETE POURING TESTS

Figure 5  
112

██████████

The data are being analyzed. The results should be available soon and will be the subject of a separate report.

Construction-Scale Pouring Tests - (Rockwell, Krum, Goodman). Nearly forty tons, or eight cubic yards, of MO concrete were poured in tests to determine if this concrete can be handled in standard Portland cement handling equipment.

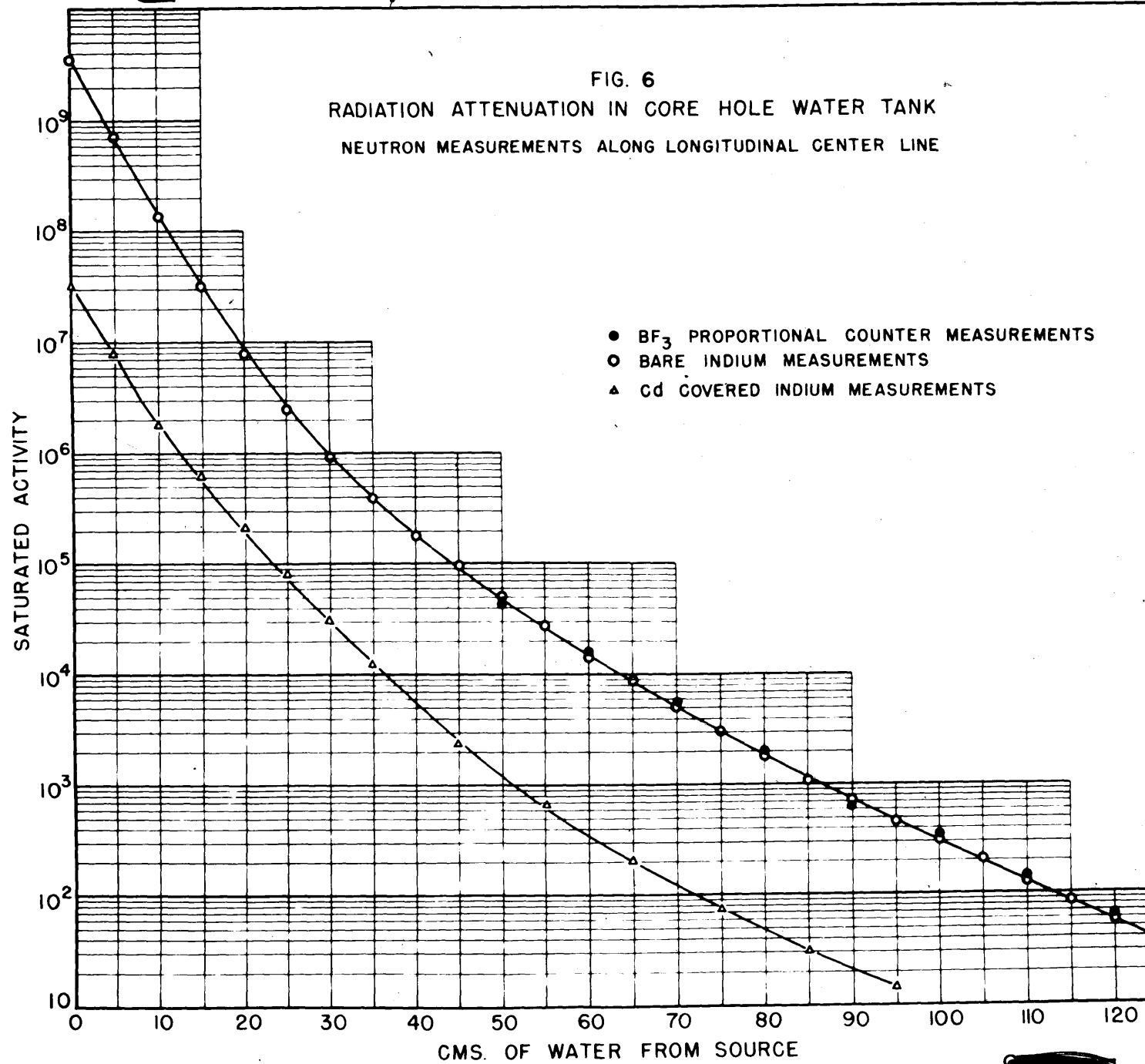
The transit truck mixer used in the tests was built to hold twelve tons of Portland cement concrete. When loaded with about eight tons of MO concrete with steel punchings, the mixer stalled.

The truck was able to handle only five tons of MO concrete. Figures 4 and 5 show the tests being conducted. Difficulty was encountered with the concrete pump when it was attempted to pump the MO through an 8" steel pipe about 200 feet long and with a 50 foot rise. Insufficient power could be supplied. The pump could be turned by rotation of the flywheels by hand indicating lack of power rather than to too stiff a mix.

On some tests the concrete set very rapidly. This has been attributed to too active MgO. Representatives of the Oxychloride Cement Association assure us that less active MgO can be supplied as desired. For this reason the large scale tests have been discontinued until less active MgO is received.

The workability, cohesiveness, and lack of segregation of the mix was noted with approval by the experienced construction field men who observed the work. Experienced personnel would have absolutely no difficulty in the use of this material in large scale work.

A sensitive position recorder has been developed which will be used to observe shrinkage and expansion of concretes during setting, from which thermal expansion coefficients can be calculated. A large constant temperature chamber has been obtained to hold the entire sample and holding jig.



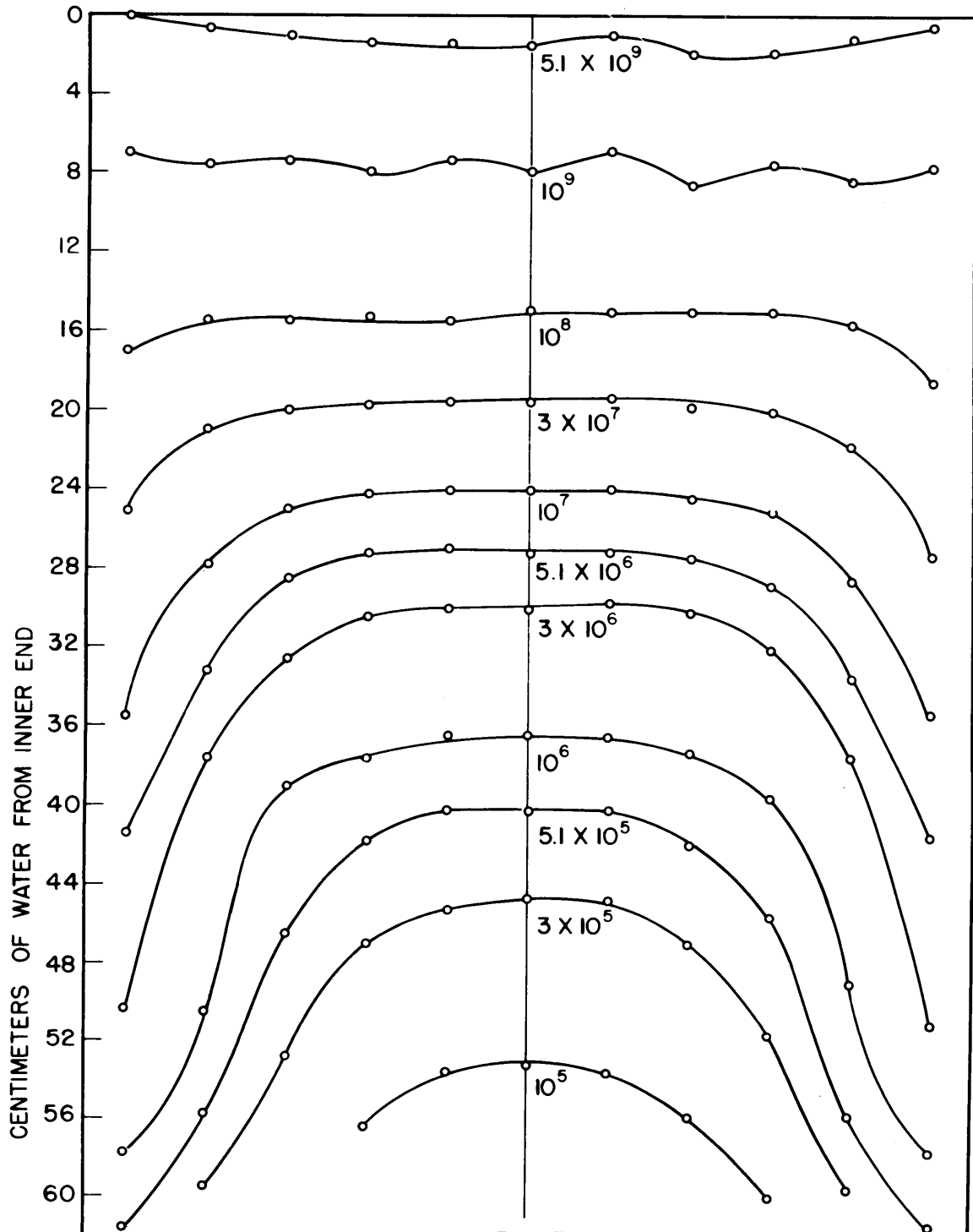


FIG. 7

NEUTRON MAP SHOWING LINES OF EQUAL FLUX IN WATER TANK

INDIUM FOIL DATA

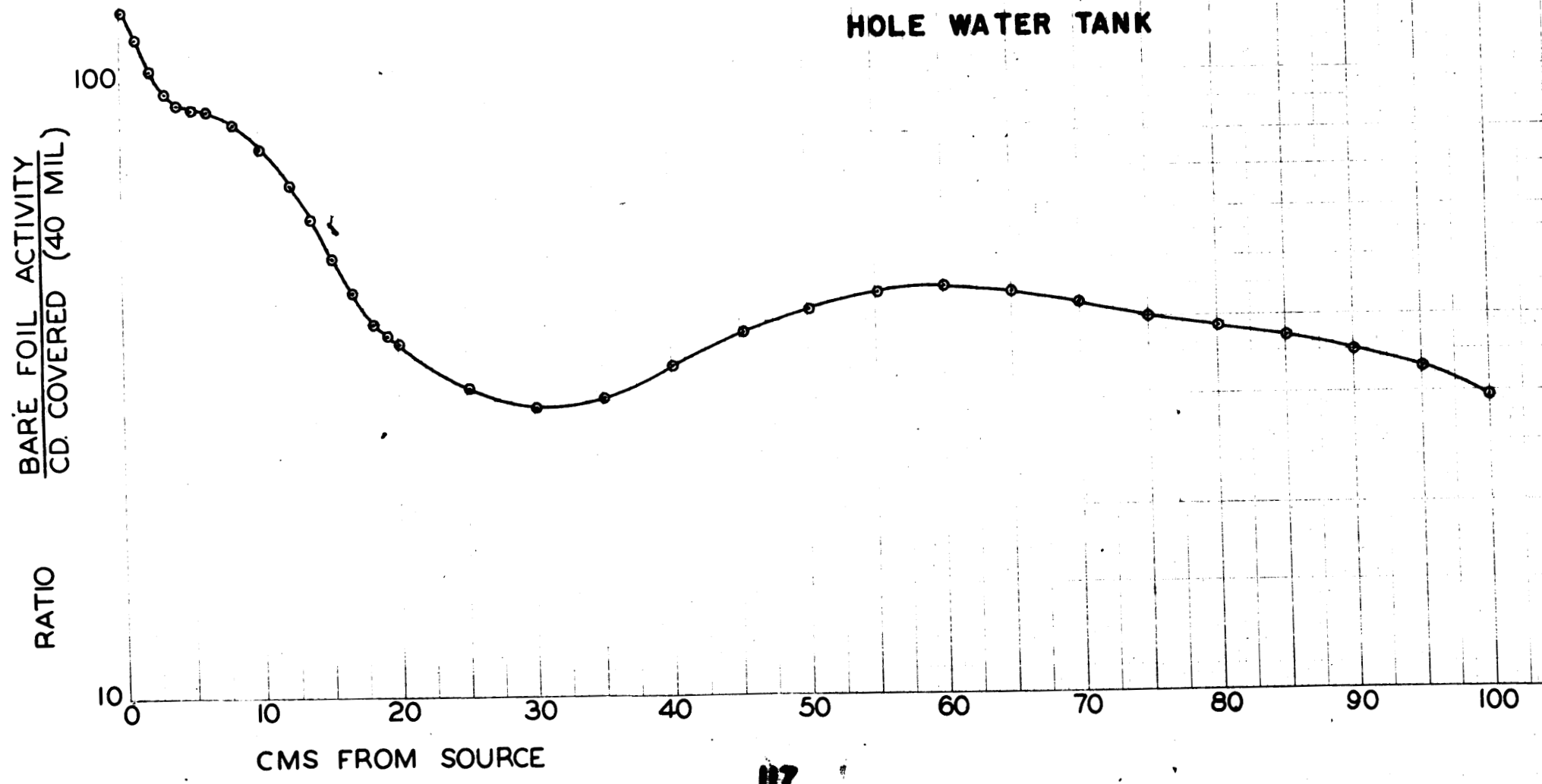
VERTICAL TRAVERSE

Cm Down -25 -20 -15 -10 -5 -0 + 5 10 15 20 25 Cm Up  
CENTIMETERS OF WATER

DT 6102

FIG. 8  
CADMIUM RATIOS ALONG  
CENTERLINE OF CORE  
HOLE WATER TANK

~~SECRET~~



██████████

with a  $\text{BF}_3$  proportional counter were used to extend the data on thermals to 120 cms. Gold foils were also used in the region close to the source to determine flux in terms of a standard, and also to compare the distribution shown by gold with that for indium. The distribution shown by gold was identical with that from indium.

Figure 6 shows the flux measured along the center line of the tank. Both Cd covered and bare foils readings out to a distance of 120 cms are shown. Figure 7 is a neutron map showing lines of equal flux in the vertical centerline plane. It is evident from this figure that transverse leakage of neutrons becomes important at 40 cms and beyond.

Figure 8 shows the cadmium ratio for indium foils along the centerline of the tank.

Correlation Between ORNL and Chicago Gamma Attenuation Data - (Sleeper, T. Arnette, Blizard). Some questions have arisen concerning the agreement between early Chicago gamma data and recent data taken at Oak Ridge National Laboratory. The analyses of the correlation between Zinn's data (CP-684) and our data (ORNL-32) presented in ORNL-32 seem to be ambiguous. A re-evaluation of Zinn's data, plotted in Figure 8 of ORNL-32, shows that the change in slope at 40 cm is due to the absence of paraffin laminations beyond that point. Probably this is due to the diminished rate of production of secondary gammas. Zinn's data were taken with a G. M. counter presumably comparable with the ORNL technique. The relaxation length for the last 20 cm of iron in Zinn's measurements is 3.85 cms, which is to be compared with 4.47 cms, obtained by Clifford and Palladino in a similar experiment (Central Files No. 47-11-33). This gives a ratio of 1.16 between the two relaxation lengths.

Zinn's iron-paraffin data indicate a relaxation length of 8.6 cms for a Hanford shield. This is to be compared to the value of 10.2 reported in ORNL-32, exhibiting a ratio of 1.18 between the two measurements.

Borst reported values of 7.9 cm for G. M. measurements and

██████████

██████████

8.5 cm for ion chamber measurements on a Hanford shield facsimile (CP-1202) on the basis of only two points each. The available data indicate a difference of about 17% between the Chicago and ORNL gamma relaxation lengths measured with a G. M. counter.

A study of notes and graphs taken from an unpublished report by Zinn reveals that both ion chamber and G. M. counter measurements yield the same equilibrium relaxation lengths, as might be expected. The measurements for iron were 3.7 cm and 3.8 cm respectively. The major difference observed was in the absolute value of the radiation intensity, different by a factor of about 10 for the two measurements. This depends on the conditions of the experiment, which cannot be evaluated from information available here.

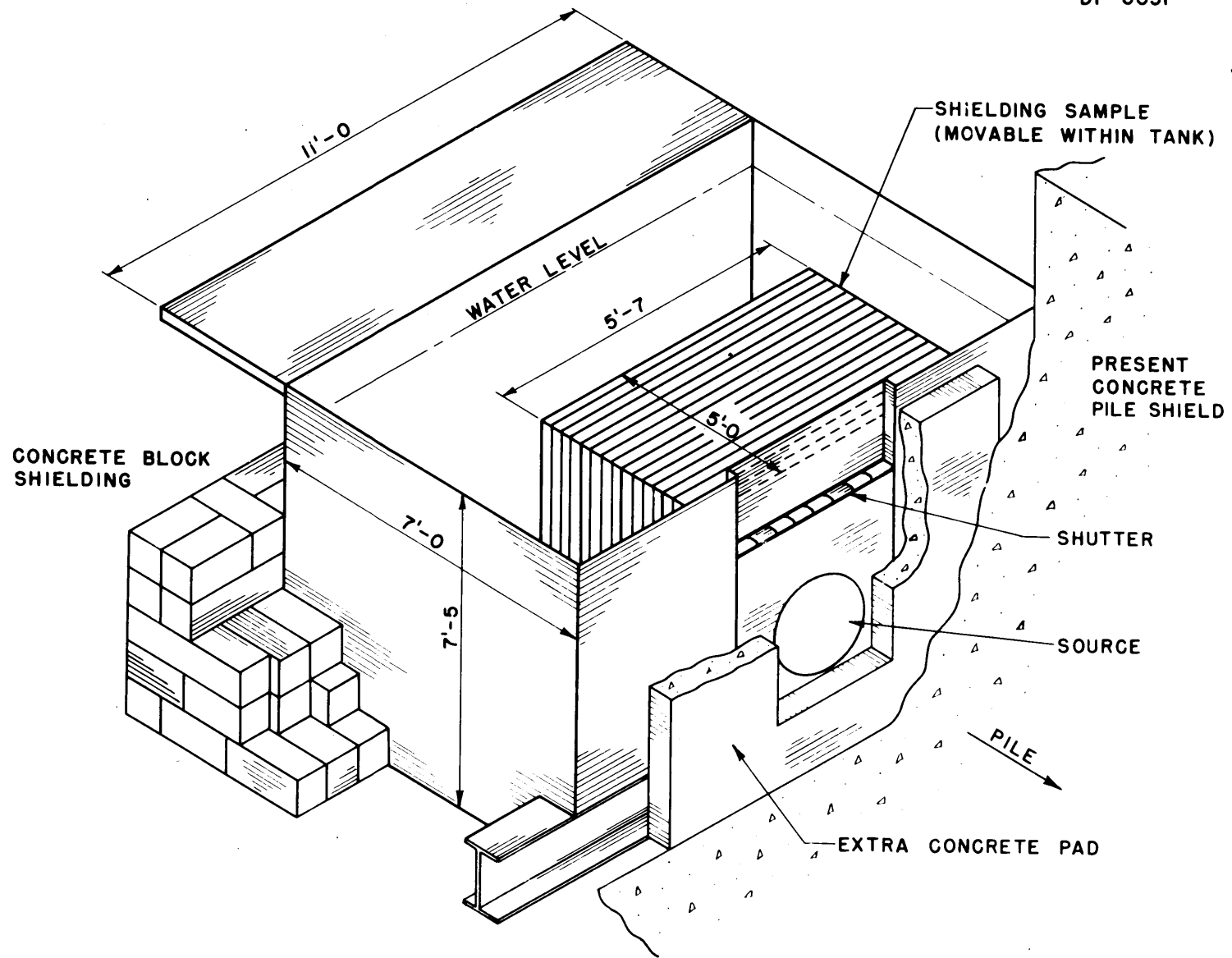
Gamma attenuation measurements have been made at ORNL with the G. M. counter surrounded by 8" of lead, except for an open tube looking at the core hole. The measurements were made 8' from the pile shield. These measurements have been compared with those taken with the same tube held against the shield block under test, and no significant differences were observed.

To study the effects of the geometry further, a 10 mc. radium point source of gammas was used with the brass walled G. M. tube surrounded by lead, except for the opening along its axis. Several horizontal traverses were taken with the source at different distances from the counter. The integral

$$2 \pi \int_0^{16"} N r \, dr$$

was evaluated to compare the contribution from a circle of 16" radius at the four different distances. N is the number of counts/min at a given distance from the center line, "r" is the distance of source from counter axis, and 16" is about half the width of the core hole. At radii greater than 16", a few counts are registered from the Oak Ridge shield. In the range covered, 95% of the counts were measured within a radius of 14" or less, indicating that in ORNL-32 geometry we are measuring test shield characteristics and not those of the surrounding Oak Ridge shield.

██████████



ISOMETRIC VIEW OF LID TANK

FIG. 9

██████████

To date, measurements indicate that the most likely cause of the difference between Chicago and ORNL data may be the difference in source spectrum. The extra hardening of the spectrum due to visible slug array opposite the ORNL core hole may be the explanation. Borst's measurements were made without such a lattice.

Lid Test - (Clifford, Blizard). Designs have been completed for the large water tank for testing shield materials with a fission source at the core hole exit. Figure 9 shows the proposed tank in place. Completion is anticipated during October. It is a steel tank measuring about seven by seven by ten feet, with a lead neutron-window opening into the present core hole. The tank will rest on the balcony, tight against the core-hole through the shield, will be filled with water, and will be open on top. At the lead window will be a converter plate made of Oak Ridge slugs, which will absorb thermal neutrons from the pile and emit fast neutrons. The present core-tank, when filled with water, will shut off the supply of thermal neutrons and act as a shut-off valve for the system.

With a slab of experimental shielding material in place, gamma and neutron distributions will be observed in the water back of the slab, and compared with similar data taken with a different number of slabs. There are three important features of the system:

1. The streaming of neutrons from the sides will be calculable since the samples will be five feet square and the flux at the edge will be known.
2. In addition to the usual measurement of attenuation through each slab, changes in the spectrum can also be observed from the slow neutron distribution in the water behind the last slab.
3. Samples can be inserted and removed without requiring pile shutdown.

Instrument development - (Clifford). An arrangement is being made to set up movable Sb gamma source and a fixed RaBe neutron source to investigate the effect of gamma flux on neutron detectors. An attempt

██████████

██████████

will be made during the slab test referred to above, section entitled "Tests of MC Concrete" , to use aluminum foil for detecting fast neutrons. It is anticipated that this will require some ingenuity.

If the schedule permits, measurements will be taken in the water tank filled with saturated  $B_2O_3$  solution; it is hoped that some information can be gleaned on the effect of boron on the gamma flux through a shield. In this connection, an attempt has been made to measure the 0.5 MeV gammas which have been reported to result from 90% of the neutron captures in boron. This has been quantitatively measured by only one experimenter, but there is good indirect evidence of its existence. An aluminum-walled, air-filled ion chamber was calibrated for 0.5 MeV gammas at the National Bureau of Standards, and then readings were taken in the strong neutron flux in the water tank. The measurements were repeated with a thin coating of boron over the tube, and again with a thick coating. The readings were successively less, which would seem to indicate that a capture gamma was either not being emitted or not being detected. The thickest coating plus the chamber wall was still appreciably less than the range of 0.5 MeV gammas. K. Way has suggested that the gamma may be highly converted.

Battery Test - (Clifford, T. Arnette). A report has been written (ORNL-106) which describes the experiment. Data are presented on battery behaviour during and after exposure to radiation, and a rough estimate is made of its radiation attenuation properties.

#### Other Work in Progress

Early Attenuation Data - (Blizard). Attenuation data on Portland concretes with iron aggregates and varying percentages of boron had hitherto been reported only in the Quarterly Reports. This is now being prepared more completely in ORNL report form.

Diffusion of Gamma Rays - (Blizard). No significant progress has been made recently on this work.

Boron Coating - (Rockwell). The literature study of boron coating

██████████

techniques has been continued. No actual laboratory work has been conducted recently.

Status Report on Shielding - (Entire Group). A complete summary report is being prepared. It is hoped to analyze critically all ORNL shielding experience.

Improved Isotope Shipping Containers - (Clifford, Rockwell). Experiments have been run on  $P^{32}$  and  $I^{131}$  in long plastic tubes to simulate a line source of radiation rather than a point source, since calculations indicate that considerable gain might be expected with this system under several conditions. The plastic tubes are enclosed in cardboard mailing tubes, with only a small amount of shielding needed, and are loaded and unloaded with hypodermic needles. For beta-emitters the shield contains no metals to act as x-ray targets. Some radiation, hold-up, and absorption data have been taken. These preliminary results look very promising.

Theoretical Work - (F. H. Murray). Further studies were made of the high energy neutron flux from a plane isotropic source in an infinite medium. When approximate formulas have been obtained for the flux density per unit energy interval due to a source energy  $E'$ , in the form  $nv(E', E, z)$ , a maximum of  $nv$  may occur near the value  $E'$ , and it is convenient to evaluate the integral

$$\int_{E_0}^{E'} nv(E', E, z) dE = h(E', z) \frac{e^{-p(E')z}}{p(E')z},$$

which expression defines  $h(E', z)$ . For water and some other materials one obtains from the assumption of only grazing collisions with O and H the formula

$$p(E') = \sigma(E'),$$

but the estimates only have been made for the function  $h$ .

Thermal neutron densities may be estimated from the integral over the source spectrum ( $f(E') dE'$ ),

$$(nv)_{th} = \frac{C'}{z} \int f(E') h(E', z) e^{-P(E')z} dE'$$

if variations in age near the high energy parts of the spectrum can be neglected. Analyses of the factor  $h(E')$  are being made due to its importance in estimations of the absolute value of the thermal flux at any point.

THEORETICAL PHYSICS

M. E. Rose

The Problem of Polarizing Nuclear Spins. Considerable study was made of:

- (a) Methods whereby nuclear spins may be aligned
- (b) Experiments which might be performed with such aligned nuclei.

Under (a) both direct coupling of nuclear moment and external field and hyperfine structure coupling of nuclei with the magnetic field produced by the extra nuclear electrons was considered. The latter method would simplify the problem considerably if nuclei with hfs splittings of order  $0.1 \text{ cm}^{-1}$  in the ground state can be found. This hfs coupling scheme would work only with paramagnetic substances.

Under (b) consideration was given to scattering experiments designed to yield information about the spin dependence of nuclear forces. At thermal energies where diffraction effects occur, scattering with and without polarization of nuclei and/or neutron would yield all information about spin dependence which could be desired. Fairly large changes of coherent scattering could be expected where the spin dependence of the forces is pronounced. For higher energy neutrons the change in scattering is of the order of the product of nuclear and neutron polarizations. If this can be made large enough one can get both scattering amplitudes as a function of energy. This depends on obtaining polarized neutrons at all energies which can be done if nuclear paramagnetism is achieved. The determination of angular momenta of levels of compound nuclei would be a comparatively straightforward matter with polarized nuclei and neutrons polarized at resonance energies. The latter again is a possibility with aligned nuclei.

This work was the basis of a talk given at the Oak Ridge Conference on Low Temperatures and Nuclear Physics on August 7.